ALTERNATIVE MATERIALS AND CONFIGURATIONS FOR PRESTRESSED-PRECAST CONCRETE PILE SPLICE CONNECTION

Quarterly Progress Report
For the period ending November 30, 2021

Submitted by:
PI- Armin Mehrabi, PhD, PE
Research Assistant- Seyed Saman Khedmatgozar Dolati (PhD student)

Department of Civil and Environmental Engineering
Florida International University
Miami, FL

ACCELERATED BRIDGE CONSTRUCTION
UNIVERSITY TRANSPORTATION CENTER

Submitted to:
ABC-UTC
Florida International University
Miami, FL

Disclaimer

The contents of this report reflect the views of the authors, who are responsible for the facts and the accuracy of the information presented herein. This document is disseminated in the interest of information exchange. The report is funded, partially or entirely, by a grant from the U.S. Department of Transportation's University Transportation Program. However, the U.S. Government assumes no liability for the contents or use thereof.

Table of Contents

1. Introduction and Background

Establishing bridge foundation when there is a top layer of weak soils normally requires application of deep foundations such as pile foundation. One of the options among various types of piles and installation methods is driving prestressed-precast concrete piles (PPCP) (Figure 1). Since it employs pile segments prefabricated in precast plants and delivered to the site for installation, it follows the principals of Accelerated Bridge Construction. Comparing to other types of piles, this option is in many cases more cost and time effective. Accordingly, PPCP generally reduces the construction time in line with the benefits promised by ABC methods. However traditional PPCPs which use conventional passive and none passive carbon steel reinforcements are prone to corrosion especially when they are in a marine environment. In such environments, accumulating salts in piles which are caused by alternating the level of water and water splash accelerate corrosion. Corrosion causes the piles to fail prematurely and incur costs. According to the Cost of Corrosion (Lampo et al., 1997), in highway bridges the dollar impact of corrosion on concrete and steel bridges is substantial and the indirect costs including the user and maintenance increase the overall costs tenfold. Accordingly, attempts have been made to increase corrosion resistance of PPCPs. Using Carbon Fiber Reinforced Polymers (CFRP) and High Strength Stainless Steel (HSSS) for strands and other types of reinforcements has shown a great improvement in corrosion resistance.

Figure 1: Prestressed-Precast Concrete Piles

(https://dlsprestressed.com/services/driven-concrete-piles/)

For various reasons, it becomes necessary or is desirable to splice PPCPs. The merits of casting shorter pile segments and splicing them on-site are: 1- easy handling, transporting, and driving, 2- possible reduction in concrete cracking during handling, transportation, and driving, 3- suitability of pile extension in unforeseen situations and soil conditions where longer piles become necessary, 4- reduction in transportation cost, 5- ability to be store in the precast yard and construction site (Venuti, 1980). It should be stated that these advantages can only be achieved if the use of splice is economical, can develop the structural capacity of pile section and the connection can be made quickly without the need for special skilled labors. With this in mind, splicing of pile segments has to be performed at the site to achieve longer lengths using various types of joints. There are various means of establishing bearing-type splices. Splicing with the use of corrosion-resistant material is the focus of this project. State Departments of Transportation including FDOT have Specifications and Standard Drawings showing details and designs for pile splices including those using corrosion-resistant materials.

Nevertheless, because of lack of understanding of the structural behavior and sometime complexity and cost associated with splicing, especially for the case of corrosion-resistant materials, their use has been very limited. On the other hand, much has been done in relation with ABC connections and details for bridge sub- and super-structure joints and connections, and a variety of new and effective joints have been developed and are in use. The aim of the proposed study is to build upon the experiences gathered in general for ABC connections and develop an effective yet simple splice connection for prestressed-precast concrete piles to provide the necessary pile lengths for reaching the required resistance and at the same time to promote corrosion resistance.

2. Objectives and Research Approach

The objective of this project is to explore alternative pile splice connection configurations and materials, and to investigate the feasibility of these connections in comparison with the existing epoxy dowel splice for prestressed-precast concrete piles. The project begins with reviewing literature on types of driven piles, existing pile splice configurations and materials, as well as available ABC connections implemented for bridge sub- and superstructures. This will be followed by exploring alternative connection configurations and alternative materials. The performance of the promising designs will be compared to the existing designs using analytical modeling. Among other materials, a non-proprietary Ultra-High-Performance Concrete (UHPC) mix currently under investigation by ABC-UTC will be considered in detailing of the splice connection zone as well as its use as filler/bonding material for dowels. Additionally, the use of mechanical connection types utilizing corrosion resistant materials will be explored to address the time constraint associated with pile driving operation. The project will culminate in development of the most promising alternative splice connection details and materials for prestressed-precast concrete piles. This research project focuses on the use of analytical modeling and computational means for investigation on the structural behavior, and comparison between performances of existing details for pile splices and newly developed designs using alternative configuration and material. This will include finite element modeling of pile

segments and splices, as well as section analysis using available analysis tools. Future activities will include performing experimental verification of the newly developed details.

3. Description of Research Project Tasks

The following is a description of tasks carried out to date.

Task 1 - Literature Review

3.1. Types of Driven Piles

Driven piles are divided into piles made of wood, steel, concrete, and various types of composite materials. These types of pile are reviewed briefly here, however, this study focuses on prestressed precast concrete piles to be discussed in more details.

3.1.1. Wooden Piles

Wooden piles have a long-rooted history. There are some reasons for using them. The ease and the speed of installation, being an eco-friendly or "green" construction, and being cost-effective are among the reasons that make wooden piles popular (Figure 2). However, wooden piles, especially in coastal areas, are prone to damage caused by marine borer activity. Therefore, fabricating more durable piles is needed in the marine environment and when piles are in the water, especially in the splash zone (Figure 3) (Iskander, 2003).

Figure 2: Wooden piles

(https://www.pinerivergroup.com/blog/wood-pilings)

Figure 3: Tunneling in a timber pile caused by Teredo and Bankia (M. Iskander, 2003)

3.1.2. Steel Piles

The use of steel piles has been limited due to the susceptibility to corrosion (Figure 4). Whenever employing a load-bearing steel pile foundation has been considered for a structure, the probability and the amount of corrosion have always caused concerns (OHSAKI, 1982). The rate of corrosion of steel piles immersed in fresh water is estimated to be 0.03 mm per year which increases to four times in the splash zone (Fleming et al., 2008). Localized corrosion of steel sheet piling has been investigated by E. Melchers et al. (2014) (Figure 5). In their research, samples of two types of sheet piling were exposed to natural seawater for 1, 2 and 3 years. The samples demonstrated localized corrosion in the central zone and close the flange-web junction. The corrosion in steel piles can affect the load-bearing capacity of piles dramatically. Therefore, there is a need for alternative materials for pile fabrication that are resistant to corrosion.

Figure 4: Corrosion in steel pile

(https://www.ducorr.com/ducorr-blog/2018/3/20/conventional-steel-corrosion-and-durability-design)

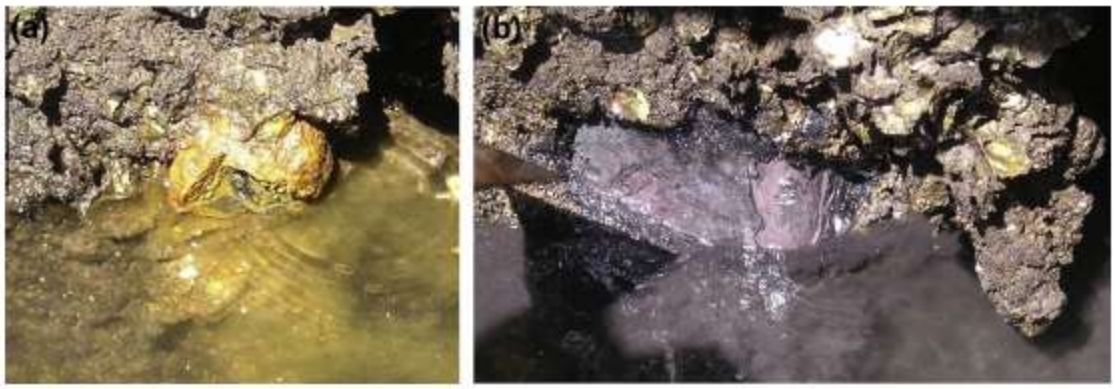

Figure 5: Local corrosion of sheet piling (Melchers et al., 2014)

3.1.3. Composite Piles

Composite materials, due to their resistance to electrochemical corrosion and versatility of fabrication, provide alternative to customary material. The price for the composite is however high. Fiber Reinforced Plastic (FRP) composites are used in some cases in hybrid construction with concrete where the concrete provides the role of bulk mass, and the FRP has a role of load carrying partner and protector of the concrete from the exterior environment. This combination provides for a cost effective use of composites. Concrete-filled FRP tubes as a hybrid system, can be used for pile fabrication (Shahawy, 2003). They have been used in many marine environments (Figure 6).

Figure 6: FRP tubes for composite piles

(https://www.harbortech.us/products/composite-pilings/)

The first recycled plastic pile was driven at the port of Los Angeles (Horeczko, 1995). It was a steel core composite pile. This experience showed that due to thermal stresses, the steel core composite piles experience core delamination. Therefore, producers presented a type of composite piles that included fiberglass and HDPE combined with fiberglass reinforcement and stabilizers. In 1998, Iskandar and Hassan reviewed the types of composite piles and compared them in term of material properties, durability, drivability, and the interaction between soil and piles. They found that piling materials made of FRP or fiberglass offer performance advantages for employing in harsh and marine environments. The advantages of using them are durability

and environmental benefit. However, disadvantages include high cost, less drivability and high compressibility (Iskander & Hassan, 1998).

3.1.4. Prestressed precast concrete piles

One of the options for establishing pile foundation is the use of prestressed-precast concrete piles (PPCP) (Figure 7). This option provides in many cases an economic alternative to other pile foundation types and accelerates the construction process, especially in marine environments. In PPCPs, prestressed strands provide the pile with the required tensile strength during the driving process. The strands, provide the extra strength to resist the moment bending which will be caused during lifting, transporting, and the bending moment as a result of lateral loads. PPCPs have been made in different shapes with different types of materials for strands.

© https://www.gimrock.com/FoundationWork.html

Figure 7: Prestressed-Precast Concrete Piles in marine environment

3.1.4.1. Prestressed Precast Concrete Piles Using Conventional Prestressed Strand

Prestressed concrete piles can be reinforced with prestressing strands including threaded rebars (e.g., Dywidag rods), prestressing wire or seven-wire strands (Figure 8), and with other reinforcing bars and welded wire mesh. The most commonly used prestressing reinforcement is seven-wire strands. Two types of seven-wire strands have been used: 1- stress-relieved 2- low-relaxation. The difference in the behavior of these two types of strands is shown (Figure 9). In conventional PPCPs, the low relaxation seven-wire strands with the various nominal diameters including the common 0.5 and 0.6 inches have been used. However, traditional prestressed piles that use carbon steel strands and bars are prone to corrosion, especially when they are in marine environments. In such environments, alternating water levels and water splash promote deposit and migration of chlorides into the pile and provides a condition for accelerating the corrosion. Among other states departments of transportation, the Florida Department of Transportation (FDOT) has also implemented programs for the utilization of alternative prestressing strand materials that are corrosion resistant. The use of Carbon Fiber Reinforced Polymers (CRFP) and High Strength Stainless Steel (HSSS) for strands, longitudinal and transverse reinforcement in

the precast concrete piles have shown great improvements to resistance against corrosion (Belarbi et al., 2017; Mullins et al., 2014; Rambo-Roddenberry et al., 2016).

(a) Deformed bars (b) Prestressing seven-wire strands

Figure 8: Type of reinforcement for prestressing

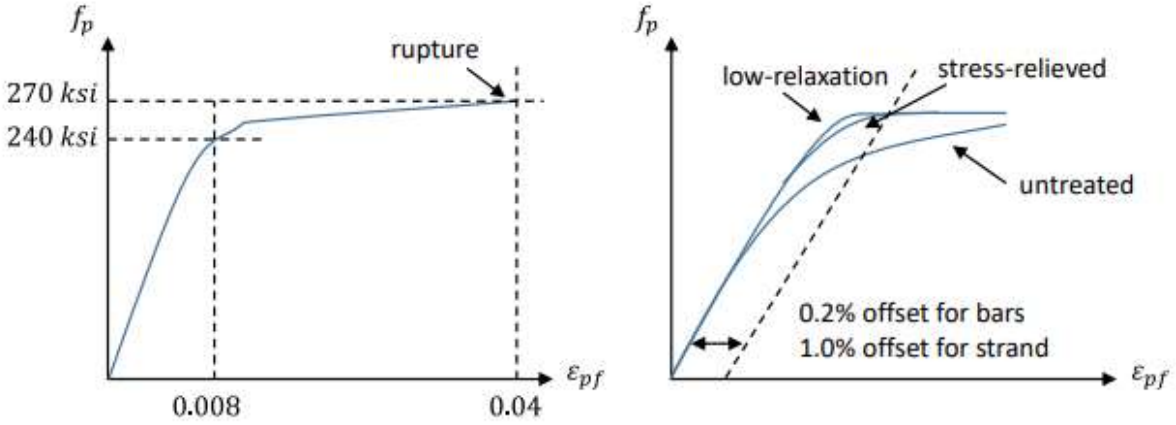

Figure 9: Difference in the behavior of the low-relaxation and stress relieved strands

3.1.4.2. Prestressed Precast Concrete Piles Using Alternative Strand Materials

There have been several investigations on the application and performance of PPCP using alternative prestressing strand material. CFRP and its variant Carbon Fiber Composite Cable (CFCC) is one of the materials that has shown great promise for replacing the normal prestressing strands. ACI-440-04 covers an extensive review of the background, material properties and design recommendation for the use of these materials and other FRPs. CFCC has shown high bond strength to concrete (about twice of that of steel), has light weight and high tensile strength, its relaxation is less than steel, and can be coiled in its twisted wire form. However, CFCC is more expensive than steel, has low impact resistance, and it is brittle in failure not as ductile as its steel counterpart (Rambo-Roddenberry et al., 2016). Grace (2007) used CFRP for post-tensioning tendons and reinforcing bars for the first time in the Bridge Street Bridge in Southfield, MI. His study monitored the performance for long period of time and demonstrated its suitability for use in prestressing/post-tensioning applications. Roddenberry et

al. (2014, 2016) tested PPCP using CFCC of various lengths to investigate the flexural strength, transfer length, development length, and drivability (Figure 10). They concluded that transfer and development length for CFCC is noticeably shorter than that of steel, and flexural strength higher than anticipated. Pile driving and installation were without any major damage to the pile despite the hard condition and high stress level. Some challenges in production were noted and modifications recommended including use of wood versus steel cap, care in installation and handling, lower stress rate, avoiding the use of regular vibrator, and strong quality control (QC).

Figure 10: Flexural testing of PPCP with CFCC (Roddenberry et al., 2014)

PPCP using HSSS strands and spirals have also been studied as another alternative to carbon steel strand piles. Mullins et al. (2014) tested three types of stainless steel material that are available in strand form and compared their corrosion resistance and structural performance to conventional carbon steel prestressing strand. They showed that the use of HSSS strands had no adverse effect on transfer length, while it improves the corrosion resistance significantly (Figure 11). Paul et al. (2015) demonstrated through testing that transfer and development length for HSSS-2205 prestressing strands are considerably smaller than that predicted by AASHTO LRFD, the flexural and shear strengths of piles using SS were greater than predicted by both ACI-318 and AASHTO LRFD, and the stress loss was smaller than that predicted by AASHTO LRFD refined method. These properties were not affected after installation and extraction.

Figure 11: PPCP with Stainless Steel Strand and Spiral (Mullins et al., 2014)

Prestressed Precast Concrete Piles (PPCP) often require splicing for one or more of the following reasons such as (i) limits on length for shipping and transportation, (ii) limited pile-driving headroom that will force planned splicing, (iii) and when the required capacity is not achieved with the piles existing lengths resulting in unforeseen splicing, and others (Figure 12). The focus of this report is on the types of splices for precast prestressed concrete piles which can provide the piles with corrosion resistant materials and accommodates a time effective method.

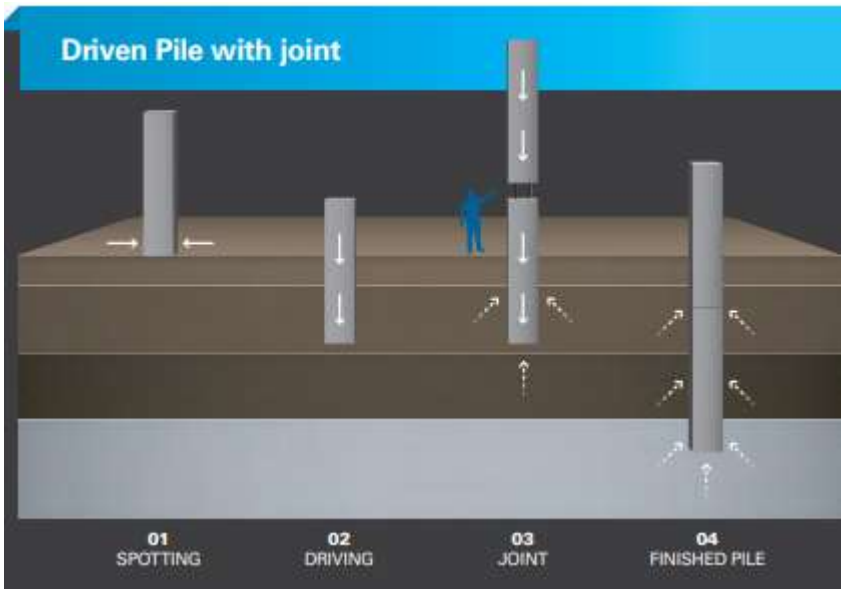

Figure 12: Driven pile with joint/splice

3.2. Pile Splices

3.2.1. Existing Splice Systems for Driven Piles

There are various means for establishing bearing-type splices including wedge, pinned, welded end plates, post-tensioned, sleeve, connecting ring, mechanical and finally dowel splices as illustrated in Figure 13.

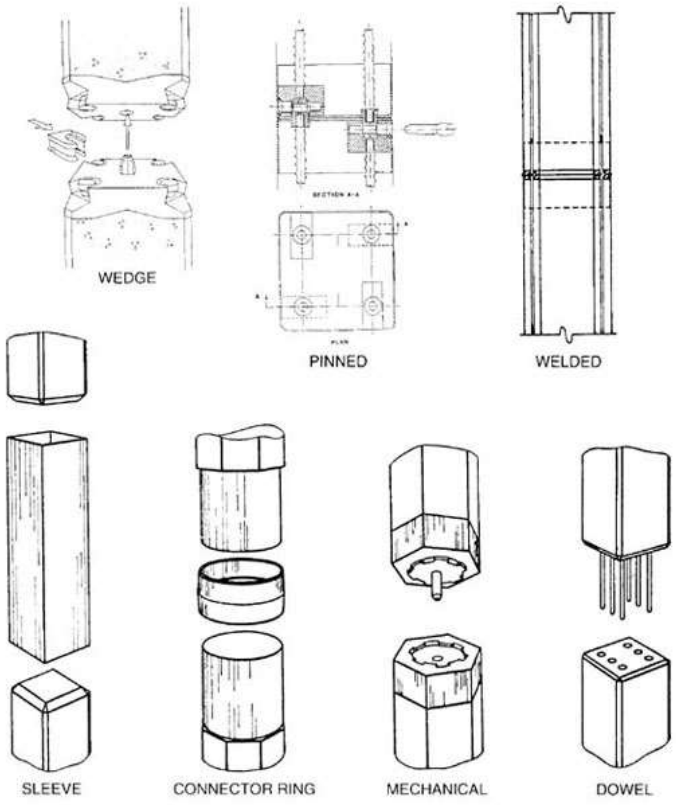

Figure 13: Various types of existing pile splicing (Pile Buck Magazine, http://www.pilebuck.com/education/pile-points/concrete-pile-splices/ 1/7)

Gerwick (1968) reviewed the formation, utilization, and installation of the PPCPs, and discussed their failure and damages. In his work, epoxy dowel splices were mentioned as the most desired type in providing resistance for piles in flexural design. He also mentioned that mechanical splices are the most economical type of pile splices. In 1970, Liu presented a report which helped designers with splices. Driving and no driving conditions, the required concrete strength for piles, driving stress, head and tip design practice, and the requirements for an ideal splice were discussed. A combination of sleeve and wedge for establishing pile splices were discussed by Alley (1970). This splice was used in Seattle, WA, for splicing octagonal piles. The splice includes outer and inner steel sleeves which were connected to four steel wedges welded to form the piles. In 1971, a chapter in a textbook by Gerwick (1971) discussed typical detail of prestressing pile splices used in the U.S, Japan, Sweden, and Norway. In 1974, a comprehensive research was carried out on 20 types of splices by Bruce and Hebert (1974a). Details of various splices and their strengths were presented in this study. Also, the performance of each splice in tension, compression, and flexural was discussed. The results of this investigation is summarized in Table 1 (Bruce Jr & Hebert, 1974a).

Table 1: Type of splices (Bruce Jr & Hebert, 1974a)

Type of Splices for Piles					
Type	**Splice type**	**Does this detail require preplanning?**	**Time needed (minutes)**	**Labor skill (procedure)**	**Country of Origin**
Mechanical	Marier Splice	yes	minimal-30	average	Canada
Mechanical	Herkules Splice	yes	minimal-20	simple	Sweden
Mechanical	ABB Splice	yes	minimal-20	simple	Sweden, western Europe
Welded	NCS Splice	yes	high-60	average	Japan, Pacific, Northwest
Welded	Tokyu Splice	yes	high-60	average	Japan(Tokyo)
Welded	Raymond Cylinder	yes	high-90	average	USA
Welded	Bolognesi-Moretto Splice	yes	minimal-50	average	Argentina
Bolted	Japanese Bolted Splice	yes	minimal-30	average	Japan
Connecting Ring	Brunspile Connector Ring	yes	minimal-20	simple	USA
Sleeve	Anderson Splice	**no**	minimal-20	simple	USA
Welded Sleeve	Fuentes Splice	yes	minimal-30	average	USA(Puerto Rico)
Sleeve	Hamilton Form Company Splice	**no**	high-90	simple	USA
Dowel	Cement-Dowel Splice	yes	average-45	simple	USA
Post Tensioned	Macalloy Splice	yes	high-120	average	Great Britain.
Combination	Mouton Splice	yes	minimal-20	simple	USA
Combination (Sleeve and Wedge)	Raymond Wedge Splice	yes	minimal-40	simple	USA
Connecting Ring	Pile Coupler Splice	yes	minimal-20	simple	USA
Mechanical	Nilsson Splice	yes	minimal-20	average	Sweden
Wedge	Wennstrom Splice	yes	minimal-20	simple	Sweden
Mechanical	Pogonowski Splice	yes	minimal-20	average	USA

In Table 1, types of splice, the required time for installation, the skill of labor which needed during construction, and the country of origin are shown. This table also specifies whether preplanning is required to establish each type of splices. The installation time, as it is on any ABC method, is of extreme importance. By reducing the construction time, the impact of splicing on the overall bridge construction time will be reduced and the bridge usage by the public is greatly improved, especially when the replacement of an existing bridge is involved. In addition to requiring minimal time to establish the splice, the splice should be strong enough to resist all load effects including tension, compression, shear, and flexural. In Table 2, the performance of these splices has been summarized (Bruce Jr & Hebert, 1974a).

Table 2: Performance of the splices in compression, tension, and flexure in comparison with un-spliced pile (Bruce Jr & Hebert, 1974a)

Type of Splices for Piles					
Type	**Splice Type**	**Splice Performance in Compression**	**Splice Performance in Tension**	**Splice Performance in Flexure**	**Patent**
Mechanical	Marier Splice	100 percent of pile strength	100 percent of pile strength	100 percent of pile strength	yes
Mechanical	Herkules Splice	100 percent of pile strength	100 percent of pile strength	100 percent of pile strength	yes
Mechanical	ABB Splice	100 percent of pile strength	100 percent of pile strength	100 percent of pile strength	yes
Welded	NCS Splice	100 percent of pile strength	100 percent of pile strength	100 percent of pile strength	yes
Welded	Tokyu Splice	100 percent of pile strength	100 percent of pile strength	100 percent of pile strength	yes
Welded	Raymond Cylinder	100 percent of pile strength	100 percent of pile strength	100 percent of pile strength	yes
Welded	Bolognesi-Moretto Splice	100 percent of pile strength	50 percent of pile strength	100 percent of pile strength	yes
Bolted	Japanese Bolted Splice	100 percent of pile strength	90 percent of pile strength	90 percent of pile strength	yes
Connecting Ring	Brunspile Connector Ring	100 percent of pile strength	20 percent of pile strength	50 percent of pile strength	yes
Sleeve	Anderson Splice	100 percent of pile strength	no strength	100 percent of pile strength	no
Welded Sleeve	Fuentes Splice	100 percent of pile strength	100 percent of pile strength	100 percent of pile strength	yes
Sleeve	Hamilton Form Company Splice	100 percent of pile strength	75 percent of pile strength	100 percent of pile strength	no
Dowel	Cement-Dowel Splice	100 percent of pile strength	40 percent of pile strength	65 percent of pile strength	no
Post Tensioned	Macalloy Splice	100 percent of pile strength	100 percent of pile strength	100 percent of pile strength	yes
Combination	Mouton Splice	100 percent of pile strength	40 percent of pile strength	100 percent of pile strength	yes
Combination(sleeve and Wedge)	Raymond Wedge Splice	100 percent of pile strength	100 percent of pile strength	100 percent of pile strength	yes
Connecting Ring	Pile Coupler Splice	100 percent of pile strength	100 percent of pile strength	100 percent of pile strength	yes
Mechanical	Nilsson Splice	100 percent of pile strength	100 percent of pile strength	100 percent of pile strength	yes
Wedge	Wennstrom Splice	100 percent of pile strength	100 percent of pile strength	100 percent of pile strength	yes
Mechanical	Pogonowski Splice	100 percent of pile strength	100 percent of pile strength	100 percent of pile strength	yes

As it was shown, splice types Bolognesi-Moretto, Japanese Bolted, Brunspile Connector Ring, Anderson, Hamilton Form Company, Cement-Dowel, and Mouton Splice are weak in tension. Also, Japanese Bolted, Brunspile Connector Ring, and Cement-Dowel Splice could not pass the flexural design requirement. In the following sections, various types of splices and their advantages/disadvantages are discussed.

3.2.1.1. Wedge Splices

This type of splice which is also called mechanical wedges is used mainly for square piling but it is also used for octagonal, round, and hollow cross sections. In Scandinavia and Western Europe, it is used for precast reinforced concrete piles. Also, Venuti (1980) in his research successfully employed this type of splice for precast prestressed concrete piles. Both the lower and upper part of pile to be spliced have to be the same shape (Figure 14). It is made of two plates, cone, and four internally threaded bolts. The piles internal reinforcing bars are threaded into the bolts (Figure 15). The procedure of wedge splice is simple. The alignment cone is placed into the center of the lower pile. The upper pile section then is placed on the lower part till the splice plates are in their correct position. After that, the wedges are driven into each of the four corners of the splice by using a sledgehammer. The wedge become locked in the splice. This detail applies directly to reinforce concrete piles. However, with some modification, i.e., pre-installation of auxiliary bars inside the pile, it can also apply to prestressed piles.

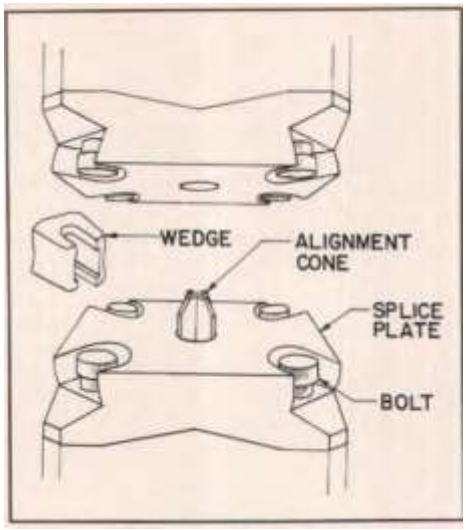

Figure 14: mechanical wedge splice (Venuti, 1980)

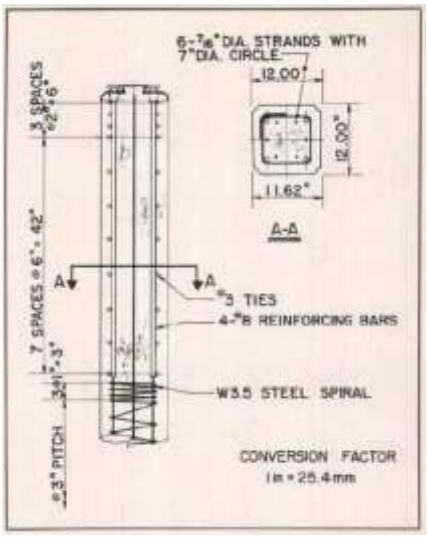

Figure15: mechanical wedge splice details (Venuti, 1980)

According to the investigation of Venuti (1980), this type of splice is designed to perform similar to un-spliced section in compression, tension, torsion, shear, and bending. After experimental testing on this type of splice, he concluded that wedge splice; 1- can develop the full capacity of the pile in tension, compression, and bending, 2- has the same strength for both the torsion and shear in all direction 3- requires minimum space for storage, 4- can be fabricated and handled simpler and faster since the splice parts are the same in each plie section, 5- can be installed easily and quickly and does not need skilled labor forces, 6- due to having zinc alloy alignment cone has a sacrificial role and improves corrosion resistant. The only disadvantage of using this splice is the need for careful and quality fabrication at a prestressing plant.

3.2.1.2. Welded Splices

One of the problems with using welded splices is its corrosion potential, especially in corrosive soils and marine environment. Also, the lack of certified field labor and concerns with the quality of field welds have limited the use of welding systems (Michael P Culmo, 2009). Figure 16 shows welding of pile segments in welded splice (Li et al, 2014). Nippon Concrete Systems (NCS) type welded splice is a very common type of welded splice in the State of Washington. Tokyo splice can be used in prestressed concrete cylindrical piles. Also, temperature due to welding does not seem to affect concrete and the strength will not be reduced. Raymond splice can also be used in cylindrical piles. However, its use is limited due to longer time for installation. The last type of welded splice is Bolognesi-Moretto which is not common because the use of dowel in the plate causes warping (Bruce Jr & Hebert, 1974a).

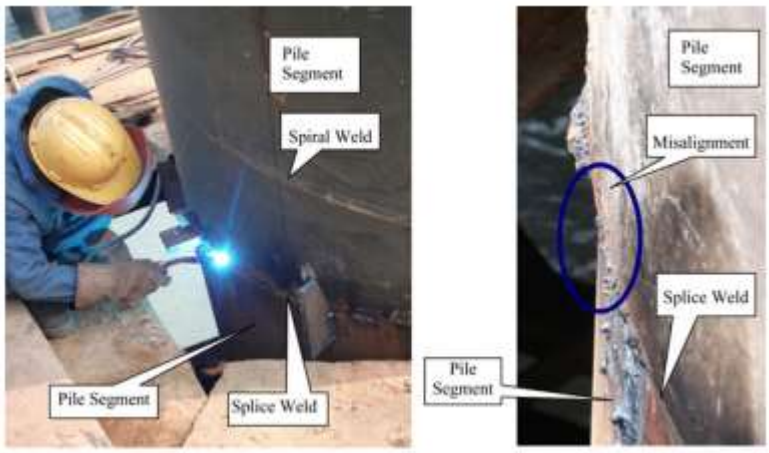

Figure 16: welded splice (Li et al., 2014)

3.2.1.3. *Dowel Splices*

The most common type of pile spliced used in the state of Florida is dowel splices. In this type of splice, holes are cast or field drilled into the top of the pile segment driven into the ground. Rebar dowels which are protruding of the end of the top pile segment are placed into the holes of the bottom pile and filler/bonding material is used to fill the spaces around the dowels in the holes and to bond them to the lower segment (Figures 17,18)(Wu, 2016). Dowel rebars can be made of conventional carbon steel or Stainless Steel (SS), Carbon Fiber Reinforced Polymer (CFRP) or Glass Fiber Reinforced Polymer (GFRP). Different types of resin and cement can be used as filler and bonding agent to connect the piles section. The setting time and the amount of strength that can be resisted by the filler and bonding materials should be considered in choosing (Bruce Jr & Hebert, 1974b; Canner, 2005). Installation of this type of splice causes the construction delay since it requires the top section of pile to be held till the filler or bonding materials cure. Epoxy is the most common type of bonding material that is used for PPCP splices. There have been efforts to decrease the curing time of epoxy (Navaratnarajah, 1981). Also, it is realized that some filler and bonding materials that are effective require more setting time. One of these materials which is under investigation by the FIU and UF researchers on ABC-UTC projects is non-proprietary UHPC. The bond strength of bars (No. 8 and No. 11) embedded with UHPC is 8 times of the bond strength between bars and conventional concrete (Tazarv & Saiidi, 2017). It is also realized that time to set and time to achieve desirable strength may be a challenge for the use of UHPC.

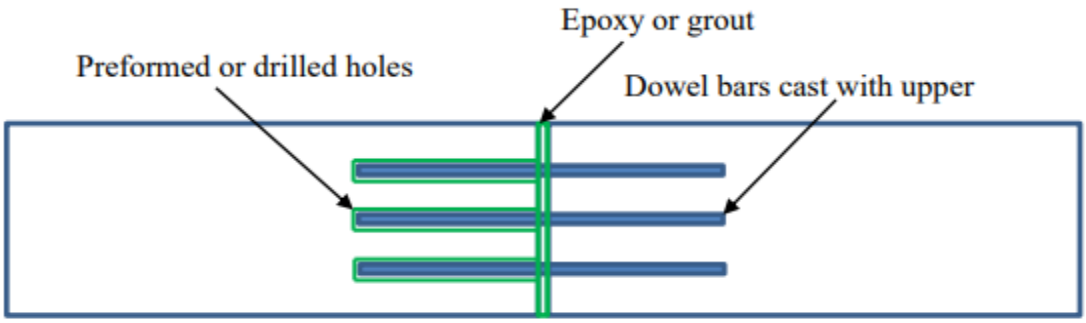

Figure 17: Dowel splice (Wu, 2016)

A: Step 1: Inserting dowel rebars B: step 2: Filler or bonding material C: Step 3: Final installation

Figure 18: Dowel splice process at Econfina River Bridge in Taylor County, Florida

3.2.1.4. Sleeve Splice

In this method, between two segments of voided piles, a steel tube is inserted (Cook & McVay, 2003). The steel tube is grouted to the pile for bond and transferring the load (Figure 19). Also, for improving the bond between the steel tube and the pile segments, spiral bars are welded to the steel tube. The required time for establishing the sleeve splice depends on the time needed for grout to reach the desired strength. The grout should reach the required strength before driving, otherwise, driving will fail (Wu, 2016).

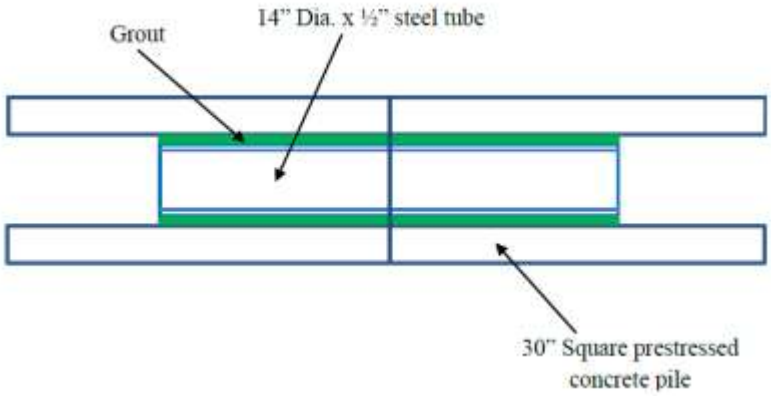

Figure 19: Sleeve splice (Wu, 2016)

3.2.1.5. Mechanical Splices

Mechanical splice has been considered as the most economical type of splices. It needs minimal installation time, can provide good flexural and tensile capacity (500-1000psi tensile) and can develop full bending capacity. In general, there are several types of mechanical splices that can be used. One type of mechanical splice, often with octagonal PPCS, uses steel caps, one male and one female. At the end of the each pile matching holes or grooves are devised. The steel caps are mechanically connected with high strength steel pins inserted into the holes. (Figure 20) (Mullins & Sen, 2015).

Figure 20: Mechanical splice (Mullins & Sen, 2015)

In 1990, Gamble and Bruce investigated another type of splice called ABB splice. They experimentally investigated the behavior of ABB splice under different loading conditions and found that this splice which previously was used for shorter piles, can be used to extend piles to longer lengths. ABB splices are used often for square piles (Gamble & Bruce Jr, 1990) (Figure 21). In the late 1990s, GYA mechanical splice was developed (Figure 22) that is made of two steel caps, four grooved pins and four holes. This type of splice has performed well in load tests and is currently used in many projects (Korin, 2004).

Figure 21: ABB splice

Figure 22: GYA mechanical splice (Korin, 2004)

3.2.1.6. Grouted Post-Tensioning Duct Connections

Recently, a new splice system was proposed by G. Mullins and R. Sen (2015) that used post-tensioning to establish the pile splice. In grouted post-tensioning duct connections, protruding reinforcements from one prefabricated element are embedded into the post-tensioning ducts cast at the end of the receiving prefabricated element. The duct is then filled with grout. The main difference between this splice with grouted coupler is that the reinforcing steel is not spliced but bonded to concrete. The mechanical coupler is a structural member. The role of grout is to transfer the force from the bar to the coupler. However, the grouted duct is a non-structural member that transfers the force from the reinforcement to the surrounding concrete. There have been much research that investigated the grouted post-tensioning duct connection. The research

has shown that using duct reduces the development length of bars in mass concrete. Also, it decreases the probability of cracking in the element at the ultimate load (Michael P Culmo et al., 2017).

G. Mullins and R. Sen (2015) after reviewing all the pile splices, proposed an alternative method to splice post-tensioned pile segments (Figure 29). In this splice system, the embedded anchorages are cast into the ends of splice pile segments where the stress due to post-tensioning was localized (Figure 30). This embedded anchorage provides the concrete near the end of pile segments with tensile capacity provided by the post-tensioning process. This type of splice like Macalloy (see Table 2) splice is established by post-tensioning of the strands.

Figure 29: Alternative method to splice post tensioned pile segments (Mullins & Sen, 2015)

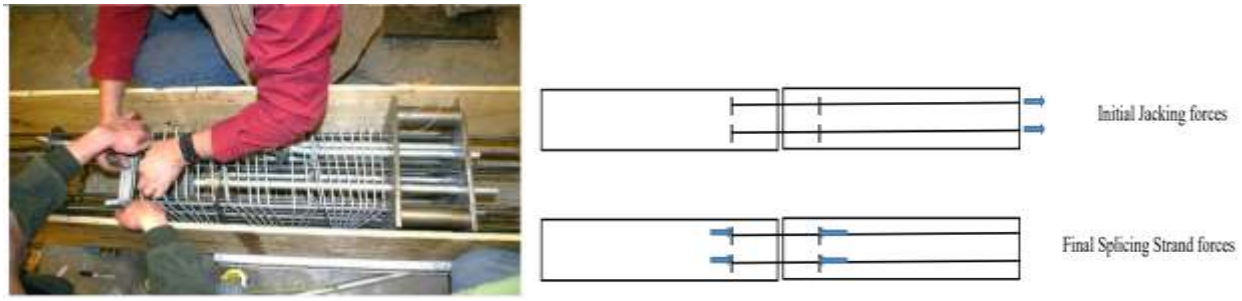

Figure 30: Embedded anchorages (Mullins & Sen, 2015)

G. Mullins and R. Sen (2015) performed numerical modeling, laboratory testing, a full-scale bending test, and a pile-driving demonstration using their proposed spliced pile. To investigate the performance of the proposed splice system, scaled specimens that included four 20ft-long, 14-inch square piles were constructed, spliced, and tested in bending (Figure 31). They found that the cracking moment was unaffected by the splice indicating that the splice was successful in transferring the tensile capacity. Based on the lessons learned from scaled specimens test, full-scale testing was also conducted. Three, 40ft-long piles were spliced and tested in bending (Figure 32). The results again indicated that the proposed splice system could provide the piles

with the same cracking moment and 96% of the ultimate moment of the un-spliced pile. For the final part of their research, 100ft-long spliced pile specimens were constructed and driven at the field to assure the feasibility of the splice system (Figure 33). They concluded that the developed splice system could effectively restore the full capacity to withstand pile driving installation and structural loading. They also indicated that the spliced system can be practiced in the marine environment since the concrete cover provides full protection against corrosion for strands.

Figure 31: Bending testing of scaled spliced pile specimen (Mullins & Sen, 2015)

Figure 32: Bending testing of full-scale spliced pile specimen (Mullins & Sen, 2015)

Figure 33: Pile driving using spliced pile specimen (Mullins & Sen, 2015)

3.2.2. Other Pile Splices under Development

In 2019, FDOT initiated an investigating on the behavior and effectiveness of epoxy dowel splice, experimentally and analytically, for prestressed precast concrete piles using corrosion resistant material for dowels (SS, CFRP, and GFRP), and comparing their performance to conventional carbon steel dowel splices. This investigation is being performed by researchers at Florida International University (FIU). They are investigating the effectiveness of GFRP dowels to economically substitute other corrosion-resistant dowels (Mehrabi & Farhangdoust, 2019).

3.3. ABC Connections with Potential for Using in Piles

There has been a large amount of research in relation with joints and connections in Accelerated Bridge Construction (ABC), and many types of joints are implemented successfully and perform well (Khedmatgozar Dolati & Mehrabi, 2021). Some of these connections are used for connecting columns to pier caps, columns to footing, or column segments to each other. These concepts can be adopted or modified for pile splices. Table below summarizes some of the available concepts for connecting ABC columns.

Table 3 Different connections of cap beam and column (Mehrabi, A.B., and Torrealba, 2019)

Type	Connection method	Usage
Formed in cap beam	Grouted sleeve	-Connect precast cap beam to cast-in-place or precast concrete column
	Grouted pocket	-Connect precast cap beam and precast or cast-in-place concrete column -Connect precast cap beam and steel pile or column
Formed along the Columns	UHPC column segment	-Connect precast cap beam and precast concrete column
	Grouted sleeve	-Connect precast cap beam and precast concrete column
	Mechanical couplers	-Connect precast column to cap beam
Other types	Welding	-Connect precast cap beam and steel pile or column
Cap beam segments	Closure pour	-Connect precast cap beam segments
	Mechanical couplers	-Connect precast cap beam segments to create moment connection

Following describes some of ABC connections with more relevance to pile splices. Figure 23 shows an example of grouted sleeve connection for column to cap formed inside the cap (left) and a grouted sleeve connection for column to footing connection (right). The concept of mechanical couplers perhaps is closer to the application to pile splices. Figure 24 shows connection of column to footing using mechanical coupler and a series of commercially available

couplers. This type of coupler has been used also for connecting column segments and therefore, conceptually applicable to pile splices. One challenge in adopting these concepts would be their corrosion resistance that is a major issue for pile performance especially in the marine environment. Hence, emphasis should be on the use of alternative material to establish such connections. Use of corrosion resistant materials such as stainless steel (SS) and fiber reinforced plastics (FRP) has been investigated broadly and showed promising to be included in precast elements that are exposed to harsh and corrosive environment. Accordingly, these materials will be considered in this study for reinforcement as well as for establishing mechanical connections. SS material has been incorporated in almost all types of reinforcing and prestressing elements and therefore can establish forms, mechanisms and systems equivalent to conventional carbon steel. It has also been attempted widely to create shapes and mechanisms for FRP material so that they can be used as replacement to carbon steel. To this end, bars, strands and various profiles have been introduced. FRP threaded rods and fasteners are also becoming more available. Figure 25 shows some of these products that are available in the market. Production of FRP elements are quite versatile and can be adjusted to the project details if needed. These elements can be configured to accommodate connections similar to grouted sleeve and other mechanical connections for pile splice. This way, both strength and durability can be provided for piles and pile splices in corrosive environment. In the following mechanical couplers and grouted post-tensioning connections are discussed further.

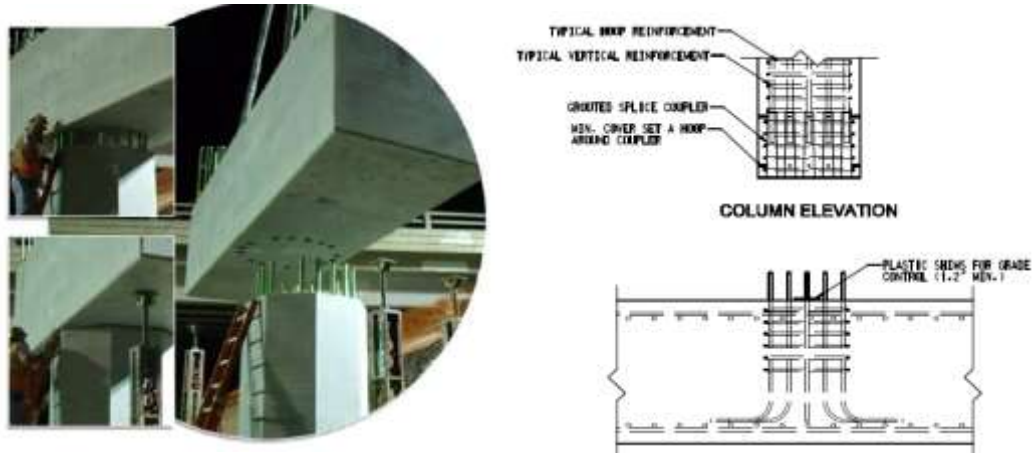

Figure 23: Grouted sleeve connection for column to cap (left- (Roddenberry & Servos, 2012)) and column to footing (right-(M P Culmo, 2009))

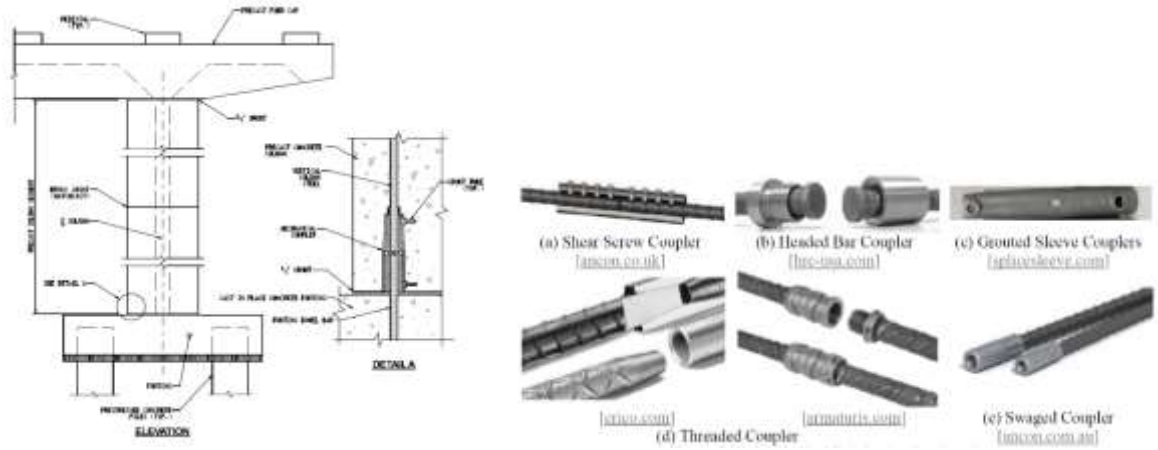

Figure 24: Mechanical coupler connection for column to footing (M P Culmo, 2009; Michael P Culmo et al., 2017)

Figure 25: FRP bars, bolts and fasteners

3.3.1. Mechanical Couplers

Prefabricated elements are often joined by splicing steel reinforcement. Joining prefabricated elements can therefore be performed using mechanical splicer. According to the AASHTO LRFD Bridge Design Specifications, mechanical bar splices, also called couplers should provide 125% of the specified yield strength of the bars which are connected to (Michael P Culmo et al., 2017). Several types of couplers are in the market (Figure 26). In general, they are divided into five categories (Figure 27). These are: (a) shear screw couplers, (b) headed bar couplers, (c) grouted sleeve couplers, (d) threaded couplers, and (e) swaged couplers. Shear screw splice is made of lock shear screw, shear rails, and coupling sleeve. Equal length of bars is placed into the sleeve, then the screws are tightened till the heads of screw shear off. In headed bar couplers, the plated end of bars are encased in sleeves that are threaded into each other. In grouted sleeve, two bars are connected to each other by placing them into a steel sleeve. Then the sleeve is filled with grout. In one version of grouted sleeve splice, the length required for coupler is reduced by threads inside the sleeve. In threaded couplers, the threaded bars are installed in a coupler with matching internal threads. Both straight and tapered threads can be used for the bar. In swaged coupler, straight bars are connected to pressed steel sleeve (Tazarv & Saiidi, 2016). The most

common type of mechanical couplers are grouted splice couplers. They transfer loads between bars based on the grout filled device. The load is transferred between the bars by the coupler. They have been used to connect prefabricated elements. One prefabricated element has the role of host. There are holes at the face of the host element to receive the protruding bars from the element to be connected. The connection between the host and the joining element is established when the bars are inserted into the sleeves and filled with the grout (Figure 28). Pouring the grout in the sleeve can be performed before the positioning of the bars, referred to pre-grout, or it can be done after placing the bars in the sleeve by use of grout pump (Michael P Culmo et al., 2017).

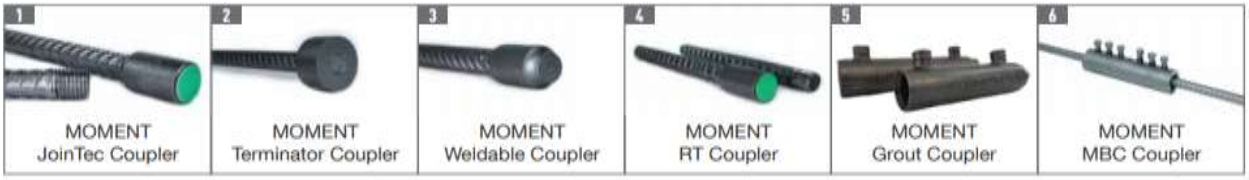

Figure 26: Mechanical couplers in market (Nvent)

(https://www.nvent.com/us/en/products/concrete-reinforcing-steel-connections.html**)**

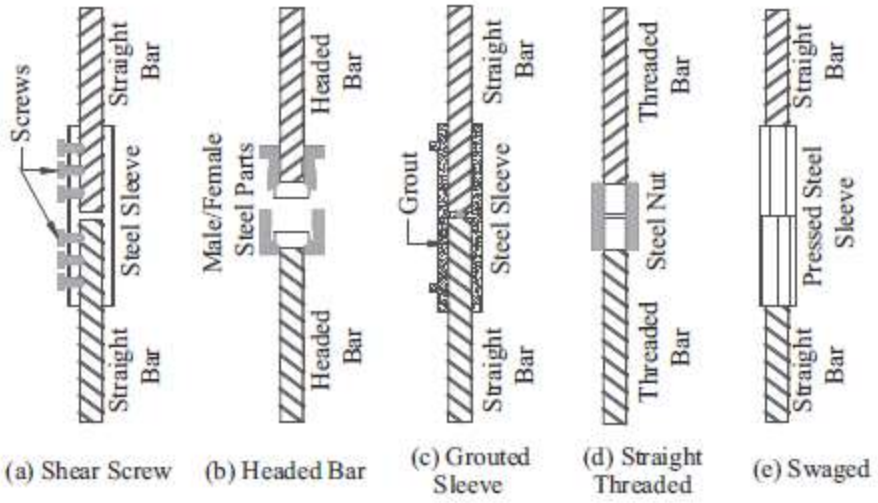

Figure 27: Types of mechanical couplers (Tazarv & Saiidi, 2016)

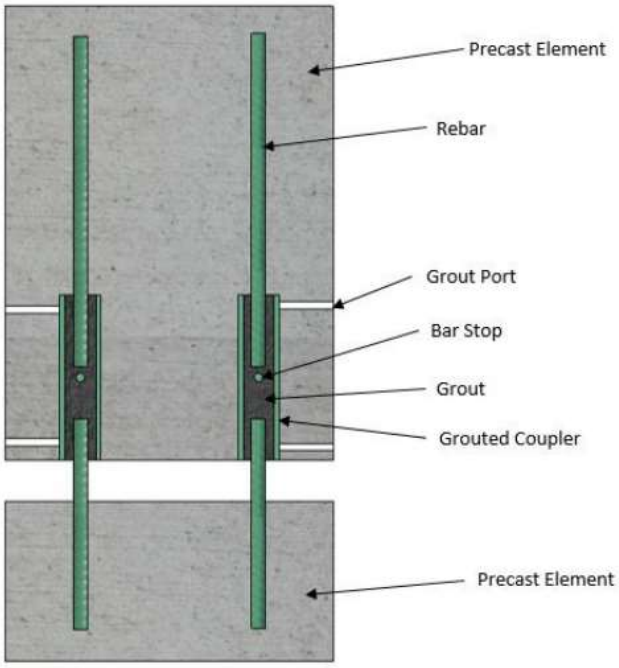

Figure 28: Grouted coupler in precast element (Redd, 2016)

3.4. Filler or Bonding Material

Regardless of what configuration are used for connecting precast-prestressed pile segments, some kind of material is needed to perform as bonding, filler or coating agent. Different types of cement and resin are used as filler or bonding materials at the connection of the precast concrete structures. The properties that are of utmost importance for choosing proper grouts to be used in connections are durability, strength, and constructability. These properties are tabulated in Table 4 (Scholz et al., 2007).

Table 4: General grout properties (Scholz et al., 2007)

Strength	Durability	Constructability
Compressive	Shrinkage	Work Time
Tensile	Freeze/Thaw	Set Time
Bond	Sulfate Resistance	Flow
	Chloride Ingress	

Filler or bonding materials shall provide the required strength for members; otherwise, premature failure will be observed. Reaching required strength is defined as their ability to provide adequate resistance for both compressive and tensile stress in a structural element.

In ABC, since one of the goals is to accelerate constructions as much as possible, the rapid strength gain for the filler or bonding materials is of importance. Most grouts used for highway patching are rated for compressive strength of 2500 psi in two hours. Initial set time is the parameter used to compare the rapid strength of grouts, although work time should be taken into account to see the feasibility of pouring the grout. Work time is defined as a time interval between the start of mixing until workability begins to decrease. Decreased workability is deemed the inability to move a grout by vibration. If the work time is too short, the pouring of grout in the connections/joints will be a problem. There is a linear relationship between work time and initial set time, measured from the start of mixing until the product shows resistance to the penetration of a thin rod (Scholz et al., 2007). Quite a bit of research has been conducted to find bonding materials with proper constructability features. In the following sections, recent research on cement and polymer grout as well as epoxy resin will be reviewed and analyzed according to their constructability, durability, and strength.

3.4.1. Cement grout:

Vasumithran et al. (2020) investigated the effects of incorporating fillers such as fine sand and fly ash in cement grouts to improve their constructability and evaluated the flowability as well as mechanical properties of the proposed mixes. They replaced 10 percent of cement mass with silica fume and up to 50 percent of cement mass with filler materials in certain mixes. Table 5 shows certain mixes of grout specimens. SF, FS, FA, and SP stand for silica fume, fine sand, fly ash, and superplasticizer, respectively.

Table 5: Mix proportion details (in kg/m3) (Vasumithran et al., 2020)

Mix type (W/C)	Cement	SF	FS	FA	Water	SP
M0(0.35)	1458.6	–	–	–	510.5	5.8
M1(0.25)	1536.9	170.8	–	–	426.9	23.8
M1(0.3)	1416.1	157.3	–	–	472.0	13.7
M1(0.35)	1312.8	145.9	–	–	510.5	7.6
M1(0.4)	1223.5	136.0	–	–	543.8	2.4
M2(0.3)	865.7	96.2	961.9	–	288.6	19.2
M2(0.35)	825.9	91.8	917.8	–	321.2	14.7
M2(0.4)	789.7	87.8	877.5	–	351	8.8
M3(0.6)	673.9	74.9	–	748.7	449.2	13.5
M3(0.65)	649.6	72.2	–	721.7	469.1	11.5

Their findings indicate that increasing the water-cement ratio (w/c) causes; 1-low mechanical strengths, 2- long setting time, 3-grout instability, and 4-excessive bleeding. The results of the set time and compressive strength of the investigated various grout mixes are summarized in Figures 34 and 35.

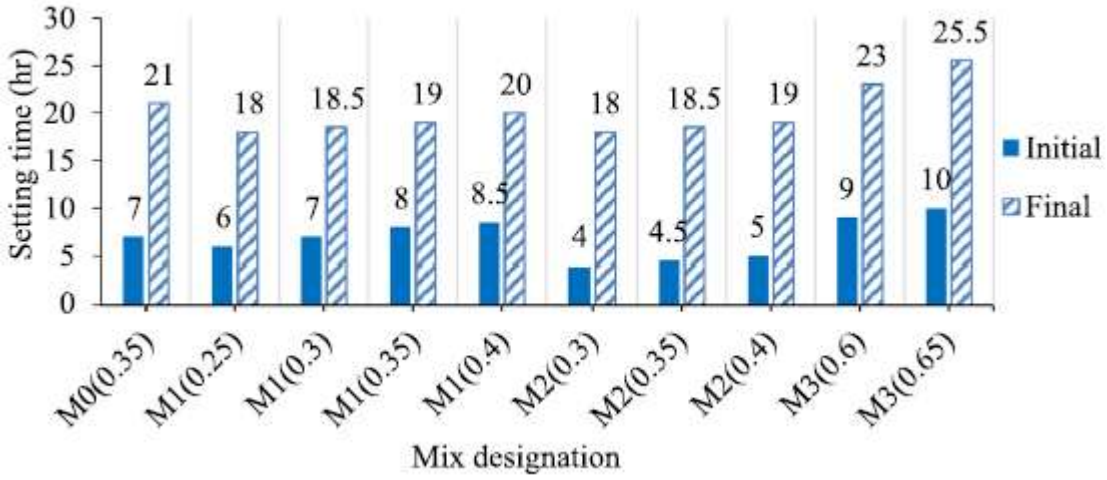

Figure 34: Setting time of the selected grout mixes (Vasumithran et al., 2020)

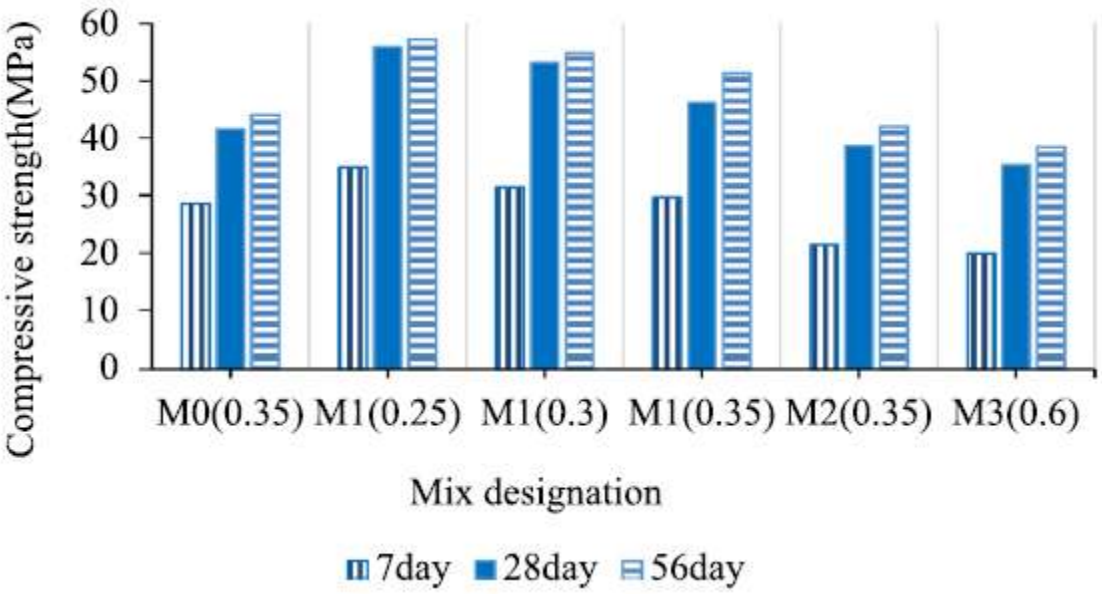

Figure 35: Compressive strength of various grout mixes (Vasumithran et al., 2020)

They also concluded that grouts with fine fillers have a better performance in shrinkage and water absorption, and that fine fillers can be a proper replacement to cement since it increases the durability of grouts. They noted that replacing levels of cement with supplementary cementitious materials should be chosen wisely not to affect strength and durability properties. Otherwise, the high volume concentration of fillers in grouts can reduce the compressive strength dramatically (Vasumithran et al., 2020).

From the work by Vasumithran et al., it can be concluded that M2 grouts (see Table 5) have the least setting time, both initial and final, and as the w/c ratio increases, the setting time increases. The setting time for M2 with w/c equal to 0.3 is less than the mixes with w/c of 0.35 and 0.4 (Figure 34). Additionally, according to the Figure 35, M1 grouts have the highest compressive strength, and as the w/c increases the compressive strength decreases; the compressive strength for M1 with the w/c equal to 0.25 is more than that type of grout with the higher w/c of 0.3.

Jansson (2008) investigated the impact of two types of grout, Erico HY10L and Nissco SS Mortar, used for mechanical reinforcement splices (Figure 36). HY10L is a non-shrink metallic grout. Small steel fragments are used in the grout to improve the ductility of the hardened product. He found that the working time for HY10L is 25 to 30 minutes. After testing three specimens, their compressive strength was measured as reported in Table 6 (Jansson, 2008).

Figure 36: Grout specimens (Jansson, 2008)

Table 6: Grout compressive strength in psi for Erico HY10L (Jansson, 2008)

	24 hours	3-Day	7-Day	28-Day
Specimen 1	6,500	9,550	11,630	14,150
Specimen 2	6,550	9,580	11,750	15,000
Specimen 3	6,500	9,600	10,880	14,950
Average	6,520	9,580	11,420	14,700

Nissco SS Mortar is a non-shrink nonmetallic grout, and the working time was measured to be 40 minutes at 70 degrees Fahrenheit. The grout compressive strength for three specimens (2x2 in.) was reported and summarized in Table 7.

Table 7: Grout compressive strength in psi for Nissco SS Mortar (Jansson, 2008)

	24 hours	3-Day	7-Day	28-Day
Specimen 1	7,320	11,500	15,000+	15,000+
Specimen 2	7,520	11,380	15,000	15,000+
Specimen 3	7,220	11,330	15,000+	15,000+
Average	7,350	11,400	15,000+	15,000+

Splice sleeve Japan Inc. also introduced SS Mortar as a filler material for NMB splice sleeve. The advantages of applying this type of grout are; 1- high early strength, approximately 30 N/mm2 in 24 hours, 2-high ultimate strength, approximately 100 N/mm2 in 28 day, 3-flowability, and 4- not having significant shrinkage. Examples of the test results, based upon ASTM tests (Figure 37), for fresh SS Mortar and hardened SS Mortar are shown in Tables 8 and 9.

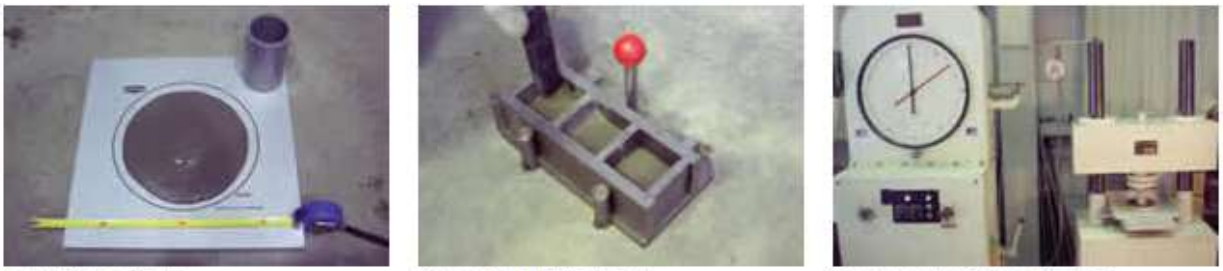

Figure 37: Compressive strength and flowability tests

(http://splicesleeve.com/ssj/ssmortar.html)

Table 8: Test result for fresh SS Mortar

(http://splicesleeve.com/ssj/ssmortar.html)

Amount of water (per bag)	Consistency (Dia. by Flow table)	Mixed temp.	Curing temp.	Bleeding ratio	Setting time (Hour-Min.)	
					Initial	Final
2.2 litters	180 mm	20°C	5°C	0%	9-31	13-35
			20°C	0%	4-18	5-55
			30°C	0%	2-23	3-20

Table 9: Test result for hardened SS Mortar

(http://splicesleeve.com/ssj/ssmortar.html)

Consistency (Flow table)	Curing temp	Compressive Strength (N/mm^2)					
		12 hrs	18 hrs	1 day	3 day	7 day	28 day
180 mm	5°C	-	4.0	10.1	42.2	56.5	86.3
	20°C	5.6	20.2	30.5	55.2	71.1	100
	30°C	18.5	36.0	49.0	68.5	79.1	101

As it is shown, the setting time of SS mortar at 30 degrees centigrade is approximately 2 hours and, as the temperature decreases, the setting time increases. In 5 degrees centigrade, it reaches approximately 9 hours. Also, the compressive strength of SS mortar in 30 degrees centigrade is approximately 101 Pascal in 28 day, and as the temperature decreases, the compressive strength decreases. The temperature is an important factor affecting the properties of grouts and should be considered in the construction.

In 2007, Potter experimentally investigated the sensitivity of grouting material to installation process. In his research, 6 NMB sleeve splices with a #9 Grade 60 bar were constructed and

filled with SS mortar (Figure 38). Half of the tested specimens were representative of poor grouting material, in that the grout material was not rodded. Others were representative of proper grouting materials since they were rodded with a 1/8" diameter wire, 10 times for a depth at least ¾ of the splice sleeve. The tensile test was applied to the specimens to find the effect of rodding on the SS mortar performance. The results indicated that rodding of SS mortar in the splice system might not affect the tensile strength of the splice system as long as sufficient amount of SS mortar is used and the placement of rebar is adequate.

Figure 38: NMB sleeve splices setup for testing the sensitivity of grout (Potter, 2007)

Varga et al. (2014) investigated 7 pre-bagged grouts used in the construction industry (Table 10).

Table 10: Grout used in the investigation (De la Varga & Graybeal, 2015)

Grout category	Solids specific gravity[a]	Nomenclature[b]
Nonmetallic cement-based	2.93	C1 - 0.16
Nonmetallic cement-based	2.93	C2 - 0.18
Nonmetallic cement-based	2.68	C3 - 0.17
Metallic cement-based	3.16	C4 - 0.167
Fly ash-based	2.84	F1 - 0.08
Epoxy-based	2.62	E1 - fluid[c]
Magnesium phosphate-based	2.59	M1 - 0.08
Ultrahigh-performance concrete	2.78	U1 - 0.18

[a]Specific gravity of the solids fraction measured using a gas (He) pycnometer.
[b]Grout nomenclature followed by the w/s used for each of the grouts.
[c]The supplier of E1 recommends two formulations: dry and fluid. In this study, the fluid formulation was used.

The results of their investigation on flowability and setting time are summarized in Table 11. Also, the results of the compressive strength of the grout cubes are summarized in Table 12.

Table 11: Flow Measurements Using ASTM C1437 Methods(Standard, 2013), Time of Set (ASTM 2008b), and Fresh Air Content (A. ASTM, 2014)

Grout	Number of drops	Flow at 5 min (%)[a]	Flow at 15 min (%)[a]	Final time of set (ASTM C403) (h)	Air content (ASTM C231) (%)
C1- 0.16	5	112	106	7.7	3.4
C2- 0.18	5	117	84	6.8	5.1
C3- 0.17	5	111	100	10.3	12
C4- 0.167	5	110	91	6.8	3.6
F1- 0.08	5	101	109	0.7	4.6
E1- fluid	N/A[b]	N/A[b]	N/A[b]	3.5	8.5
M1-0.08[a,c]	5	115	75	0.4	6.9
U1- 0.18	5	N/A[d]	>125	6.9	3.2
a	Flow slightly changes depending on mixer used. These values were measured using a medium-sized Univex mixer				
b	Material sticks in mold. Test cannot be performed.				
c	Flow was measured at 2 and 5 min because of final setting time limitations				
d	Flow was measured only at 15 min because of mixing time requirements.				

Table 12: Compressive strength results for grout cubes (De la Varga & Graybeal, 2015)

	Average compressive strength (MPa)					
Grout	4 h	8 h	1 day	3 days	7 days	28 days
C1- 0.16	___a	___a	30.5 (0.83)[b]	48.9 (2.21)	52.14 (1.17)	67.6 (2.00)
C2- 0.18	___a	___a	25.6 (0.41)	41.1 (0.90)	45.1 (0.97)	50.2 (2.35)
C3- 0.17	___a	___a	16.6 (0.48)	26.2 (0.76)	35.5 (0.21)	43.7 (0.41)
C4- 0.167	___a	___a	34.6 (0.76)	49.3 (1.52)	60.9 (0.07)	67.6 (1.52)
F1- 0.08	31.1 (0.21)	34.6 (1.38)	34.9 (1.04)	44.0 (0.90)	55.5 (1.04)	56.1 (0.35)
E1- fluid	___a	8.42 (0.14)	56.1 (1.45)	73.6 (0.35)	77.3 (0.41)	93.5 (3.24)
M1- 0.08	32.0 (2.07)	31.3 (0.41)	43.0 (2.14)	44.9 (1.93)	44.2 (1.24)	54.0 (2.35)
U1- 0.18	___a	___a	93.15 (0.28)	129.7 (3.45)	132.1 (1.59)	170.4 (0.90)
Note:	1 Mpa = 145 psi.					
a	Material had not set yet, or it was still to be tested.					
b	Numbers in parentheses indicate one standard deviation in Mpa as determined for three replicate specimens tested at each age.					

In their investigations, they also studied the shrinkage behavior of the grouts and found that although some grouts are referred to as non-shrink materials, the shrinkage was observed in most of them, especially in dry ambient conditions. The internal curing was introduced as an effective method in decreasing the shrinkage.

From their work, it can be concluded that UHPC and epoxy-based grouts have the highest compressive strength compared to others. Also, in terms of setting time, fly ash-based and magnesium phosphate-based grouts have the lowest setting time.

Scholz et al. (2007) conducted a thorough research on 8 types of grouts to develop a performance specification for grouts that fill the haunch between the top of a beam and the bottom of a deck panel (Figure 39). Standard or modified ASTM tests were used to determine the material properties of the 8 types of grout. The mix information of the candidate grouts is included in Table 13 (Scholz et al., 2007).

Figure 39: The tests for grouts that fill the haunch between the top of a beam and the bottom of a deck panel

Table 13: Candidate Grouts and Mixing Information (Scholz et al., 2007)

	ID No. and Product Name	Mixing Quantities per 50-lb, Bag					
		Initial Water, pints	Additional Water, pints	Aggregate Extension, % by weight	Aggregate Extension, lb	Yield Volume, cu. ft.	Cost per bag, $
Neat Grout	1. ThoRoc® 10-60 Rapid Mortar	5.50	1.00	0	0	0.43	12.75
	2. SikaQuick® 2500	5.00	0.50	0	0	0.43	13.75
	3. Five Star® Highway Patch	5.00	1.00	0	0	0.40	20.50
	4. Set® 45 Hot Weather	3.25	0.50	0	0	0.39	24.00
Extended Grout	5. ThoRoc® 10-60 Rapid Mortar	5.50	1.00	50	25	0.57	12.75
	6. SikaQuick® 2500	5.00	0.50	50	25	0.60	13.75
	7. Five Star® Highway Patch	5.00	1.00	80	40	0.66	20.50
	8. Set® 45 Hot Weather	3.25	0.50	60	30	0.58	24.00

As shown in Table 13, from the eight types of grouts investigated, four of them were neat grouts, and others were extended grouts. In the extended grouts, a third-eighth inch pea gravel extension was used. The ASTM tests were conducted to find the compressive as well as tensile strength ((C. ASTM, 2002),(C. ASTM, 1996)), bond strength with concrete (C. ASTM, 1999) (Figure 40), flowability (C. ASTM, 2001) (Figure 41), work time as well as set time (ASTM C 230), and shrinkage behavior (Materials, 1999). Also, the effect of extension on grouts was investigated.

Figure 40: Bond strength test between grout and concrete (Scholz et al., 2007)

Figure 41: Flowability test

Tests results of compressive strength for the 8 grouts in one and two hours as well as one and 7 day are presented in Figure 42.

	Grout	Compressive Strength, psi			
		1 hr.	2 hr.	1 day	7 day
1	ThoRoc® 10-60	**2700**	**3030**	**5210**	**6380**
2	SikaQuick® 2500	1700	2250	3540	4710
3	Five Star® Patch	910	2810	5080	5820
4	Set® 45 HW	420	2050	4930	4930
5	ThoRoc® extended	**1860**	2370	3150	5040
6	SikaQuick® extended	1020	1170	1900	2550
7	Five Star® extended	-	**2730**	**4490**	**5440**
8	Set® 45 HW extended	-	230	2650	4180

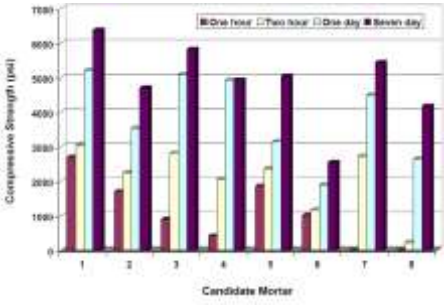

Figure 42: Compressive Strengths per ASTM C 109

Scholz et al. (2007) concluded that most grouts reached 2 Ksi in the first two hours. ThorRoc10-60 (1) had the highest compressive strength among all both in the first hour and after 7 days.

Also, the pea gravel extension reduced the compressive strength of the neat grouts. Based on ASTM C 109, a product shall meet the following requirements for compressive strength (Scholz et al., 2007):

- 1 hour: No strength
- 2 hour: Determined by engineer-of-record based on construction procedure.
- 1 day: Minimum 4000 psi
- 7 day: Minimum 5000 psi

Accordingly, ThorRoc10-60, the neat grout; Five Star Patch, both neat and with extension grouts; Set 45 HW, the neat grout meet the requirements.

Tests results for tensile strength for the grouts in one and 7 days are presented in Figure 43.

	Grout	Tensile Strength, psi	
		1 day	7 day
1	ThoRoc® 10-60	385	**540**
2	SikaQuick® 2500	255	340
3	Five Star® Patch	**485**	530
4	Set® 45 HW	380	410
5	ThoRoc® extended	410	510
6	SikaQuick® extended	280	335
7	Five Star® extended	**445**	**555**
8	Set® 45 HW extended	330	415

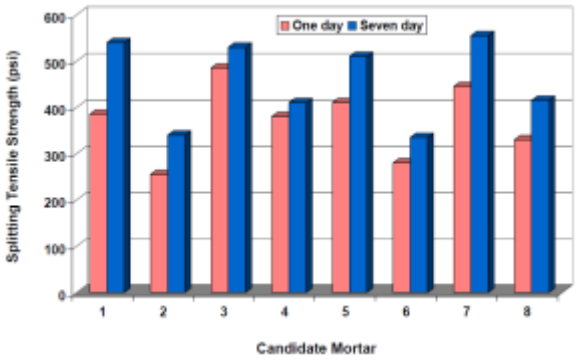

Figure 43: Splitting Tensile Strengths per ASTM C 496

Scholz et al. (2007) found that each candidate grout reached a 200 psi split tensile strength on the first day (Figure 43). In 7 days, all of them except Sika Quick 2500, both neat and extended, reached at least 400 psi split tensile strength. Based on ASTM C 496, a product shall meet the following criteria for the splitting tensile strength (Scholz et al., 2007):

- 1 day: Minimum 200 psi
- 7 day: Minimum 400 psi

If a 7 day splitting tensile strength is not available for a product, the following criteria shall be applied:

- 28 day: Minimum 600 psi

If no splitting tensile strength data is accessible for a product, the following requirement shall be applied:

- 1 day compressive strength divided by 15 must be greater than 300 psi
- 7 day compressive strength divided by 15 must be greater than 400 psi

- 28 day compressive strength divided by 15 must be greater than 500 psi

Based on the above requirements, ThorRoc10-60, both neat and with extension grouts; Five Star Patch, both neat and with extension grouts; Set 45 HW, both neat and with extension grouts, satisfy the requirements. It also can be concluded that adding pea gravel extension has not made a tangible change in the tensile strength of products.

Tests results of shrinkage for the grouts are shown in Figures 44 and 45. These results were obtained by measuring, periodically, their shrinkage behavior over 500 days (Scholz et al., 2007).

	Grout	28 Day Shrinkage		
		in.	%	με
1	ThoRoc® 10-60	0.0076	0.076	760
2	SikaQuick® 2500*	0.0080*	0.080*	800*
3	Five Star® Patch	**0.0029**	**0.029**	**290**
4	Set® 45 HW	0.0034	0.034	340

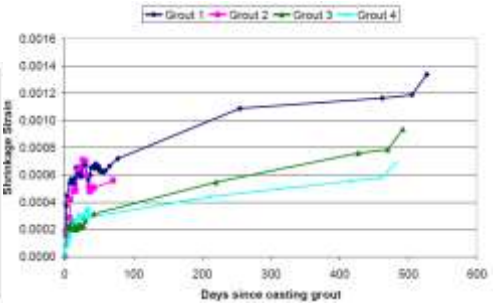

Figure 44: Neat grout shrinkage

	Grout	28 Day Shrinkage		
		in.	%	
5	ThoRoc® extended	0.0064	0.064	640
6	SikaQuick® extended	0.0089	0.089	890
7	Five Star® extended	0.0036	0.036	360
8	Set® 45 HW extended	**0.0018**	**0.018**	**180**

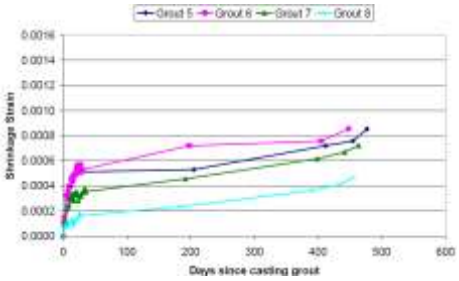

Figure 45: Extended grout shrinkage

In the shrinkage experiments, the size of the rod used in neat grouts (1 in. square cross-section bars) was different from the rod used for the extended grouts (3 in. square cross-section bars). To be able to compare these two sets of results, the ACI 209R provides correction factor (ACI-209R, 1998). The results with the correction factor are shown in Table 14.

Table 14: 28 Day Shrinkage with Volume-Surface Ratio Correction Factor (Scholz et al., 2007)

	Grout	ΔL, in.	γ_{vs}	Corrected Shrinkage, ΔL / γ_{vs}		
				in.	%	με
1	ThorRoc® 10-60	0.0076	1.165	0.0065	0.0653	653
5	ThorRoc® extended	0.0064	1.097	0.0058	0.0584	584
2	SikaQuick® 2500	0.0080	1.165	0.0069	0.0687	687
6	SikaQuick® extended	0.0089	1.097	0.0081	0.0812	812
3	Five Star® Patch	0.0029	1.165	0.0025	0.0249	249
7	Five Star® extended	0.0036	1.097	0.0033	0.0328	328
4	Set® 45 HW	0.0034	1.165	0.0029	0.0292	292
8	Set® 45 HW extended	0.0018	1.097	0.0016	0.0164	164

The shrinkage results showed that SikaQuick®2500 (2) and Five Star® Patch (3) had less amount of shrinkage than their corresponding extended grouts (6 & 7). Adding pea gravel extension increased the amount of shrinkage for ThorRoc10-60 and Set 45 HW. The effect of extension on grouts need further investigations. Based on either ASTM C 157 or ASTM C 596, a grout to be acceptable in shrinkage behavior shall meet the following criteria:

- 28 day: Maximum allowable shrinkage is 0.04% (400 micro strain)

Considering the above requirement, SikaQuick®2500 and ThorRoc10-60, both neat and with extension violate the requirements, although they are in use today.

The results of their work on the work time, initial set time in minutes are presented in Table 15 (Scholz et al., 2007).

Table 15: Candidate Grout Workability Observations (Scholz et al., 2007)

	Grout	Work Time, min.	Initial Set Time, min.	Consistency	Haunch Flow Observation
1	ThoRoc® 10-60	8	16	Thick	poor
2	SikaQuick® 2500	15	24	Medium	good
3	Five Star® Patch	18	30	Medium	good
4	Set® 45 HW	**28**	**44**	Runny	**very good**
5	ThoRoc® extended	10	19	Thick	fair
6	SikaQuick® extended	21	29	Medium	**good**
7	Five Star® extended	15	26	Thick	fair
8	Set® 45 HW extended	**24**	**35**	Medium	**good**

They found that ThoRoc® 10-60 has the shortest work time and set time among all candidate grouts. Although the short set time of ThoRoc® 10-60 seems to be beneficial for accelerating the construction, its short work time impacts negatively the flowability. ThoRoc® 10-60 is not preferable to be used in the connections/ joints with large space. However, using ThoRoc® 10-60 as filler and bonding agent in mechanical couplers can be a good option provided its

shrinkage does not make any tensile crack. It also can be concluded that adding pea gravel extension to the neat grout candidates increases their work and set time.

3.4.2. Polymeric grouts:

Mantawy et al. (2019) investigated the impact of using polymer, polymethyl methacrylate (PMMA) in place of Portland cement on the grout as filler materials (Table 16). Three tests were conducted to find the development as well as lap splice length and shear strength of the polymeric grout. The results of Polymer concrete, also called PC, were compared with ultra-high performance concrete with the mix shown in Table 17.

Table 16: Mixture Proportions of PMMA-PC (kg/m3) (Mantawy et al., 2019)

	PMMA-PC	Properties
Mixture	MMA Polymer	159.5
	Aggregate	2224.6

Table 17: Mixture Proportions of Ultra-High Performance Concrete (UHPC) (kg/m3) (Mantawy et al., 2019)

Cement	1029
Water	227.5
Aggregate (Clean Medium Sand)	910
Silica Fume	306.6
Superplasticizer (Glenium 3030 NS)	26.7

They found the minimum development length for PC in the range between 3.6 and 4.1 times of the reinforcing bar diameter that is considerably lower than the minimum development length for UHPC (Figure 46).

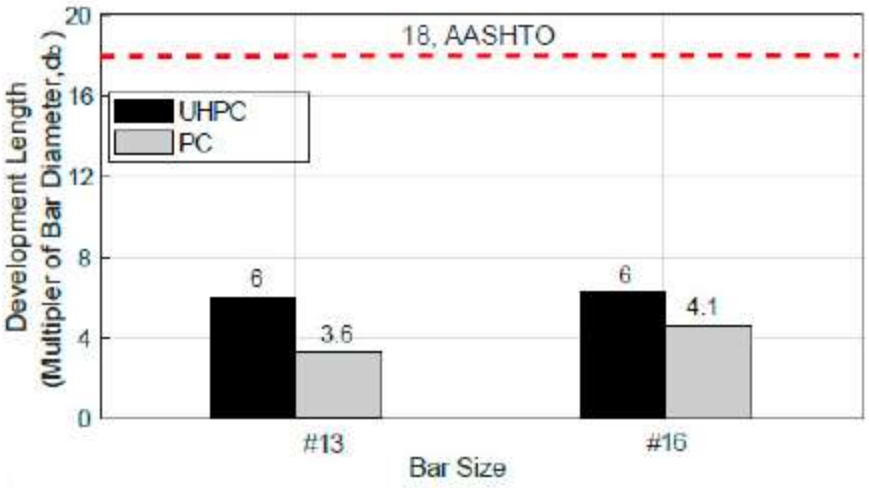

Figure 46: The comparison of minimum development length between PC and UHPC (Mantawy et al., 2019)

The minimum lap splice length needed for steel bars in PC for achieving yield stress found to be 4.1 times of the reinforcing bar diameter, whereas for the UHPC it is 4.5 times the reinforcing bar diameter (Figure 47) (Mantawy et al., 2019).

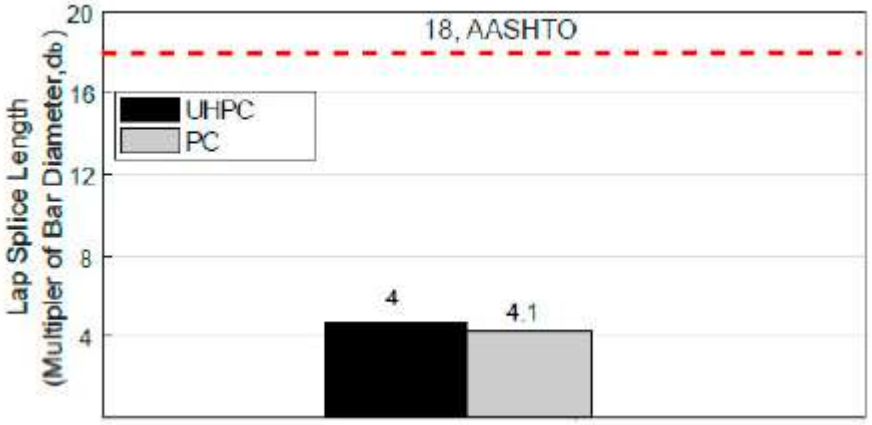

Figure 47: The comparison of minimum splice length between PC and UHPC (Mantawy et al., 2019)

Shear strength for PC was found much higher than both UHPC and normal concrete (Figure 48).

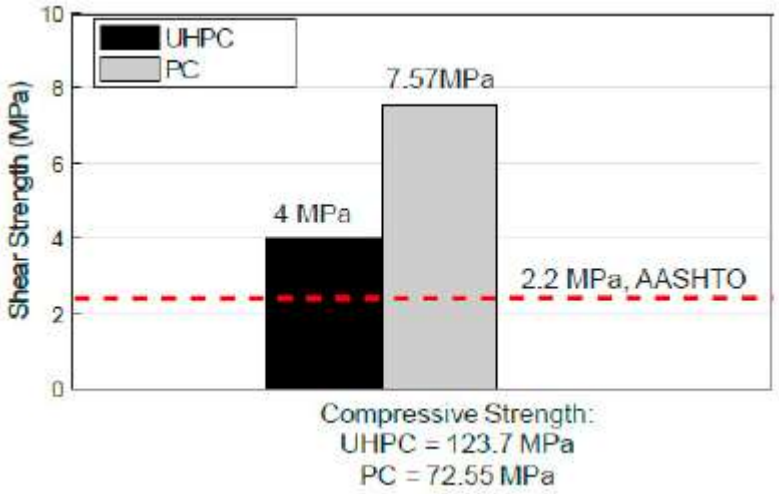

Figure 48: The comparison of shear strength between PC and UHPC (Mantawy et al., 2019)

The use of polymeric materials in grouts can effectively increase the compressive strength and reduce the required lap splice and development length.

3.4.3. Epoxy resin:

The internal stresses in cement-based bonding material are caused by the natural tendency of cement to shrink during solidification and differences in physical properties of fresh cement paste as well as hardened concrete. The internal stresses lead to circumferential tensile cracks in the surrounding concrete and thus reduce the bond strength. One solution to prevent or decrease circumferential tensile cracks is to select an adhesive that is compatible with materials to be joined as much as possible. Since the formulation within one class of adhesives varies widely impacting its physical properties, finding the best adhesive for a specific application is not easy. In selecting the adhesive materials, the properties of materials to be bonded, and the economy of bonding operations should be considered. For example, polymer adhesives cannot be applied to all types of materials. A disadvantage of applying polymer adhesives is that they have a much higher tendency to creep than concrete. One type of adhesive material that has shown a high adhesion strength to both steel and concrete is epoxy (Çolak, 2001). Epoxy compounds are formulated normally in two parts, A and B. Part A is the portion including the epoxy resin; part B is a hardener material. They can be used for grouting or pressure injection of cracks to restore the tensile strength of concrete or other materials. ASTM provides a specification for epoxy bonding system (ASTM C 881-83). It divides the epoxy material into classes, types, and grades. Type I is used for bonding hardened concrete to each other or other materials to hardened concrete. Type II is used for bonding fresh concrete to hardened concrete. The term Grade is used to define viscosity. Grade 1 is a low viscosity that can be used for filling fine cracks. Grade 2 is a medium viscosity, and grade 3 has non-sagging consistency. The class is used to define the set time that can be affected by the ambient temperature. Class A is used in applications below 40 degrees Fahrenheit, class B for applications between 40 and 60 degrees Fahrenheit, and class C for applications above 60 degrees Fahrenheit. Since their properties, including strength as well as deformation and fire resistance are not well established, care is advised in their use. Also,

most of the epoxies degrade due to creep in high temperatures in the range of 140 to 150 degrees Fahrenheit. Much research has been conducted to investigate epoxy adhesives (Sturm & Shaikh, 1988).

Adnan (2001) investigated 4 types of epoxy adhesives (Table 18) and found that the presence of filler above 46 percent in adhesive formulation decreases the shear strength of epoxy adhesives dramatically (Figure 49).

Table 18: Types of epoxy adhesive formulation (Çolak, 2001)

Epoxy adhesive formulations

Type of epoxy adhesive formulation	Resin	Reactive diluent	Curing agent	Filler
EP1	DGEBA	Diglycidyl ether	Tri methyl hexa methylene diamine	—
EP2	DGEBA	Diglycidyl ether	Tri methyl hexa methylene diamine	Quartz sand
EP3	DGEBA	Diglycidyl ether	Tri ethylene tetra amine	—
EP4	DGEBA	Diglycidyl ether	Tri ethylene tetra amine	Quartz sand

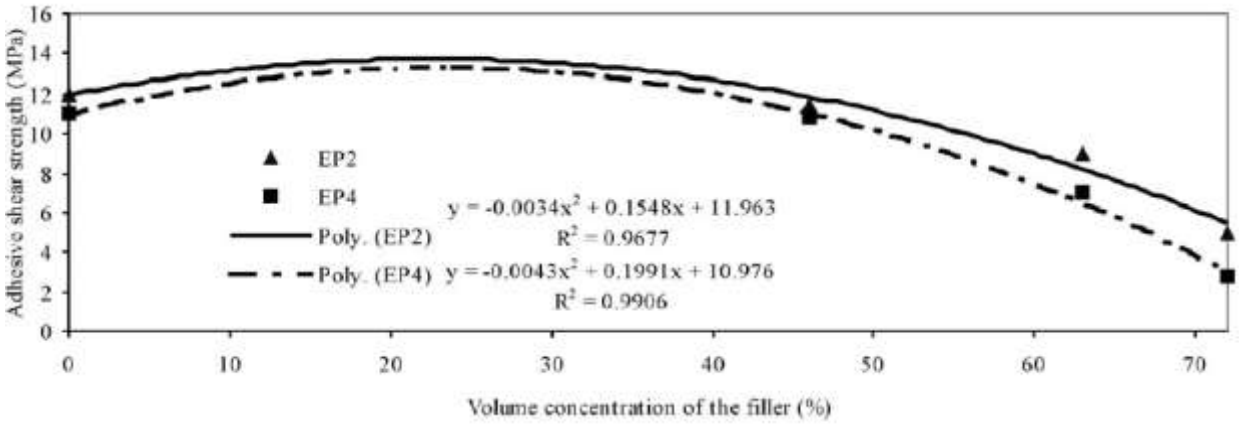

Figure 49: The effect of volume concentration of the filler on the adhesive shear strength (Çolak, 2001)

To establish proper bond in prestressed concrete piles using dowel connection, epoxy grout is commonly used. There are many types of epoxy grouts with different formulations in the market (Figure 50). The curing time of epoxy can be accelerated by heating methods such as enclosing the joints with a steam jacket (Navaratnarajah, 1981). Canner (2005) studied the CONCRESIVE® 1420 (currently known as MasterEmaco ADH® 1420) as a general-purpose gel epoxy adhesive used in prestressed concrete piles spliced with steel pipes. In his investigation, CONCRESIVE® 1420 was introduced as a proper product for the splice mating surface due to its ability to adhere to the surface and its high strength performance. The convenient way for applying epoxy is to mix them simultaneously in a larger container and pour it fast to prevent the setting of the epoxy before the completion of the process (Canner, 2005).

Figure 50: Different epoxies in the market

(https://coastalone.com/epoxy.html)

According to the Florida Department of Transportation, epoxy materials shall meet the requirements of Section 937. It also asserts the material should be on the FDOT's Approved Product List (APL) unless an alternative product is approved by the Department.

3.4.4. Sprayed polymer:

Choi et al. (2014) experimentally investigated the behavior and effectiveness of polymeric material, Polyurea, when sprayed as coating over cementitious concrete. Polyurea was sprayed on the surface of two types of specimens made of high-performance cementitious composites, PVB and PVA. The mix proportions for PVB and PVA fiber concretes is presented in Table 19.

Table 19: Mix proportions for PVB and PVA fiber concretes (Choi et al., 2014)

Constituents/concrete mix	PVB mix (without fiber)	PVA fiber mix
Cement	832.96	832.96
Metakaolin	79.30	79.30
B - 79 (Butvar - PVB)	182.39	182.39
B -75 (Butvar - PVB)	118.95	118.95
Water	364.78	364.78
Sika	26.68	26.68
PVA Fiber (RECS7)	0	7.93 (Vf = 0.6)[a]
W/C	0.438	0.438

[a]Fiber volume fraction (Vf) is constant for all PVA specimens.

In their work, two tests were conducted to investigate the effect of the sprayed Polyurea on the specimens. The first test investigated the flexural strength of coated and uncoated specimens (Figure 51). In this test, they found that coating by plain Polyuria increased the flexural strength of specimens by at least by 60 percent (Figure 52).

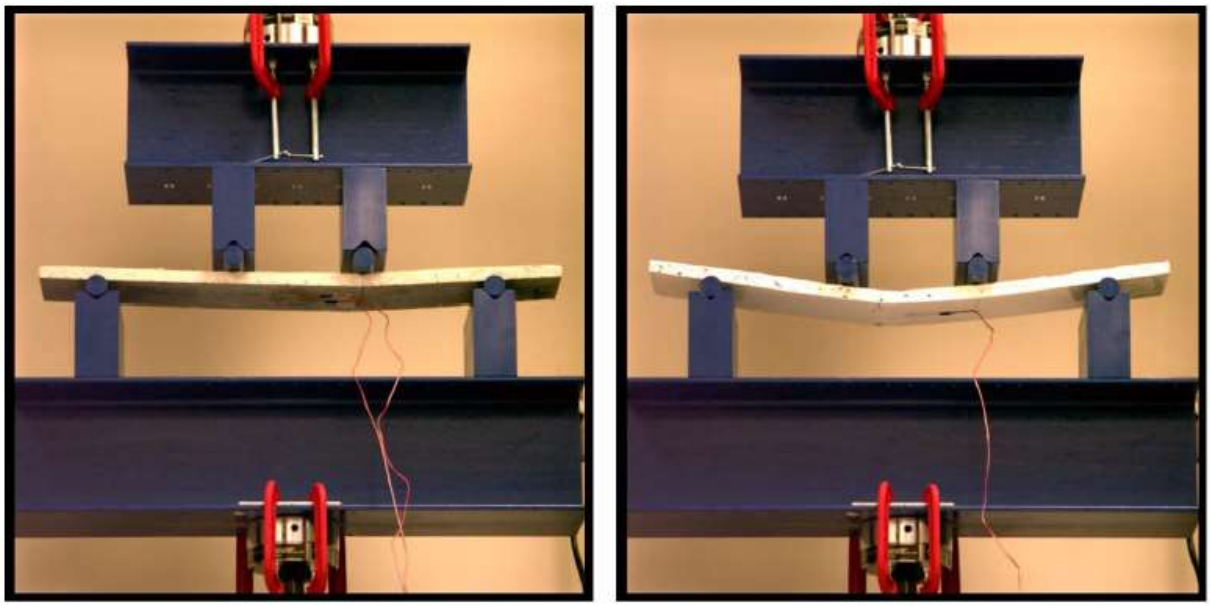

Figure 51: Flexure tests were conducted on (a) uncoated; (b) coated plates (Choi et al., 2014)

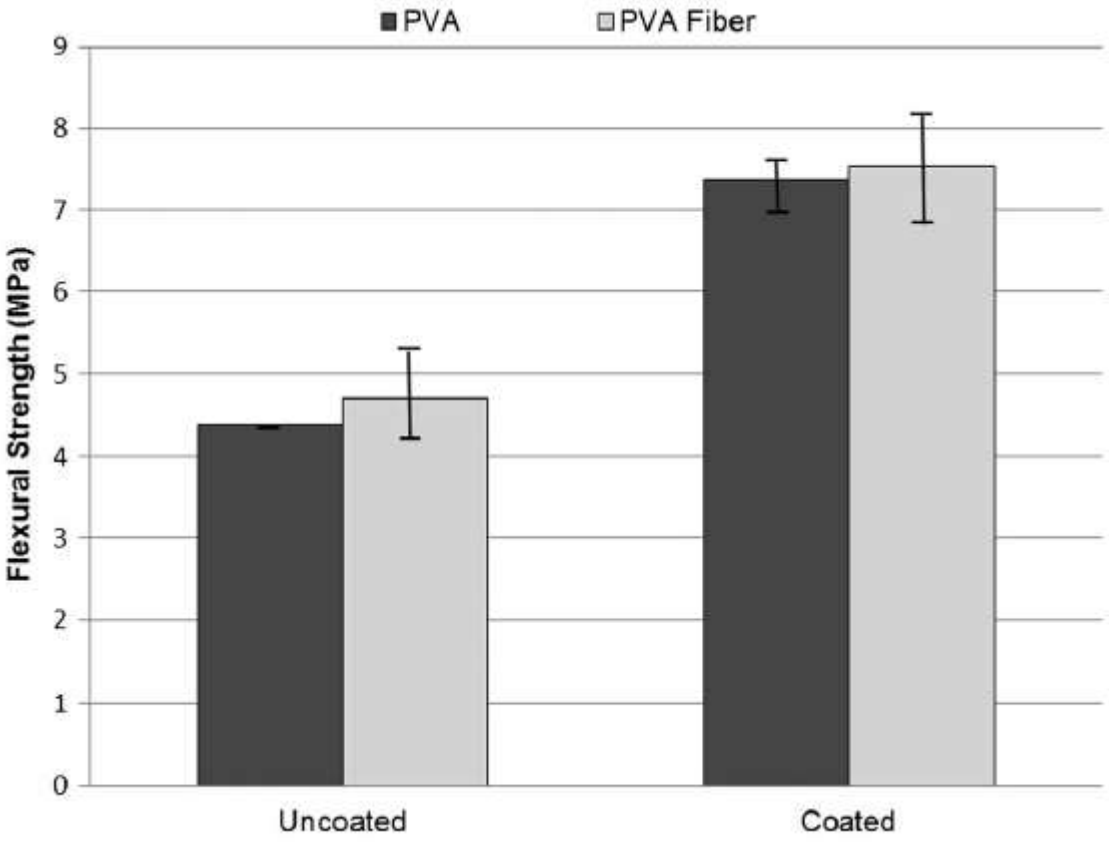

Figure 52: Flexural strengths for uncoated and coated specimens (Choi et al., 2014)

The second test, drop-weight tests, investigated the resistance of coated specimens to blast loads. The impact of sprayed Polyuria was investigated to see the proper location for spraying, top or bottom of specimens. They concluded that coating any surface is preferable to coating none. Also, coating the surface in the opposite direction of the striker is preferable to the coating the surface facing the striker, and coating both surfaces worked best (Table 20).

Table 20: Post impact Panel Condition for a Constant Drop Height of 2.74 m (Choi et al., 2014)

Specimen number	Location of polyurea coating	Condition of upper/lower surfaces
PVB mix		
#1	Bottom	F / F
#2	Both	P / P
PVA fiber mix		
#1	Bottom	F / F
#2	Both	P / P

Note: F = failure due to cracking; P = pass where no cracks were observed.

3.4.5. Candidate Grouts:

Among all grouts investigated in this section, Table 21 shows the candidates that can be used in the promising splice based on the work and set time as well as compressive strength. Further investigations in the current study will determine the grout (or epoxy) mix(es) that are most promising for the purpose of establishing splice connection for precast-prestressed concrete piles.

Table 21: Candidate Grouts for the promising splice

			Compreesive strength - psi							
Row	Type	Grout	1 hour	2 hour	1 day	7 day	28 day	Work time (hr)	Set time (hr)	Reference
1	Cement grout	Five Star® Highway Patch	910	2810	5080	5820		0.3	0.5	1
2	Cement grout	Erico HY10L			6520	11420	14700	0.4		2
3	Cement grout	M1(0.25)				5500			6	3
4	Cement grout	Nissco 5S Mortar			7350	12000	15000+	0.5	2.5-9.5*	2
5	Cement grout	Fly ash-based		4509***	5061	8047	8134	can reach 2000 psi in less than 4 hour		4
6	Epoxy based grout	Epoxy based grout			6235	11208	13558	can reach 5000 psi in less than 8 hour		4
7	Cement grout	Set 45® Hot Weather Grout	420	2050	4930	4930		0.2	0.75	1
8	Cement grout	ThoRoc® 10-60	2700	3030	5210	6380		0.1	0.2	1
9	epoxy resin-based grout	Masterflow 647R			4900	10000+	10000+	0.17-0.7**		5
10	epoxy resin-based grout	10-60 RAPID MORTAR	2000	3000	6500		8000	0.13	0.27	5

	*	set time depends on curing temperature		
	**: temperature F(C) minutes	90 (32) 10–20	***	2 to 4 hour
		75 (24) 20–30		
		55 (13) 30–40		
	Reference 1	Scholz et al., 2007		
	Reference 2	Jansson, 2008		
	Reference 3	Vasumithran et al., 2020		
	Reference 4	De la Varga & Graybeal, 2015		
	Reference 5	www.bestmaterials.com		

3.5. Type of Splices Selected for Further Investigation:

3.5.1. Mechanical bar couplers:

Mechanical bar couplers have been in use since 1973 (Yee, 1973). Among all types of mechanical bar couplers that include 1- Shear screw coupler, 2-Headed bar coupler, 3- Grouted sleeve couplers, 4- Threaded coupler, and 5- Swaged couplers, only grouted sleeve couplers are mostly in use for precast members. Also, the combination of threaded and grouted sleeve couplers have recently attracted many manufacturers.

3.5.1.1. grouted sleeve couplers

Much research has been conducted to investigate the capacity, behavior, suitability, and effectiveness of grouted sleeve couplers that are used in concrete members. Their ability in carrying the tension loads have been proven effective through several pull-out experiments. Examples include:

1- One type of grouted sleeve in the market (NMB) tested under monotonic loading by Einea et al., 1995, and Jansson at Michigan DOT, 2008 (Einea et al., 1995; Jansson, 2008);
2- Static and dynamic tests of grouted sleeve and headed bars sleeve couplers at the University of Nevada, Reno, by Haber, 2013 and Tazarv, 2014;

3- Dynamic and impact testing of grouted splices by Noureddine, 1995) and Rowell and Hager, 2010; and
4- Multiple tests of splice sleeves in Japan and Malaysia (NMB Splice Sleeve).

The application of grouted sleeve splices/couplers in seismic regions has been limited because of their presumed role in reduction of ductility (ACI Committee, 2014; Michael P Culmo et al., 2017). Their use is allowed with additional consideration as per ACI 318-14 and NCHRP report. The reason for reducing the ductility is that the coupler region is more rigid than the bar region; thus, couplers cannot be yielded at the same time as bars. The following paragraphs will go into details of the investigation on the tensile and ductile behavior of the grouted sleeve couplers which should help in introducing the most effective configuration of them for splicing the PPCPs.

3.5.1.1.1. Grouted sleeve couplers under gravity loads

Alias et al. (2010) experimentally investigated the performance of grouted sleeve couplers under axial loads in which the connector employed a mild steel pipe filled with non-shrinkage grout. The role of the grout was to bond the reinforcing rebars with the connector. The sleeve connector received a bar at each end, and the bars met each other at the mid-length of the connector as the grout was poured into the sleeve. Figure 53 shows the typical configuration of the connector.

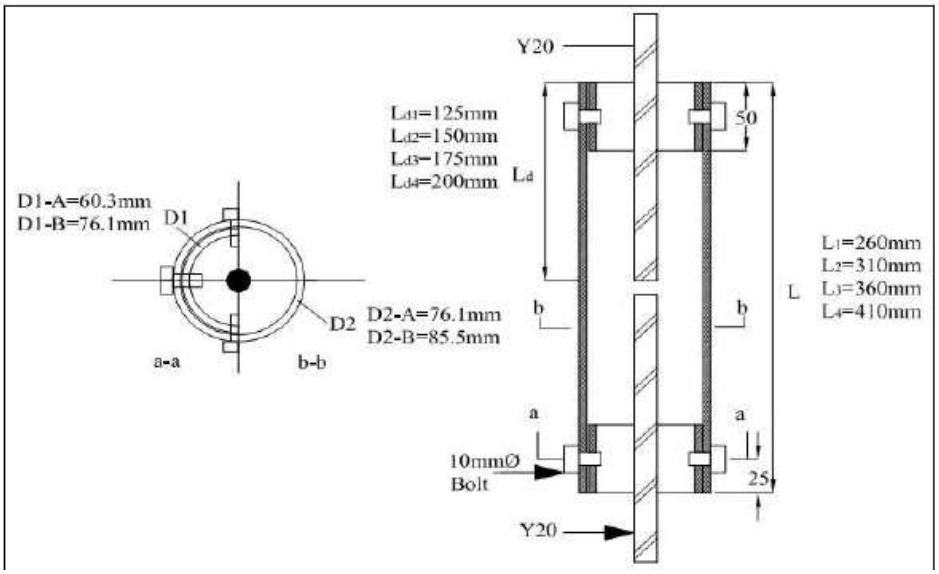

Figure 53: Detailing of grouted splice sleeve connector (Alias et al., 2014)

They conducted pull out tests to investigate the performance of the connection under tensile loads. Eight specimens were built and tested (Table 22 and Figure 54).

Table 22: Detailed dimensions of grouted splice sleeve connector (Alias et al., 2014)

Specimen	External Sleeve (mm)		Internal Sleeve (mm)		Development Length (mm)
	Diameter	Length	Diameter	Length	
Control Bar	-	-	-	-	600
A-20-125	76.1	260	60.3	50	125
A-20-150		310			150
A-20-175		360			175
A-20-200		410			200
B-20-125	85.5	260	76.1	50	125
B-20-150		310			150
B-20-175		360			175
B-20-200		410			200

Figure 54: Grouted splice sleeve connectors (Alias et al., 2014)

All specimens were tested under incremental tensile loads until failure by using Universal Testing Machine (Figure 55). The average grout compressive strength at the time of the

experiment was 6700 psi (46 N/mm^2), and the tensile loads were applied to the splices/couplers with an average rate of 13.5 lbf/s (0.06 kN/s). Three modes of failure were identified in the pull out tests; 1- fracture of the bar outside the connector (Figure 56a); 2- pull out of the bar from the grout (Figure 56b); and 3- pull out of the grout from the sleeve (internal sleeve-grout failure) (Figure 56c).

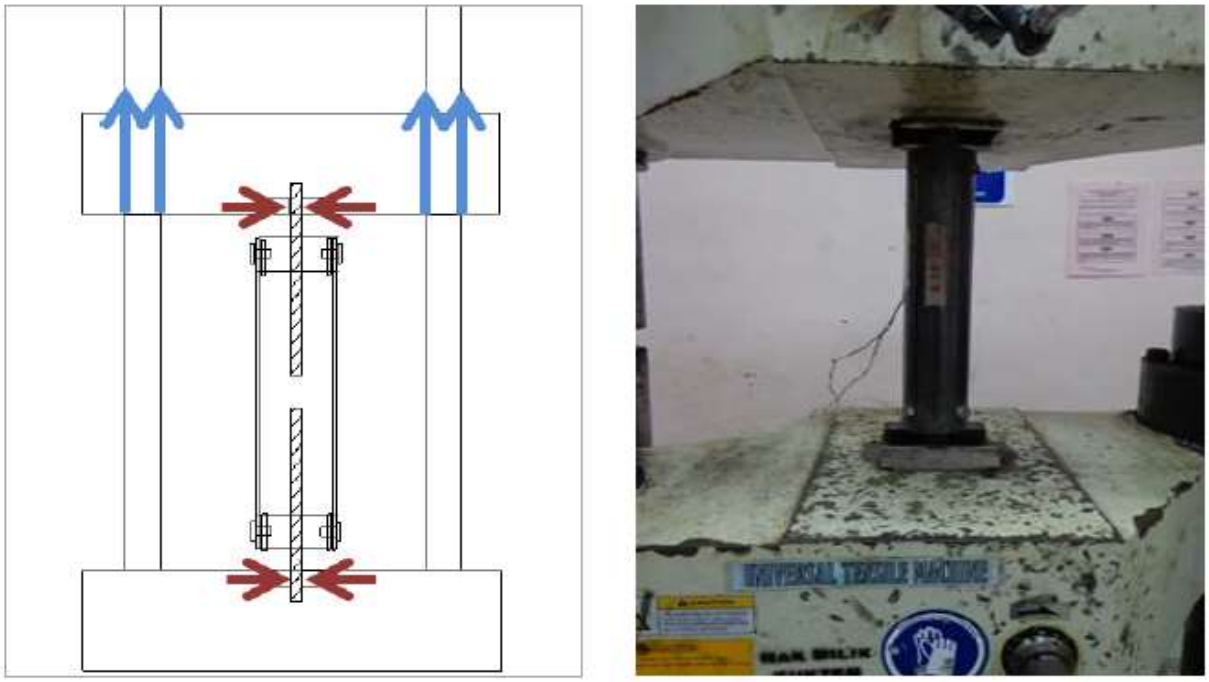

Figure 55: Test set-up (Alias et al., 2014)

Figure 56: Modes of failure: (a) bar fracture (b) bar pull out (c) internal sleeve-grout failure (Alias et al., 2014)

Table 23 shows the test results.

Table 23: Tensile test result of grouted splice sleeve connector (Alias et al., 2014)

Specimen	Pu (kN)	fu (N/mm2)	fu/fy,s (ACI 318) >1.25fy,s	*Ld / Øbar (BS 8110 =40Ø)*	*Mode of Failure*
Control Bar	207.3	659.86	1.43	-	*Bar fracture*
A-20-125	162.6	517.57	1.13	*6.3Ø*	*Bar pullout*
A-20-150	174.3	554.81	1.21	*7.5Ø*	*Bar pullout*
A-20-175	186.5	593.65	1.29	*8.8Ø*	*Bar pullout*
A-20-200	200.5	638.21	1.39	*10Ø*	*Bar fracture*
B-20-125	159.0	506.11	1.10	*6.3Ø*	*Internal sleeve pullout*
B-20-150	172.6	549.40	1.19	*7.5Ø*	*Internal sleeve pullout*
B-20-175	178.0	566.59	1.23	*8.8Ø*	*Bar pullout*
B-20-200	182.3	580.28	1.26	*10Ø*	*Bar fracture*

Also, Figure 57 shows load-displacements plot of the pull out tests.

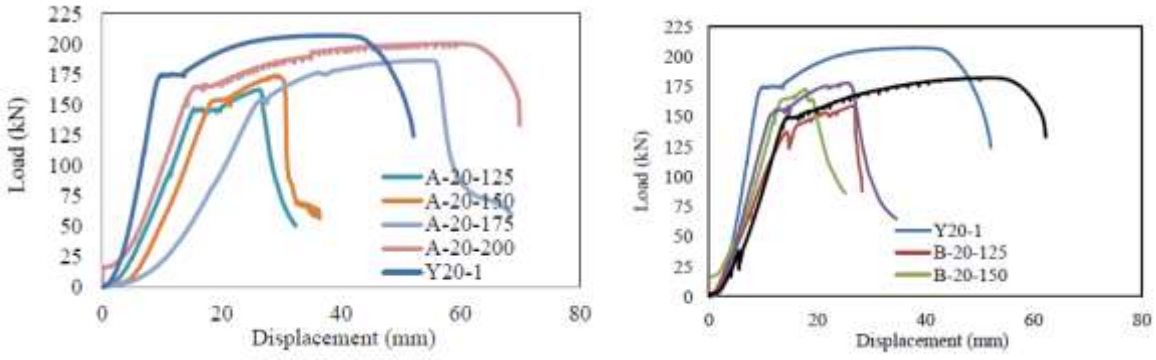

Figure 57: Load-displacement graph of connectors (Alias et al., 2014)

Based on the results, they concluded that the development length of the reinforcing bar is the most effective parameter in the performance of the connectors. Additionally, the required development length can be reduced to 10 times diameter, where, in the design standards, it is considered 40 times of bar diameter (Alias et al., 2014).

Einea et al. (1995) experimentally investigated the average bond strength of grouted sleeve couplers at failure. Yield strength of the bar, compressive and tensile strength of the grout, the

properties of the sleeve, and the geometry of the bar as well as its confining condition were identified as variables that impacted the bond strength of reinforcing bars confined with sleeve. The bar diameter as well as its embedment length into the confined grout, the sleeve's wall thickness, and the geometry of the sleeve's ends were also of importance. They found a linear relationship between the bond strength at failure, U, and the square root of grout strength (Equation 1):

$$U = K\sqrt{f'_c} \quad (1)$$

Where the K is constant and its value varies from 25 to 30.

They also stated that, confining pressure on grouted sleeve couplers, f_n, can be calculated based upon the Equation 2:

$$f_n = \frac{2\varepsilon_s tE}{d_i} \quad (2)$$

Where ε_s, t, E, and d_i are tangential strain in the sleeve, the thickness of sleeve wall, the module of elasticity of the sleeve material, and inside diameter of the sleeve, respectively (Einea et al., 1995). From their work, it can be seen that as the inside diameter of the sleeve increases without changing its thickness wall, the confining pressure decreases. Hence, the ultimate bond strength decreases. With decreasing bond, the capacity of the splice decreases. Also, as the wall thickness of the sleeve, t, increases, the confining pressure increases. Thus, the ultimate bond stress increases. Accordingly, the splice capacity increases.

Seo et al. (2016) experimentally investigated a type of mechanical grouted coupler called headed-splice sleeve (HSS) (Figure 58). This splice has a large and a small diameter end opening. Through the large opening, the rebar with head, connected mechanically to the rebar, is inserted into the sleeve. The smaller opening is threaded and received another rebar threaded to the sleeve. The grout is poured into the sleeve to bond and anchor the headed rebar and to provide the splice with its capacity. In their investigation, the bond behavior of the splice system was studied. Variables of their studies were development length of the rebar, and presence and size of the head part. They found that the presence of the head prevented the brittle failure of splice. In other words, it caused the failure to occur with the rapture of the rebar rather than the grout failure. Also, they noticed that the diameter of the head was dependent on the geometry of the sleeve and calculated the proper ratio of diameter of the sleeve to diameter of the head to be 1.3.

Figure 58: shape of HSS (Einea et al., 1995)

In their work, the bond strength of the HSS was calculated by Equation 3.

$$P_m = \tau\pi d_b l + A_{hb} k f_m \quad (3)$$

Where P_m is the maximum bond strength (N or lb); k is 3.4, based on the analysis results; l is the development length of rebar (mm or in.); and τ is the bond stress obtained in the experimental test (N/mm^2or psi) and calculated by Equation 4. A_{hb} is the improved bearing area by head anchorage device (mm^2 or in^2), calculated by Equation 5.

$$\tau = 0.9 \frac{l}{d_b} \sqrt{f_m} \quad (4)$$

Where d_b is the diameter of the rebar (mm or in.), and f_m is the compressive strength of grout mortar (N/mm^2 or psi).

$$A_{hb} = \sqrt{A_m A_h} \quad (5)$$

Where A_m is the mortar bearing surface area (area inside the sleeve) (mm^2 or in^2), and A_h is the bearing area of head (mm^2 or in^2) (Seo et al., 2016).

Henin and Moracous (2014) experimentally investigated a type of grouted sleeve coupler that is more cost-efficient and easier to implement in precast members (Figure 59) than the proprietary couplers including, NMB Splice Sleeve, Sleeve Lock by Dayton Superior, and Lenton Interlok (Henin & Morcous, 2015).

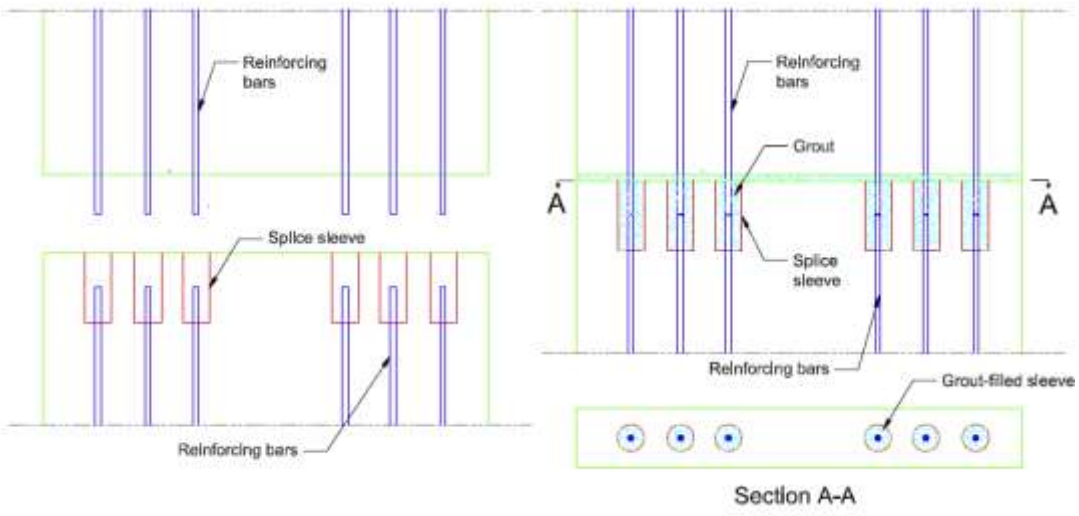

Figure 59: Precast concrete components before (left) and after (right) connecting, using bar splice sleeves (Henin & Morcous, 2015)

The proposed sleeve coupler is a grout-filled round pipe in which the diameter, length, and thickness of the sleeve rely on the bars to be spliced. Design of the sleeve is based upon shear-friction theory for transferring the force of one bar to the grout, next from the grout to the steel pipe, then from the steel pipe to the grout, and at the end from the grout to the other bar.

In their investigation, two types of grouted sleeve coupler, type P and T, as shown in Figure 60, were designed and tested. Type T had threads along the interior surface of the sleeve in both the upper and bottom of the splice, while Type P had the threads at the upper part only and was welded to the steel plate at the bottom part.

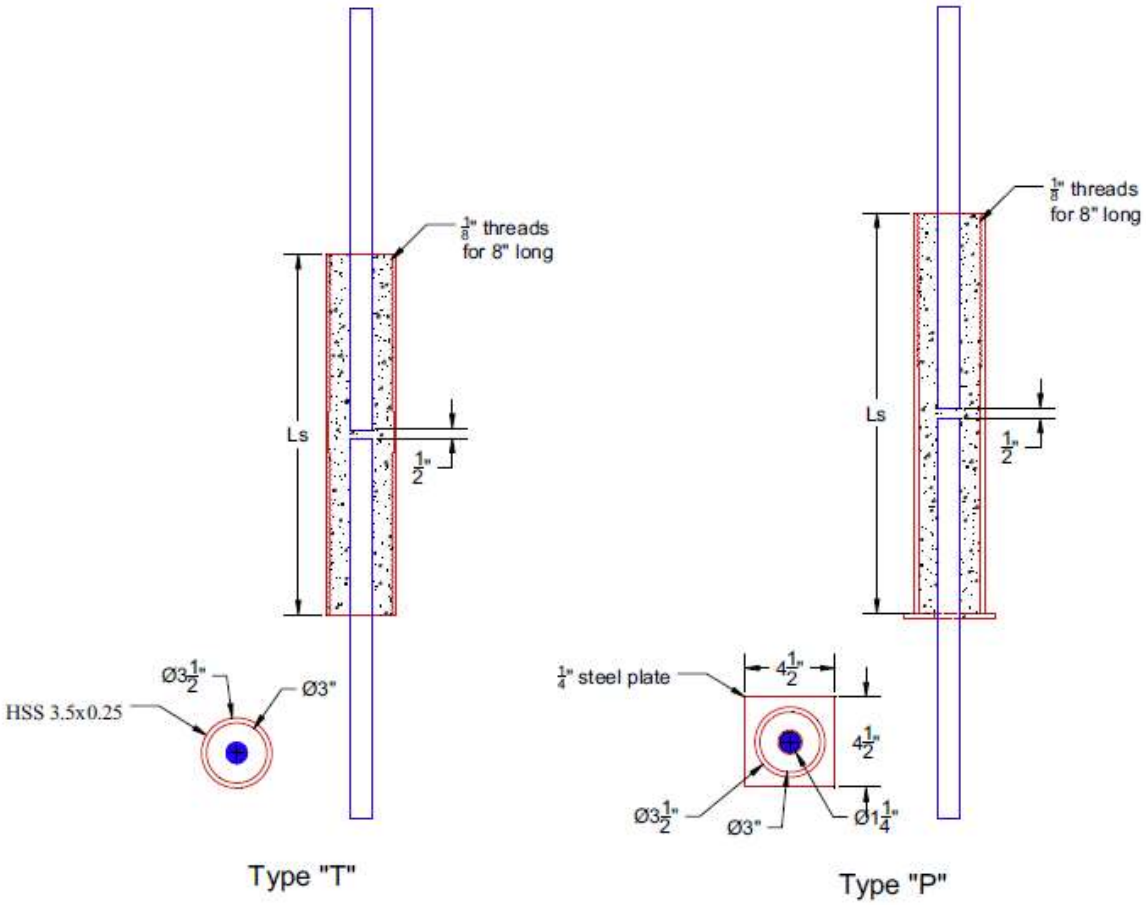

Figure 60: Two types of bar splice sleeves tested by (Henin & Morcous, 2015)

Their study included testing of 18 specimens, 9 specimens of each type with different sleeve length (Table 24).

Table 24: The details of investigated specimens (Henin & Morcous, 2015)

Specimen ID	Bar size	Sleeve length (Ls), in.	Sleeve type	Number of specimens
8T16	# 8	16	T	2
8P16	# 8	16	P	2
8T18	# 8	18	T	2
8P18	# 8	18	P	2
8T20	# 8	20	T	2
9T16	# 9	16	T	2
9P16	# 9	16	P	2
9T20	# 9	20	T	2
9P20	# 9	20	P	2
			Total	18

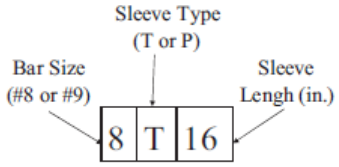

According to the test results, the embedment length of bar (l_b) was calculated (Equation 6), in which d_b is the diameter of the bar, P is the force, and F_b is the bond strength between the bar and the surrounding grout.

$$l_b = \frac{P}{\pi d_b F_b} \quad (6)$$

Where the bond strength between the grout and the bar (F_b) was found based on the shear-friction theory and estimated according to the radial confinement stress (F_n) multiplied by the coefficient friction between grout and bar (μ) (Equation 7).

$$F_b = F_n \mu \quad (7)$$

The coefficient of friction between grout and bar (μ) was considered 1 for the deformed bar surface. For calculating the radial confinement stress (F_n), the equilibrium of forces in one unit-long section of the half sleeve was used (Equation 8).

$$F_n = \frac{2tF_s}{d} \quad (8)$$

Where t, F_s, and d are the wall thickness, yield stress, and inside diameter of the sleeve, respectively. They also found that to avoid crushing failure of grout, the radial confinement stress should be less than $0.2f'c$, where $f'c$ is the compressive strength of the grout. Finally, for the proposed sleeve coupler, the required embedment length of splices was calculated based on Equation 9.

$$l_b = \frac{P}{\pi\, d\, min\left(0.2f'_c, \frac{2tF_s}{d}\right)} \quad (9)$$

They also calculated the required sleeve length (l_s) to be twice the embedment length rounded up to the nearest inch (Henin & Morcous, 2015).

3.5.1.1.2. Grouted sleeve couplers for elements subject to lateral loads:

Although strength has been the most important criterion for the application of grouted sleeve couplers for many years, reaching sufficient ductility has recently emerged as a concern (Marsh, 2011). Significant amount of research has been conducted to investigate the effect of grouted sleeve couplers on the ductility of the precast members in seismic regions. It was found, in many cases, that the connection made with grouted couplers is too rigid to allow yielding within its length. Thus, the entire elongation occurs in the rebar close to the end of the sleeve. Therefore, the ductility of the member is reduced. Many approaches, including debonding the bars and moving the grouted sleeve couplers farther inside the elements, have been implemented to improve the ductility performance of these connectors in the precast elements.

Haber et al., 2013, and Pantelides et al., 2014, investigated the displacement ductility of several precast column connections using grouted and headed sleeve couplers. The results are summarized in Table 25.

Table 25: Displacement Ductility (Haber, 2013; Pantelides et al., 2014)

Connector				$\left(\frac{\mu_D^{P/C}}{\mu_D^{CIP}}\right)_2$	Ref.$_3$
Type	Length$_1$	Embedding Element	Distance from Interface		
GC	$14.6d_b$	Footing	0	0.69	1
GC	$14.6d_b$	Column	0	0.61	1
HC	$3.6d_b$	Column	4.0 in.	0.88	2

[1] Expressed in terms of column longitudinal bar diameters, d_b

[2] Displacement ductility capacity of p/c connection to displacement ductility capacity of reference CIP.

[3] Ref. 1: Pantelides et al., (2014); Ref. 2: Haber et al., (2013)

As shown in Table 25, for precast column connections with long embedment length like grout filled coupler (GC), displacement ductility ratio is as low as 60 % of that of cast-in-place (CIP) connections.

In their research, Tazarv and Saiidi, 2014, 2015, and 2016, developed an approach to quantify the reduction in the displacement ductility. Based on the pull-out tests and numerical simulations, they found that reduced analytical plastic hinge length, L_p^{sp}, due to the presence of any type of mechanical coupler can be calculated based on Equation 10 (Tazarv, 2014; Tazarv & Saiidi, 2015, 2016).

$$L_p^{sp} = L_p - \left(1 - \frac{H_{sp}}{L_p}\right) \leq L_p \qquad (10)$$

Where:

L_p^{sp}: Reduced analytical plastic hinge length due to the presence of the mechanical coupler (in.)

L_p : Analytical plastic hinge length for CIP members as defined in AASHTO Guide Specification for LRFD Seismic Bridge Design (2011) (in.)

H_{sp}: Distance from the top surface of member to the nearest end of the mechanical coupler (in.)

Figure 61 shows the actual and idealized curvature diagram for the column with grouted sleeve coupler in the plastic hinge region.

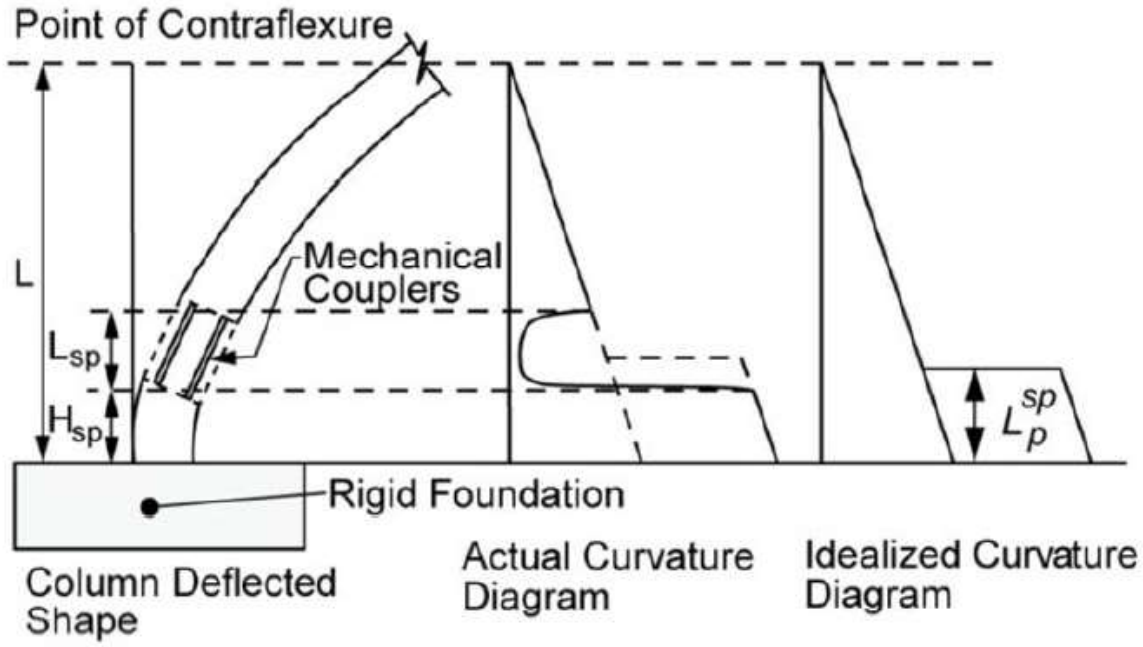

Figure 61: Actual and idealized curvature diagram (Michael P Culmo et al., 2017)

To improve the ductility behavior of the grouted sleeve couplers in precast members, many investigations have been conducted. Debonding of connected bars outside the coupler (Figure 62) was found to be an effective approach since it postpones the rebar fracture and reduces spalling of adjacent capacity-protected elements (Belleri & Riva, 2012; Cohagen et al., 2008; Mashal et al., 2014). Accordingly, the ductility of the system and as a result, the energy dissipation capacity of the structure will be increased with debonding solution. Pantelides et al., 2014, experimentally studied the effect of debonding of bars on the ductility of the member. They found that debonding increased the displacement ductility capacity from 5.4 to 6.8. There is a need for more research to investigate the effect of debonding material, debonding length, and location of debonding on the ductility behavior of a member in seismic regions.

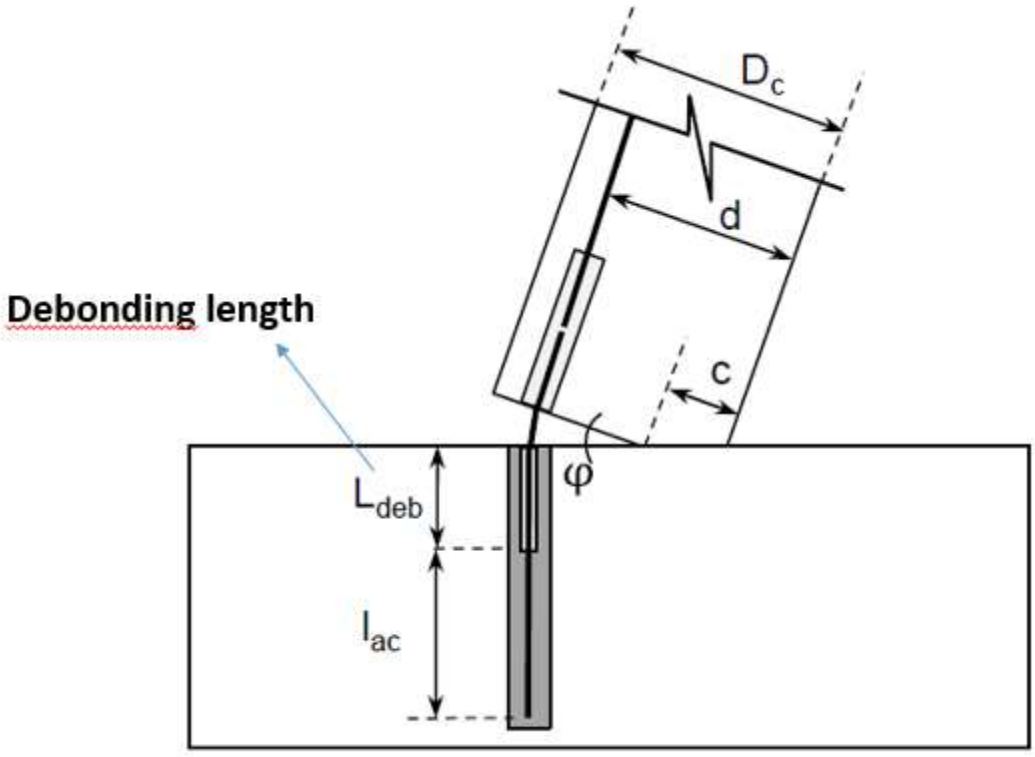

Figure 62: Debonding of the mechanical coupler (Michael P Culmo et al., 2017)

Tazarv and saeidi (2014) investigated another approach to improve the ductility of the system. They shifted away the location of the grouted sleeve couplers from the column ends to emulate the seismic response of CIP counterparts in terms of energy dissipation and displacement capacity (Figure 63). They found that this approach combined with debonding can effectively increase the ductility behavior of the system.

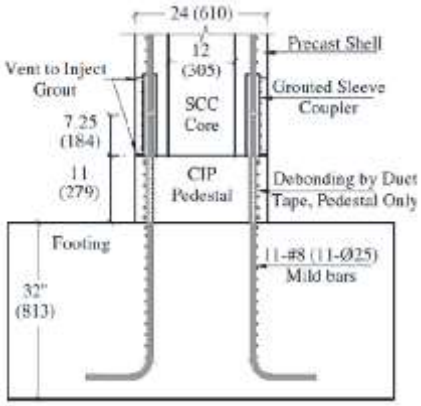

Figure 63: Shifting away the location of the grout-filled coupler from the columns ends (Tazarv, 2014)

3.5.1.1.3. Grouted sleeve couplers in the design specifications:

ACI 318-14 defines two types of mechanical bar couplers, Type 1 and Type 2. Type 1 is referred to as the connectors that are able to develop 125% of the yield strength of bars (Ab * Fy). Type 2 is referred to as the couplers that can both conform to the requirement of Type 1 and also can develop the ultimate strength (nominal tensile strength Fu) of the bars to be joined. ACI 318-14 requires using the Type 1 only in the locations in which the couplers shall not experience yielding. This requirement ensures that premature failure, bar pullout or coupler fracture will not impact the system's ductility. Therefore, Type 1 of mechanical couplers is not allowed to be implemented in plastic hinge regions for all Seismic design categories (SDCs). However, Type 2 is permitted to be used anywhere except within half a member depth from the face of the connecting element in special moment frames (SMF) with ductile connections if the connections are not "strong"(ACI Committee, 2014).

AASHTO LRFD does not use Type 1 and 2 terminologies. It requires that in SDCs C and D (seismic zone 3 and 4), any mechanical coupler be used outside the plastic hinge region (AASHTO, 2017). It also determines that in piles or shafts, where such placement is virtually impossible, mechanical couplers can be used in plastic regions if they develop the tensile strength of the bars.

Task 2 –Development of New Splice Details and Configurations

3.5.1.2. Proposed configuration for splicing PPCP

After reviewing the experiences gathered in general for ABC connections and current splice systems, two effective yet simple splice connection types for preplanned PPCP splices were developed and conceptual design has been established.

3.5.1.2.1. Preplanned pile splices

For reasons including transportation limitation and limited headroom for driving piles, splices can be preplanned for site application. This gives more choices for splicing types and allows preparing the receiving (lower) segment of piles with additional reinforcement, holes, and other embedment. As a form of mechanical connection, sleeve splice configuration was adopted for driven prestressed concrete pile segments in preplanned splicing. In the sleeve splice connections, the auxiliary bars from the lower pile segment have already inserted into the lower portion of the sleeve when that segment is fabricated. the protruding dowels from the upper segment of the piles are then inserted into the sleeves, positioned in the lower segment of piles and then sleeves are filled with non-shrink grout. The connection between auxiliary bars and sleeves can be performed in two ways which determine the type of sleeve splices. Accordingly, sleeve splices can come in two configurations; grouted and threaded sleeve splices. In threaded sleeve splice, the connection is established by threading the sleeves into auxiliary bars in the lower segment (see Figure 64a). In the other, which is called grouted sleeve splice, the auxiliary bars occupy the lower half of the sleeve and connection is established by subsequent grout injection in the sleeve performed during splicing. The connection between the auxiliary bars for grouted sleeve splice is similar to connection between the dowel and sleeve in the upper segment of pile (see figure 64b). In the threaded sleeve splices, dowels can be headed to provide better anchorage. Sleeve splices provide a simpler, cost effective, and easy to implement option to

epoxy dowel splices, and their application in precast concrete pile members can accelerate the erection and substantially reduce the required rebar lap length. Also, it guarantees higher quality assurance. To design PPCP with the splice sleeve connector, many factors should be considered such as the mechanical properties of bars and sleeves, the diameter as well as the length of sleeves, and the grout strength. The design of connectors will be included in the next progress report.

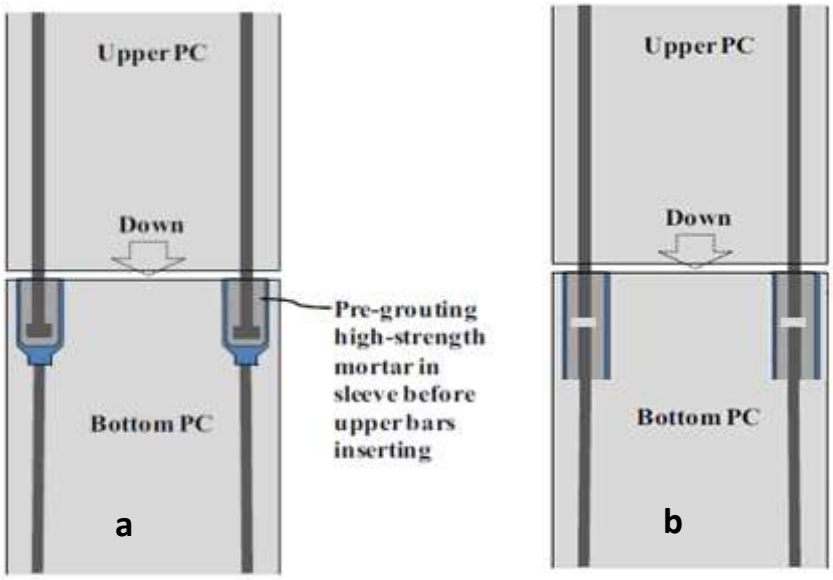

Figure 64: Proposed connections for preplanned splice; a- threaded sleeve splice b- grouted sleeve splice

3.5.1.2.1.1 Configuration of sleeve splices in the market

Tremendous research has been conducted to find the existing configuration of the sleeve splices in the market. It is found that most of the successful sleeve splices are produced by Dayton, NMB, Japan slim sleeve splice companies. Figure 65 shows a typical configuration for sleeve splices of the Dayton company, made by the USA. Dayton (Dayton Superior Corporation, 2018) has introduced the Superior D410 Sleeve-Lock Grout Sleeve as a one-piece mechanical coupler designed to butt-splice reinforcing steel in concrete structures. This sleeve system is available in seven sizes to accommodate deformed bar sizes #4 through #18. The system can effectively splice bars with the same sizes or of various sizes. The D410 Sleeve-Lock Grout Sleeve is a ductile casting with a minimum yield strength of 55,000 psi and a minimum tensile strength of 80,000 psi. It meets all known building codes and agency standards. This company also introduced Superior Sleeve-Lock Grout D490 that can achieve Type 2 Grade 60 strength criteria. Accordingly, it meets AASHTO LRFD Bridge Design specification requirements and ACI 318-14 as a Type 2 Grade 60 connection capable of more than 1,000,000 cycles at 18 ksi cyclic load range (AASHTO, 2017; ACI Committee, 2014).

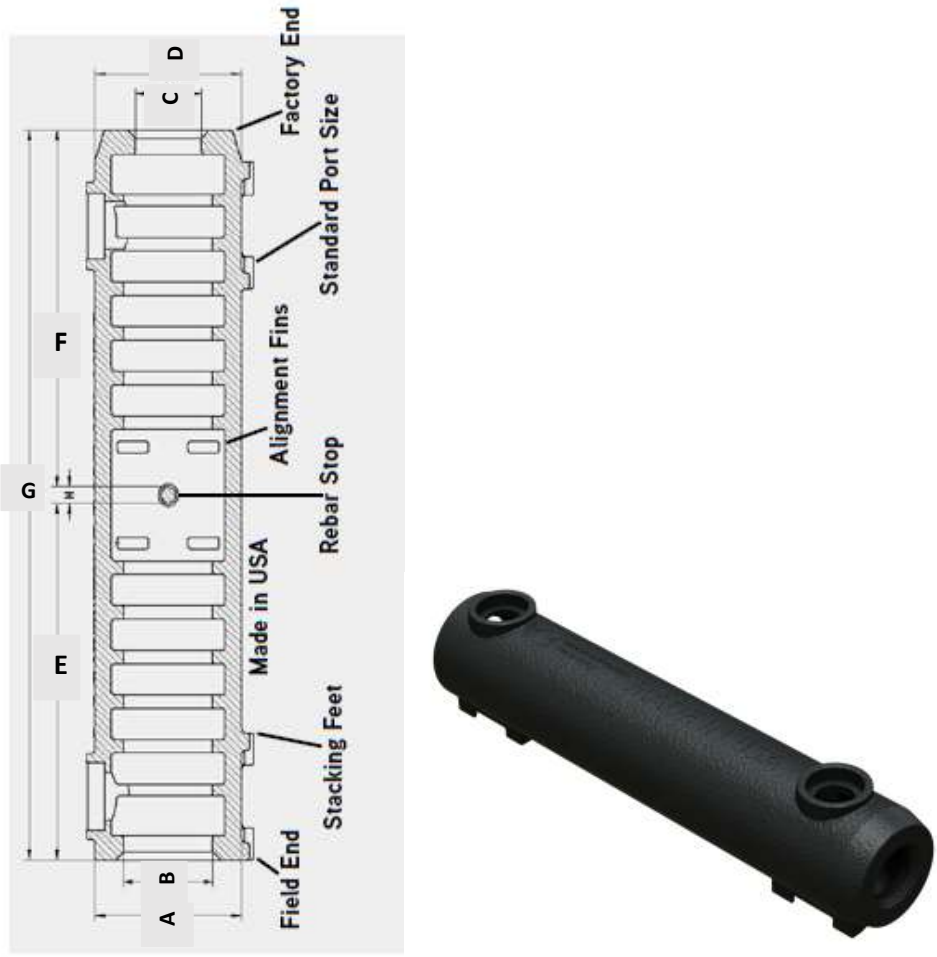

Figure 65: sleeve splices of the Dayton company (Dayton Superior Corporation, 2018)

As shown in Figure 65, the sleeve has the following features:

1- Rebar Stop – it acts as a precise stop when inserting rebar
2- Alignment Fins – Positioning fins that keep inserted rebar centered
3- Standard Port Sizes – Ports designed to accept standard 0.75" SCH40 PVC; ports use the same size PVC
4- Stacking Feet – Feet used to stabilize the product during shipping and on the shelf while assisting in wire-tying and acting as a rebar chair platform.

Table 26 shows the dimensions of the available Dayton Sleeve-Lock Grout Sleeve.

Table 26: Dayton sleeve splices dimensions (Dayton Superior Corporation, 2018)

SIZE		SLEEVE-LOCK DIMENSIONS (IN.)						REBAR EMBEDMENT LENGTH (IN.)			
		A	B	C	D	G	H	E, MAX	E, MIN	F, MAX	F, MIN
#4	13MM	2.14	1.26	0.87	2.14	9.50	0.25	4.63	3.30	4.63	3.30
#5	16MM	2.14	1.26	0.87	2.14	9.50	0.25	4.63	4.13	4.63	4.13
#6	19MM	2.61	1.73	1.14	2.61	13.00	0.25	6.38	4.92	6.38	4.92
#7	22MM	2.61	1.73	1.14	2.61	13.00	0.25	6.38	5.71	6.38	5.71
#8	25MM	2.89	2.01	1.42	2.89	16.52	0.38	8.07	6.50	8.07	6.50
#9	29MM	2.89	2.01	1.42	2.89	16.52	0.38	8.07	7.40	8.07	7.40
#10	32MM	3.04	2.16	1.57	3.04	17.99	0.50	8.75	8.19	8.75	8.19
#11	36MM	3.32	2.32	1.73	3.32	19.54	0.50	9.52	8.98	9.52	8.98
#14	43MM	3.73	2.60	2.01	3.73	24.50	0.50	12.00	11.42	12.00	11.42
#18	57MM	4.77	3.27	2.68	4.77	36.00	0.50	17.75	17.00	17.75	17.00

All dimensions are in inches

The NMB Splice-Sleeve (Splice Sleeve Nort America, 2017) is another efficient coupler in the market for splicing reinforcing bars that uses a cylindrical steel sleeve filled with SS mortar (a Portland-cement based non-shrink high early-early-strength grout). Figure 66 shows a typical configuration for NMB sleeve splices. This splice also meets the requirement of AASHTO LRFD Bridge Design specification and ACI-318-14, Types 1 and 2 (AASHTO, 2017; ACI Committee, 2014). The sleeve has an integral rebar stop in the mid-portion which assures the specified embedment of the rebar into the sleeve and an optional setscrew to hold the bar in the narrow end. Other feature of this splice is the uniform exterior dimension of the sleeve. This allows employing the same size of stirrups or hoops throughout the length of the sleeve. This sleeve system can connect bars of the same size or up to two sizes smaller than the sleeve size. The material properties of NMB Splice-Sleeve iron casting conform to the proprietary specification based on ASTM A536-84 (Annual, 1994). The grout used in the NMB must be non-metallic. Minimum grout strength will be 6500-psi for Type 1 (125%Fy) performance and 9500-psi for Type 2 (150%Fy) performance. Table 27 shows the details of the available NMB sleeve Splices.

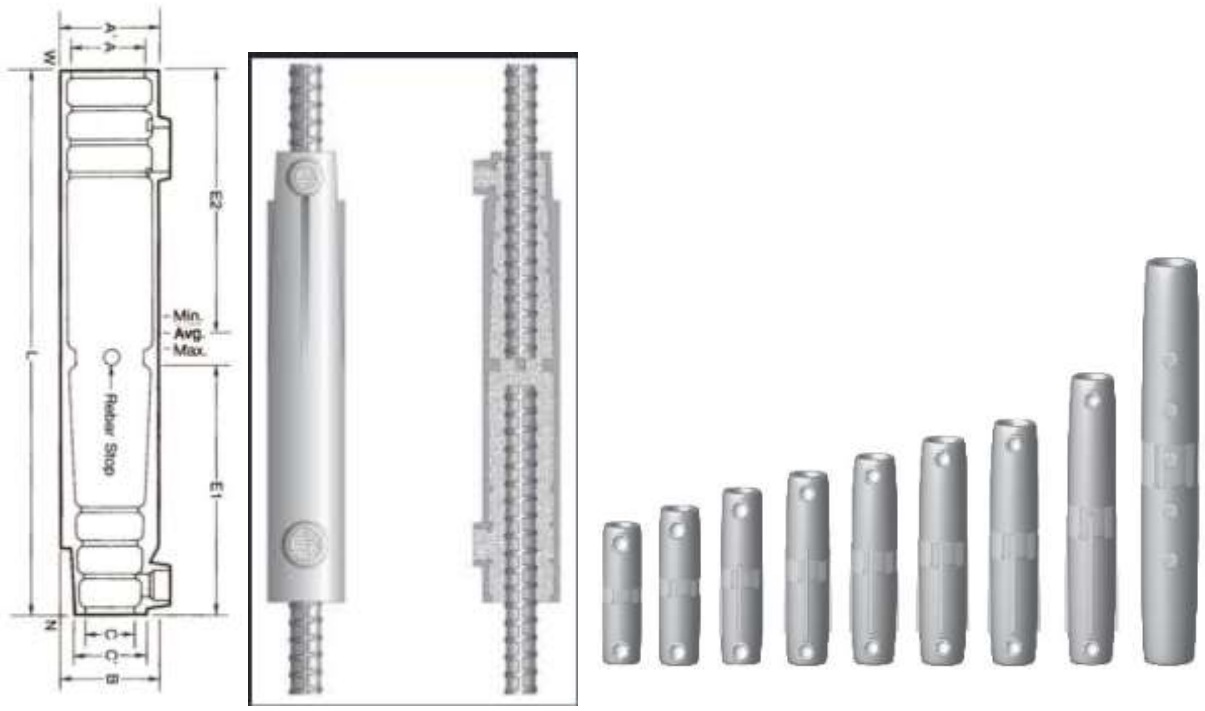

Figure 66: NMB sleeve splices (Splice Sleeve Nort America, 2017)

Table 27: NMB Splice Sleeves dimension (Splice Sleeve North America 2017)

Dimensions of NMB Splice Sleeves											Recommended Rebar Embedment Length					
Sleeve No.	Bar Dia.	Bar Size		Sleeve Length (L) inch	Narrow End Diameter		Max. Dia. (B) inch	Wide End Diameter			Factory Dowel (E1) inch		Field Dowel (E2) inch			SS Mortar lbs. per Sleeve
		ASTM	Metric Canada		I.D. (C) inch	O.D. (C') inch		I.D. (A) inch	Total Tolerance inch	O.D. (A') inch						
											Minimum	Maximum	Minimum	Average	Maximum	
5U-X	0.625	#5	15MM	9.65	0.87	1.42	1.81	1.26	0.63	1.81	4.13	4.33	4.13	4.53	4.92	1.26
6U-X	0.750	#6	20MM	11.22	1.02	1.57	1.97	1.42	0.67	1.97	4.92	5.12	4.92	5.32	5.71	1.76
7U-X	0.875	#7		12.80	1.14	1.69	2.28	1.73	0.86	2.28	5.71	5.91	5.71	6.11	6.50	2.65
8U-X	1.000	#8	25MM	14.57	1.30	1.90	2.48	1.89	0.89	2.48	6.50	6.89	6.50	6.99	7.48	3.46
9U-X	1.128	#9	30MM	16.34	1.42	2.01	2.60	2.01	0.89	2.60	7.40	7.56	7.40	7.88	8.35	3.95
10U-X	1.270	#10		17.91	1.57	2.20	2.80	2.16	0.89	2.80	8.19	8.35	8.19	8.66	9.13	4.94
11U-X	1.410	#11	35MM	19.49	1.73	2.40	3.03	2.32	0.91	3.03	8.98	9.13	8.98	9.45	9.92	6.02
SNX-11	1.410	#11	35MM	19.09	1.69	2.52	3.03	2.32	0.91	3.03	8.86	9.25	8.27	8.86	9.45	5.71
A11W	1.410	#11	35MM	19.49	1.73	3.31	3.30	2.60	1.19	3.31	8.86	9.84	8.27	8.96	9.65	6.99
14U-X	1.693	#14	45MM	24.41	2.01	2.80	3.46	2.60	0.91	3.46	11.42	11.61	11.42	11.91	12.40	9.19
18U-X	2.257	#18	55MM	36.22	2.68	3.66	4.72	3.27	1.01	4.25	17.00	18.11	17.00	17.56	18.11	25.31

Japan sleeve splices (Splice Sleeve Japan, 2015) has introduced two types of connector systems, Splice Sleeve UX (SA) and Slim-Sleeve. Type UX (SA) Splice-Sleeve connectors consist of

straight and half-tapered steel cylinders. It has a narrow end and a wide end used for splicing two non-equal-diameter or equal-diameter deformed steel reinforcing bars (Figure 67). The midsection of the interior of the sleeve has the rebar stop part, which determines the suitable embedment of the bars. Their configuration dimension is very close to the NMB Splice Sleeve but not the same.

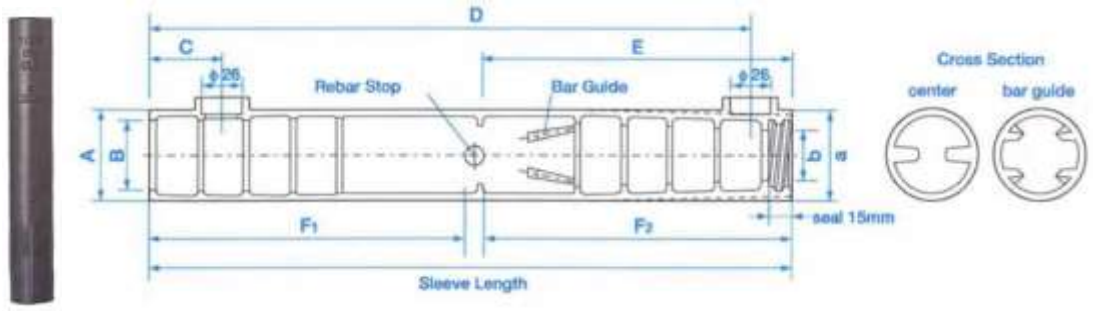

Figure 67: Splice Sleeve UX (SA) (Splice Sleeve Japan, 2015)

Slim-Sleeve connectors are similar in shape and dimension to the UX (SA) connectors except that the two ends of Slim-Sleeve are symmetrical and used to splice two equal-diameter deformed reinforcing bars (Figure 68). Table 28 shows the dimension of this sleeve splice.

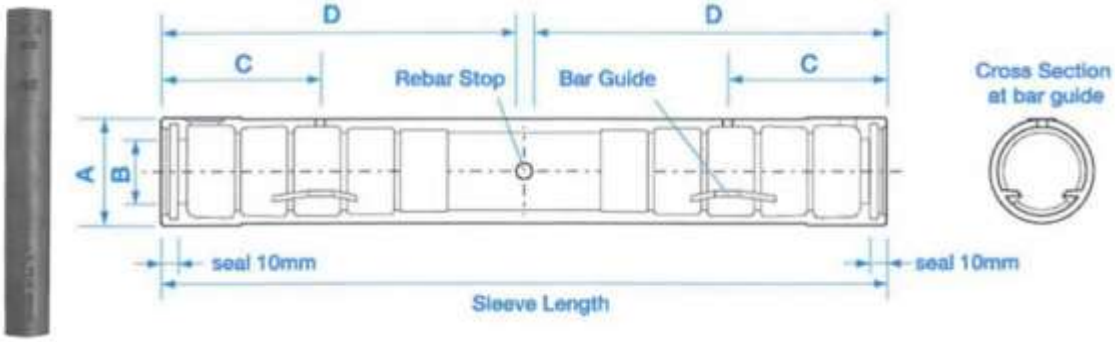

Figure 68: Japan Slim-Sleeve Splice (Splice Sleeve Japan, 2015)

Table 28: Japan Slim-Sleeve Splice dimensions (Splice Sleeve Japan, 2015)

DIMENSIONS OF NMB SLIM-SLEEVES									REQUIRED REBAR EMBEDMENT LENGTH (in.)	
Sleeve No.	Bar Diameter (in.)	Bar Size		Sleeve Length (in.)	Sleeve Diameter (in.)		Set Screw Position (C) (in.)	Rebar Stop (D) (in.)	Min	Max
		ASTM	JIS		O.D. (A)	I.D. (B)				
S6U	0.750	#6	D19	10.63	1.57	0.98	2.13	5.12	4.72	5.31
S8U	1.000	#8	D25	12.99	1.89	1.22	2.76	6.30	5.91	6.50
S9U	1.128	#9	D29	14.57	2.13	1.38	2.95	7.09	6.69	7.28
S11U	1.410	#11	D36	17.72	2.56	1.69	3.94	8.66	8.27	8.86

For SI: 1 inch = 25.4 mm.

3.5.1.2.2. Design of PPCPs using sleeve splices:

Sleeve splices can be used to connect PPCPs if they provide the splice/connection section with the required pile resistance. Accordingly, to design an effective sleeve splice system, two goals

should be achieved. Firstly, to prevent premature failure of the splice system, their failure must happen in the first mode, the rupture of the reinforcing bars outside the sleeve. Secondly, the splice section must provide adequate axial and flexural resistance. The first goal highly depends on the experimental results, including mechanical properties of the bars and sleeve as well as grout tensile and compressive strength. To achieve the first goal, a thorough investigation has been conducted by the authors (see Section 3.5.1.1) so that the proposed splice system here employs sleeve splices that meet the requirements of AASHTO LRFD Bridge Design specification and ACI 318-14, Types 1 and 2. Related to the second goal, the capacity of the splice system is investigated based on the section analysis for the ability of developing the required axial and flexural resistance.

The flexural and axial capacity of splice are calculated based on the section analysis according to ACI 318-14 (ACI Committee, 2014). Therefore, to design this splice system, the number and dimension of the bars as well as sleeves used in the section need to be determined so that it can develop the required strength. The sleeve splice configuration for an FDOT Standard 18" square prestressed concrete pile is studied here as a trial.

3.5.1.2.2.1 18'' square prestressed concrete pile:

Figure 69 shows the 18" square prestressed concrete pile based on the FDOT design standards. Its moment-axial diagram is calculated and plotted according to the following information (FDOT, 2015).

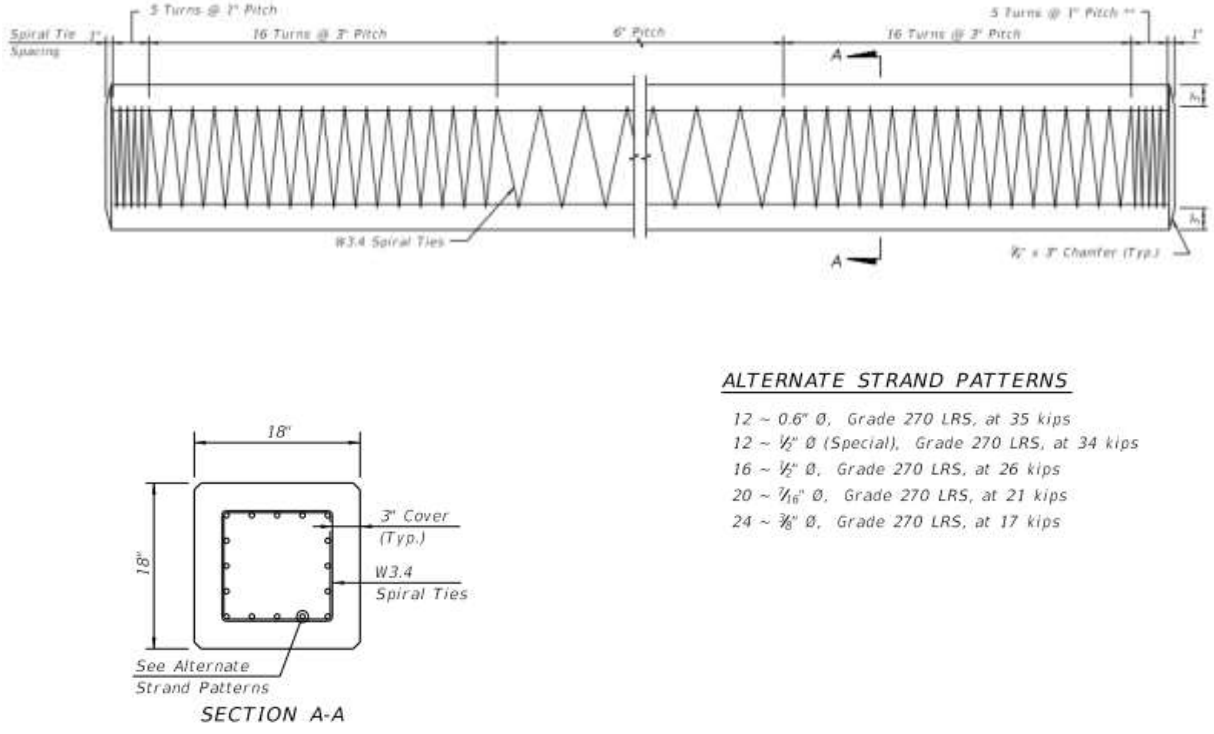

Figure 69: 18" square prestressed concrete pile - FDOT design standards (Florida Department of Transportation, 2021)

Pile Information:

Section Type:	Square
Pile Size:	18'' x 18''
Chamfer:	0.75 in.

Reinforcement:

Pretensioned Strands:

Diameter of Pretensioned Strands:	Typically, 0.5 (Special) in. dia.
Area of Strand, A_{ps}:	0.167 in^2
Strand Layout:	Square
Number of Strands:	12
Strand Modulus, E_{ps}	28500 ksi
Strength of Strand, f_{pu}:	270 ksi
Fraction of f_{pu} used for Initial Stress:	0.75
Initial Strand Stress, f_{po}:	202.5 ksi

Mild Reinforcement (Spiral/Ties):

Spiral

Wire Size:	W3.4
Wire Diameter:	0.208 in.
Minimum Cover to Face of Spiral	3 in.

Concrete Properties:

Specified Concrete Strength f'_c:	6 ksi
Concrete Unit Weight, w_c:	0.15 kcf
Ambient Relative Humidity, H:	75% (Used for creep and shrinkage Loss)
Concrete Ultimate Compressive Strain, e_{cu}:	0.003 in./in.

The moment-axial diagram and required design loads of 18 in. prestressed concrete pile calculated based on the PCI Prestressed Concrete Pile Interaction Diagram Spreadsheet (PCI, 2015) is shown in Figure 70.

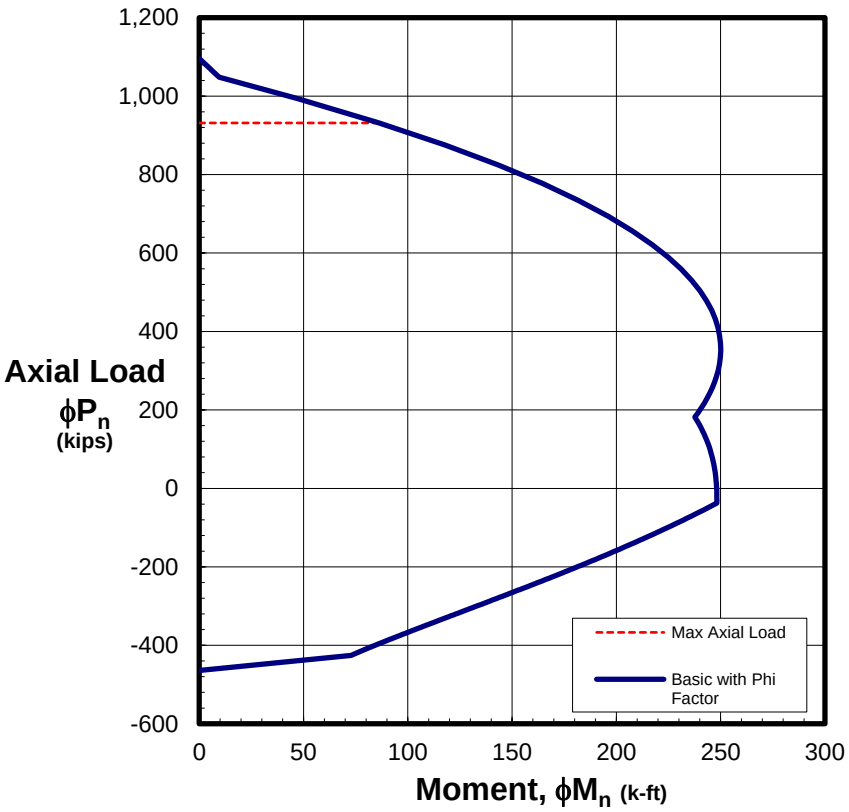

Cross-Section

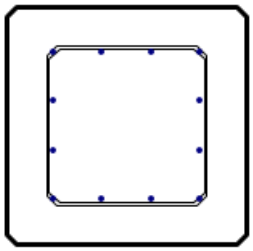

Key Points on Basic Interaction Diagram including ϕ Factors:

	Axial Load, ϕP_n (kips)	Moment, ϕM_n (k-ft)
Pure Compression	1095.8	0.0
Maximum Axial Load	931.5	86.3
Maximum Moment*	351.8	250.1
Comp. Controlled Limit	182.0	237.7
Tens. Controlled Limit	-37.4	248.2
Pure Bending	0.0	247.8
Maximum Tension	-425.6	72.7
Pure Tension	-464.1	0.0

* Based on point of maximum moment before ϕ factors are applied

**In the axial load axis, the positive and negative sign shows the compression and tension, respectively.

Figure 70: M-N interaction diagram for 18 in. prestressed concrete solid pile

As shown in the Figure above, the blue curve shows the M-N interaction diagram without considering the slenderness effect. It goes without saying that with increasing the length of the pile, the slenderness effect will be more so that the capacity of the pile will decrease. Here, to be more conservative, sleeve splices are designed to develop the pile requirements without considering the slenderness effect. Therefore, according to the M-N interaction diagram plotted above, the proposed splice system should be able to develop 247 kip-ft, 932 kips, and 425 kips in moment, compression, and tension, respectively. This compares well with the requirement set forward by FDOT Design Specification. According to FDOT Design Specification, splice systems for 18-in. square prestressed concrete piles shall meet the following requirements (FDOT, 2018):

Compressive strength = (Pile Cross sectional area) x (28-day concrete strength)

Compressive strength= (18''x18'') x (6 ksi) = 1944 kips

Nominal Compressive strength ($\beta1$=0.75) = 0.75 x 1944 kips = 1458 kips

Design Compressive strength (Brittle failure φ=0.65 for M-N Interaction Diagram) = 0.65 x 1458 kips = 947.7 kips

Tensile Strength = (Pile Cross sectional area) x 900 psi

Tensile Strength = (18''x18'') x (0.9 ksi) = 292 kips

Design Tensile Strength (for M-N Interaction Diagram) = 292 kips

Bending Strength: Shall meet the requirement in Table 29

Therefore, in the moment, splice systems should develop 245 kip-feet for a PPCP with an 18" cross-sectional area (FDOT, 2018).

Table 29: Requirement of PPCP splices in developing moment capacity according to FDOT Design Specification (FDOT, 2018)

Pile Size (inches)	Bending Strength (kip-feet)
18	245
20	325
24	600
30	950

As can be seen, the requirement determined by FDOT Design Specification (FDOT, 2018) is comparable to the capacity found from the M-N interaction diagram of 18-in. square prestressed concrete pile in bending and compression (245 kip-ft versus 247 kip-ft and 947 kips versus 932 kips, respectively). However, in tension FDOT Design Specification requires 133 kips less than the capacity that an 18-in. square prestressed concrete pile can develop. This difference can be justified by the fact that FDOT determines this number based on the feasible maximum amount of tension that pile can experience during driving or service. Here, the proposed splices capacity will be compared according to the requirements set forward by FDOT Design Specification.

The number and size of the bars as well as sleeves should be determined by section analysis using ACI 318-14 (ACI Committee, 2014). Table 30 shows the diameter and the length of the typical sleeve couplers, the size of the bars to be joined, and the suggested grout material for filling the sleeve that can be used to connect 18 in. square prestressed concrete pile segments. It is worth mentioning that the grout material can also be selected from Table 21.

Table 30: Typical sleeve splices size for connecting 18 in. prestressed concrete pile segments

Supplier/Brand	Bar Size #	Diameter (inch)	Coupler Length (inch)	Grout
Dayton	8	2.89	16.52	Epoxy
NMB		2.52	14.57	SS Mortar
HSS		2.25	4.93	BCS (Bar Connection Sleeve)
Jpan NMB		2.28	14.57	SS Mortar
Japan slim sleeve*		1.89	12.99	SS Mortar
Dayton	9	2.89	16.52	Epoxy
NMB		2.67	16.34	SS Mortar
HSS		2.56	5.71	BCS (Bar Connection Sleeve)
Jpan NMB		2.48	16.34	SS Mortar
Japan slim sleeve*		2.13	14.57	SS Mortar
Dayton	10	3.04	17.99	Epoxy
NMB		2.87	17.91	SS Mortar
Japan NMB		2.6	17.91	SS Mortar
Japan slim sleeve*	11	2.56	17.72	SS Mortar

*: Bars diameter at both ends should be the same

3.5.1.2.2.2 Design of sleeve splice system for 18-in. square prestressed concrete pile segments

As a trial, the splice system is designed with 8 #10 bars. Figure 71 shows the section detail of 18-in. square prestressed pile spliced with the splice system.

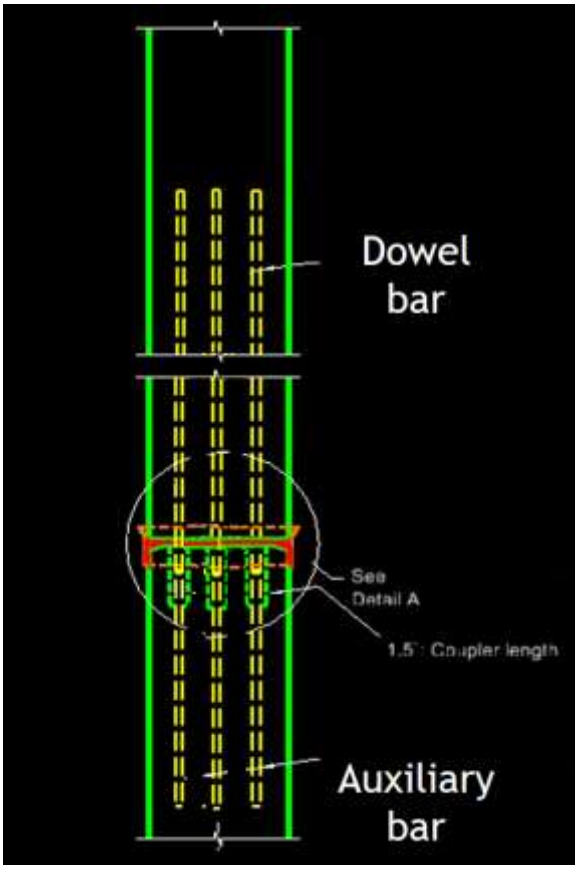

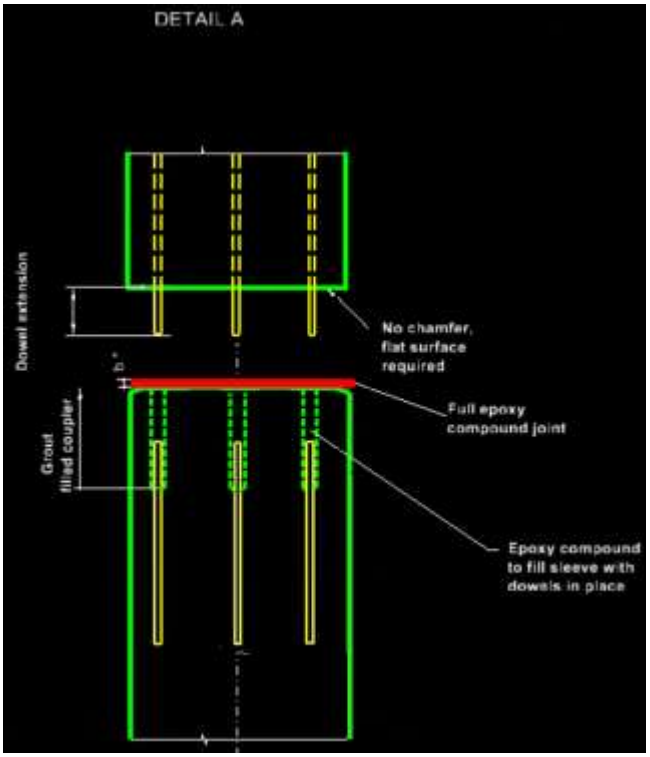

Detail A

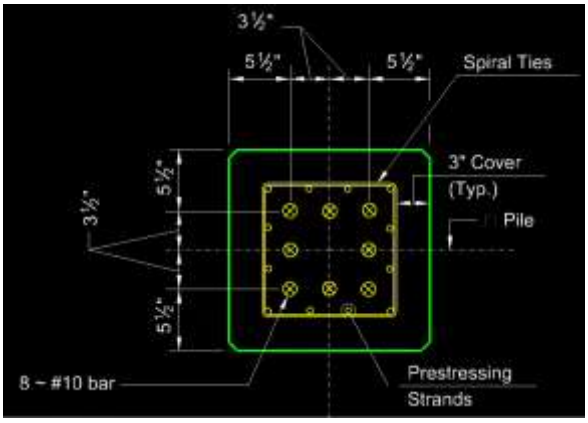

Section B

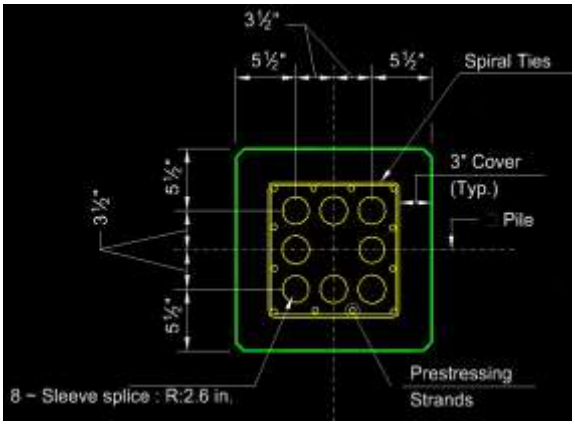

Section C

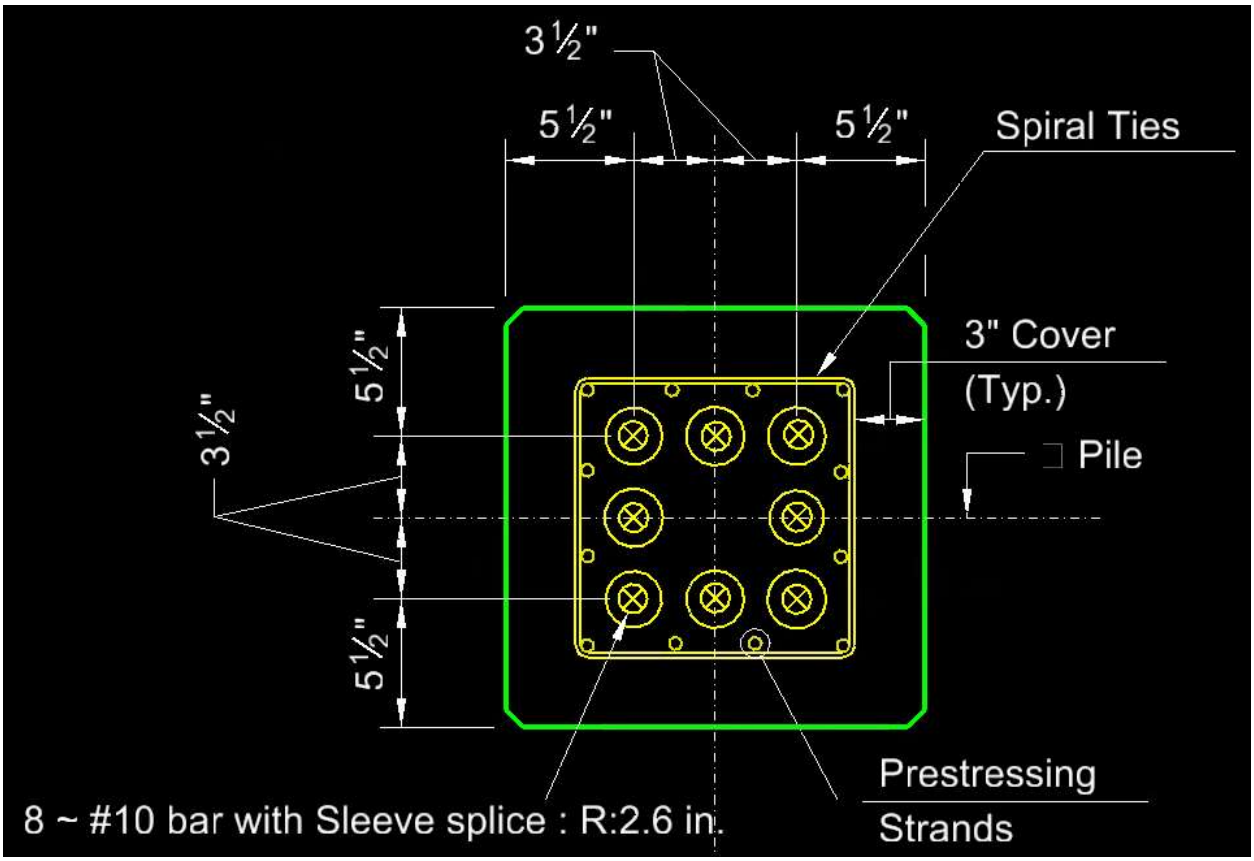

Section E

Figure 71: 18 in. square prestressed pile spliced with 8 - #10 bars

As shown in Section E, eight sleeve couplers are placed into three rows. Three of them in the first and the last row each, and two of them in the middle row, at 5.5 in., 9 in, and 12.5 in. distance from the top of the section, respectively. The spacing is selected to match that in FDOT standard design using epoxy dowels. The moment-axial interaction diagram of 18 in. square prestressed pile spliced with 8 - #10 bars calculated using ACI 318-14, is shown in Figure 72.

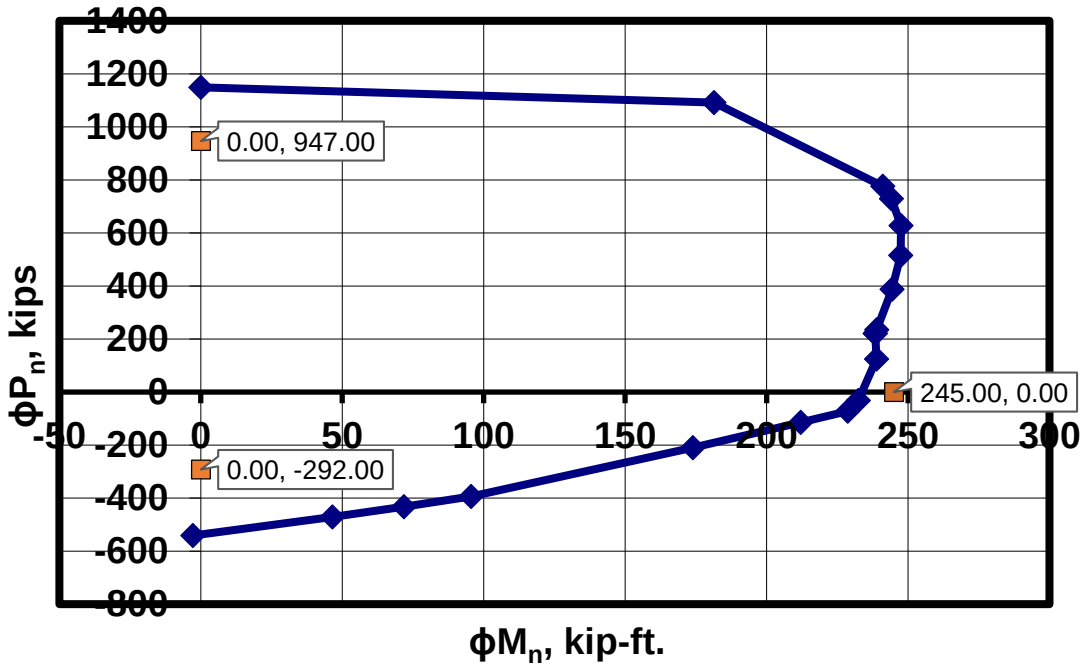

Figure 72: Location of design points in M-N interaction diagram of 18 in. square prestressed pile spliced with 8 - #10 bars

From the M-N interaction diagram shown in Figure 72, the following conclusions can be made:

Pure compression: 1149.3 kips

Pure bending: 234 kips

Maximum bending: 246 kips

Pure tension: -541 kips

The major strength combination for the M-N interaction diagram for the 18" PPCP required by FDOT Design Specification is also shown in Figure 72.

As shown in Figure 72, the proposed splice system can develop the full capacity of the pile section in compression and tension and 96% of the pile capacity in bending. However, as it can be seen in Figure 71, Section E, there is enough space to provide the section with a higher amount of moment capacity. In other words, by placing the sleeve couplers on the farthest possible left and right as well as top and bottom, symmetrically, a larger moment arm will be produced which will provide for a higher moment capacity. With this in mind, the splice system can be designed with smaller bars and sleeve sizes and diameters.

Therefore, considering placing the bars at the farthest possible location, the M-N interaction diagram for 18 in. square prestressed pile spliced with 8- #10 bars, 6- #10 bars, 9- #9 bars, 8- #9 bars, 9- #8 bars, and 8- #8 bars were calculated using ACI 318-14 (ACI Committee, 2014) and are plotted in Figures 73 through 78, respectively.

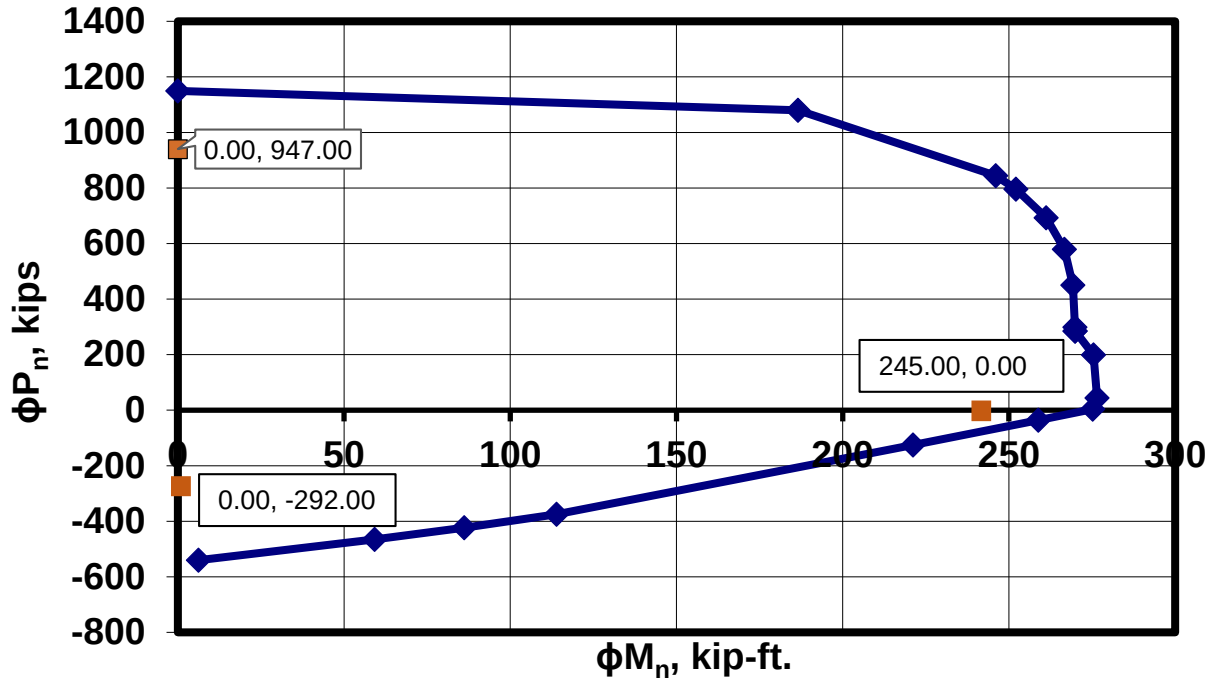

Figure 73: Moment-axial interaction diagram of 18 in. square prestressed pile spliced with 8 - #10 bars

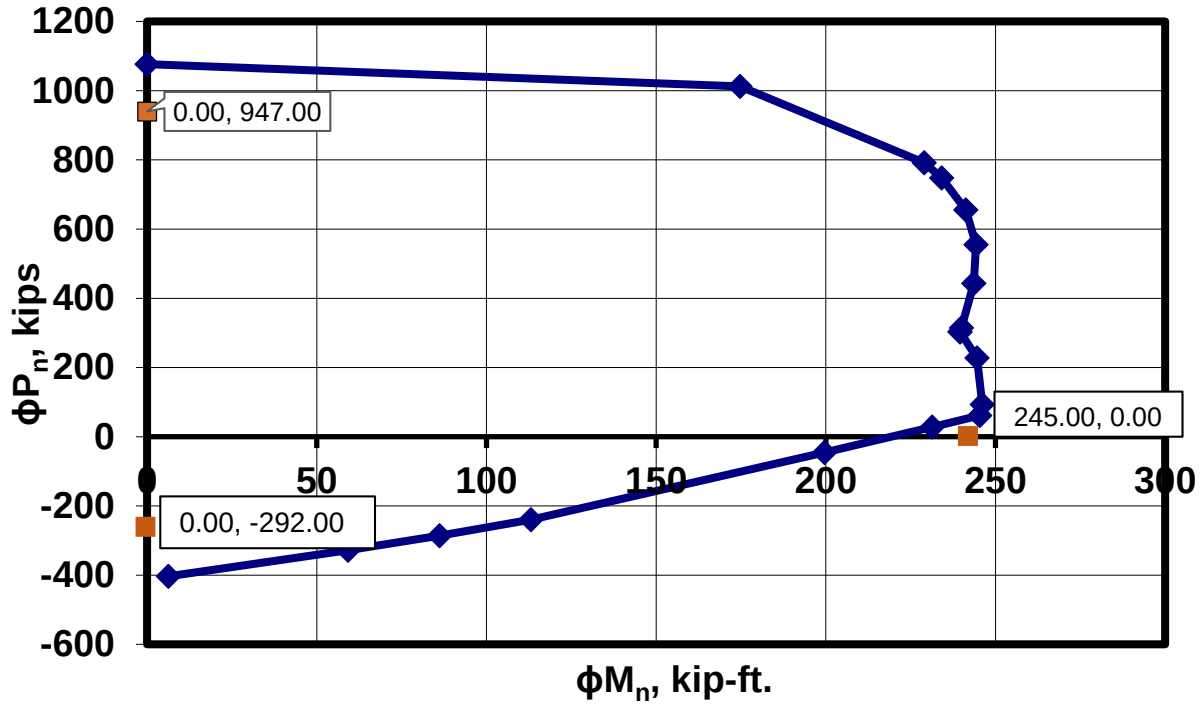

Figure 74: Moment-axial interaction diagram of 18 in. square prestressed pile spliced with 6 - #10 bars

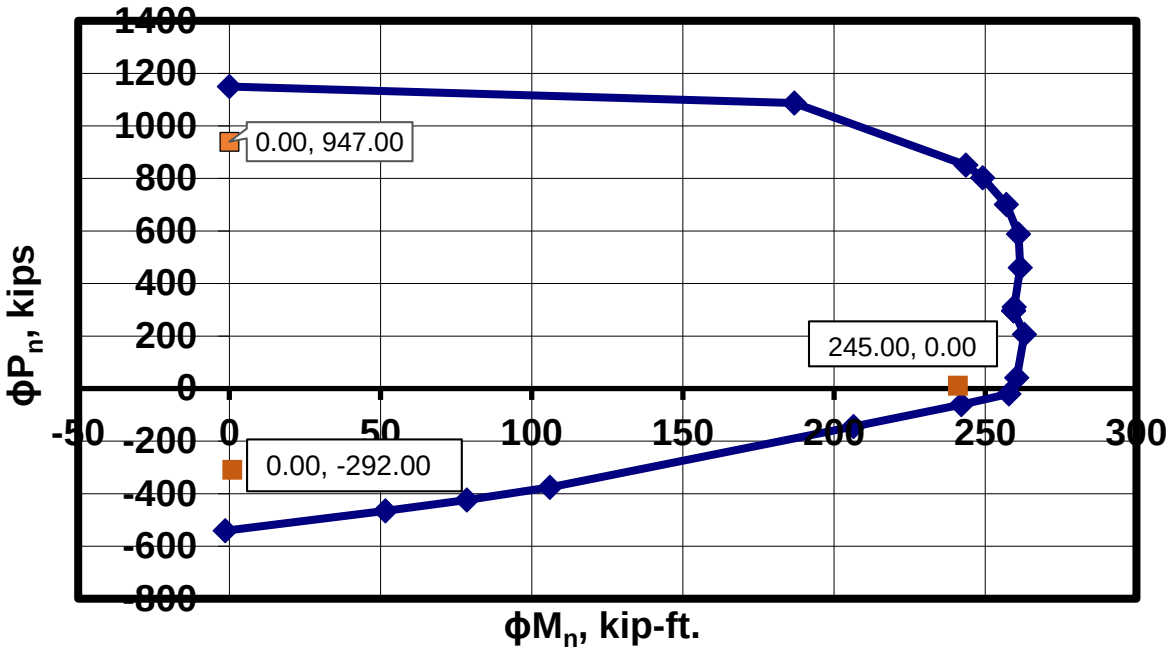

Figure 75: Moment-axial interaction diagram of 18 in. square prestressed pile spliced with 9 - #9 bars

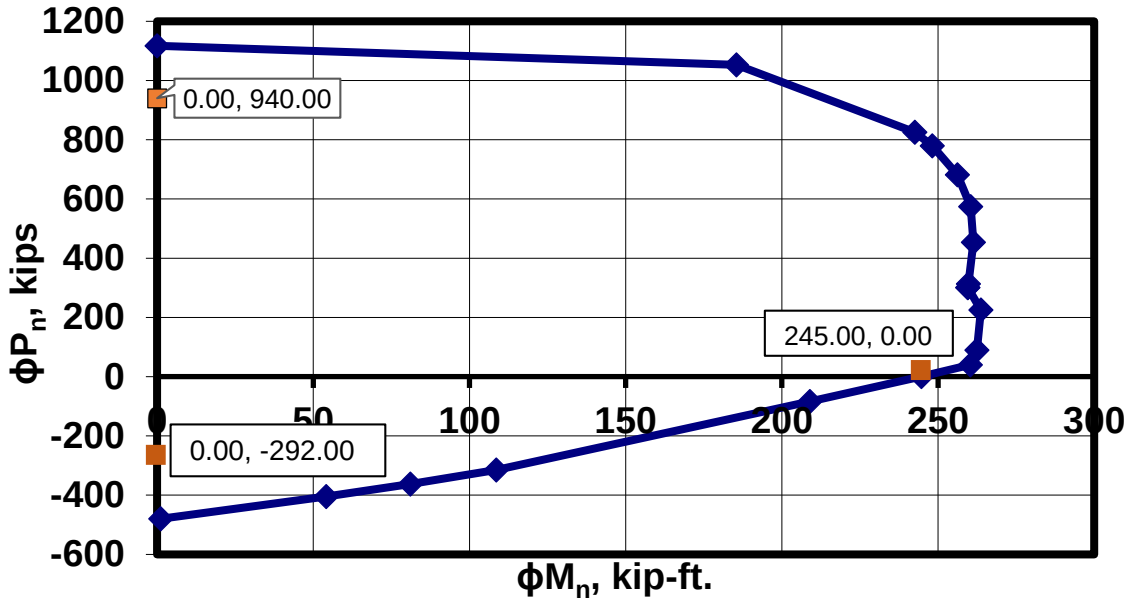

Figure 76: Moment-axial interaction diagram of 18 in. square prestressed pile spliced with 8 - #9 bars

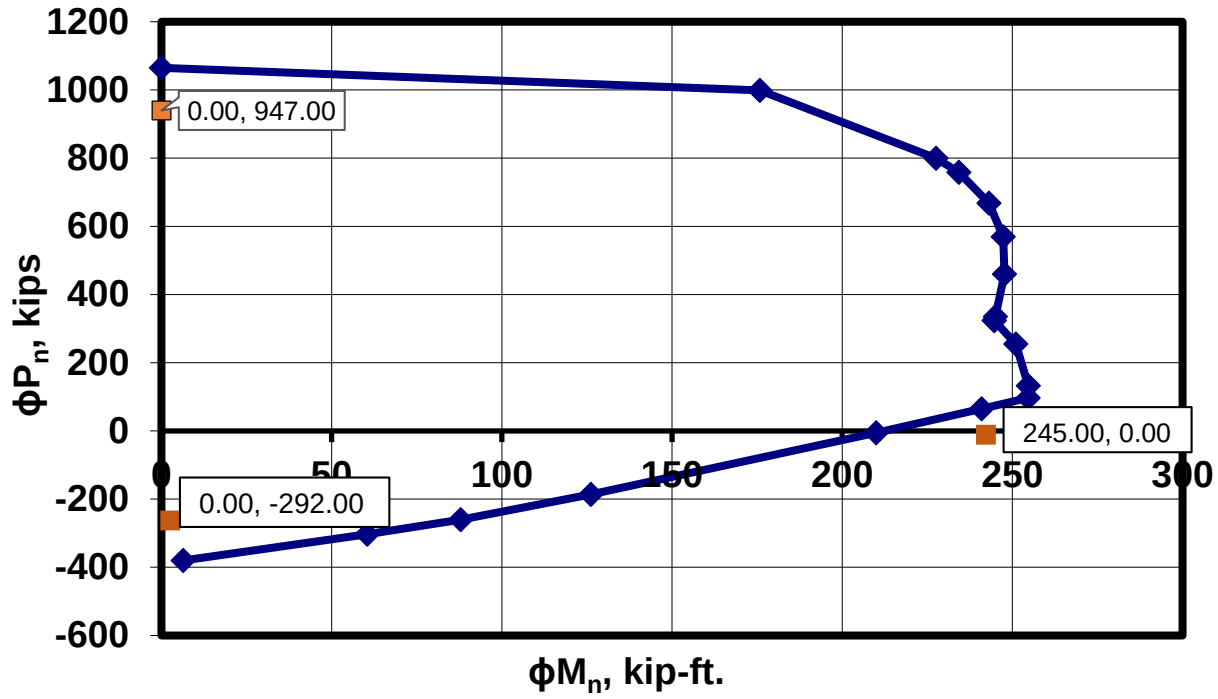

Figure 77: Moment-axial interaction diagram of 18 in. square prestressed pile spliced with 9 - #8 bars

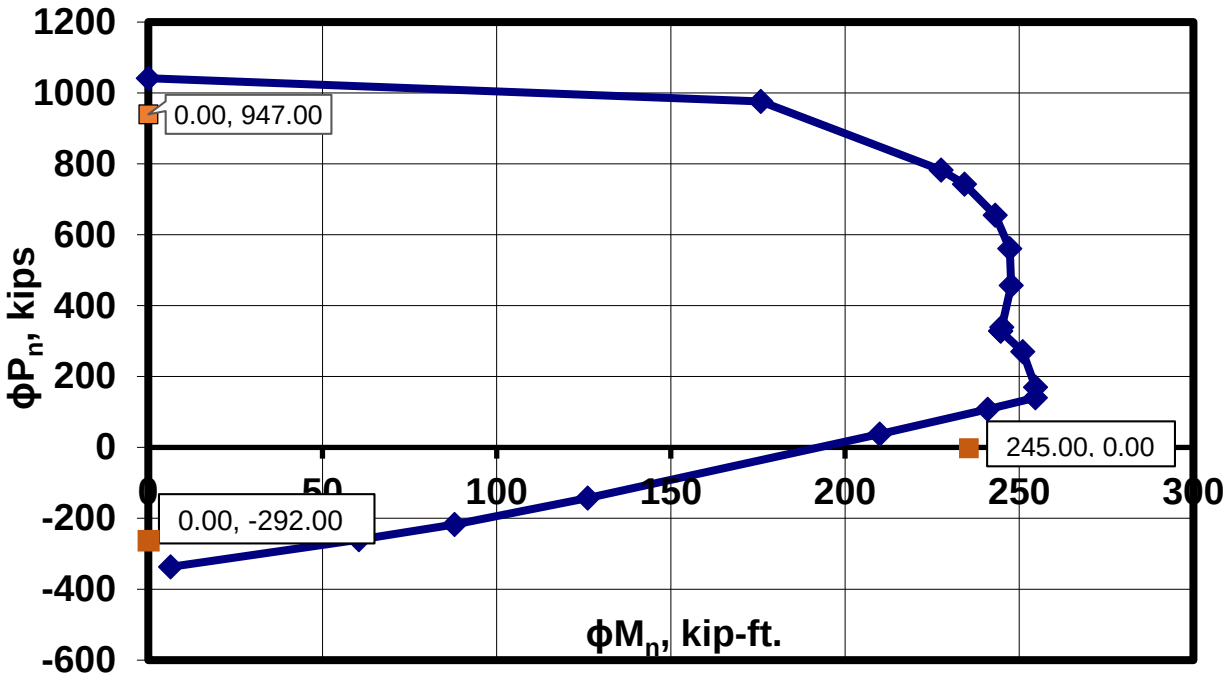

Figure 78: Moment-axial interaction diagram of 18 in. square prestressed pile spliced with 8 - #8 bars

From the M-N interaction diagrams plotted above, it can be concluded that owing to placing the sleeve splices at the farthest possible location, the required pile strengths in the bending, compression, and tension are developed with the smaller size of bars and sleeves. Table 30 shows the comparison of section capacity with the required moment, tension, and compression with various number and size of bars (and sleeves).

Table 30: Comparison of moment and tension resistance for number and size of bars

Bars			Axial and Flexural checking		
Number	# Size	Nominal diameter of bar- in.	Development of Tension and Compression (%)	Moment kip-ft	Development of Moment (%)
8	8	1	More than 100 %	210	86
9	8	1		210	86
8	9	1.128		260	105
9	9	1.128		260	105
8	10	1.27		270	110
6	10	1.27		240	98

3.5.1.2.2.3 Advantages over existing methods, impact on the construction field, and other applications

The new technology is superior to all existing methods because; a) it can be applied considerably easier, b) requires little modifications to the pile segments to be spliced, c) it is very labor-friendly and can save a great deal of time, d) it is lightweight and environmentally friendly, e) it provides for the required strength rapidly to allow pile driving to continue, and f) the required pile strengths can be developed with smaller size of bars which can save cost and time. Currently, FDOT practices epoxy dowel technique for splicing 18" square PPCPs in which 8-#10 bars are used; however, with the proposed system, the splice can be performed with 6-10# or 8-#9 bars. It should be noted that the system requires the use of auxiliary bars to develop the splice capacity into the pile segment and transfer to the strands. Their development length should be calculated accordingly. Also noted that this system will only work for the case of preplanned pile splices.

This technique will have a major impact and considerably improve the construction operation for splicing driven piles. It will also significantly enhance the strength and durability of spliced piles. With the use of corrosion-resistant materials, the durability of pile splices in marine and corrosive environments will also be increased remarkably.

3.5.2. FRP Sheet/Jacket splice system:

The FRP sheet/jacket concept has been developed as an innovative alternative to the existing methods to connect driven pile segments both in unforeseen and preplanned situations. The new system provides excellent advantage especially for the unforeseen condition when other splice systems fail to provide the required capacity. The system consists of FRP sheets and an alignment bar. One or more layers of FRP sheet are attached to each side of the pile segment at the joint location with the use of resin. An alignment bar protruded from the upper pile segment is placed into a hole at the center of the bottom pile segment to facilitate the installation as well

as ensure the alignment (Figure 79). This hole can be cast for the case of preplanned and drilled for the case of unforeseen splices. An equal amount of FRP is required on each face of the pile. The FRP for splicing can also be fabricated in a jacket form with four sides already connected like a box. In this case, the jacket can be pre-fitted and pre-attached to the upper pile segment at the precast plant (Figure 80). Many factors should be considered in designing the FRP sheet/jacket splice system: 1- the mechanical properties of FRP sheets; 2- the thickness and the number of layers in each side; and 3- the required length of FRP sheets/jacket for developing the tension in the FRP sheet (transfer of stresses to concrete and therefore to the strands in the pile) and preventing debonding of FRP sheets from concrete. Special restraint against peeling off edges and tapering the sheet ends to reduce resistance against driving are provided by addition of FRP strips in perpendicular direction. These strips will also serve as shear reinforcement at splice. The thickness and number of FRP strips as well as the spacing between them are calculated for shear resistance and confinement. In lieu of strips, bi-directional FRP sheets/jackets can be used to address the shear strength in addition to flexural capacity.

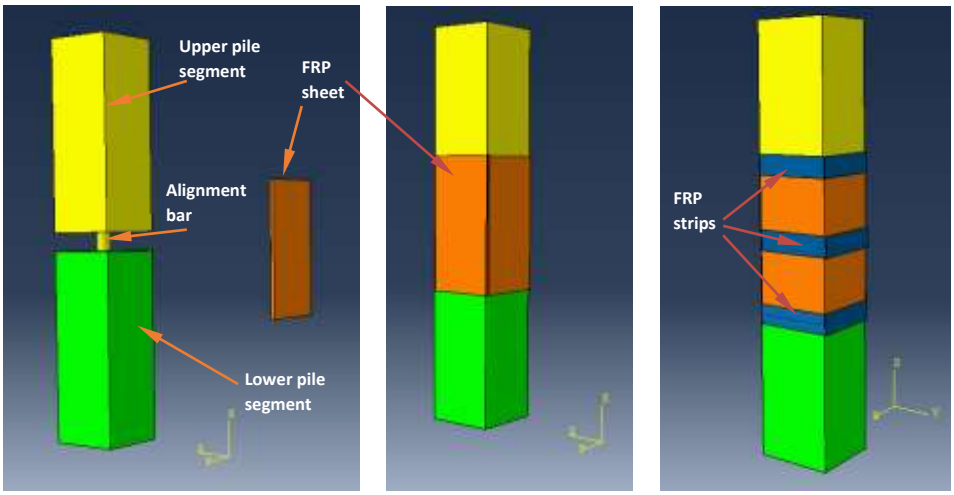

Figure 79: FRP sheet splice

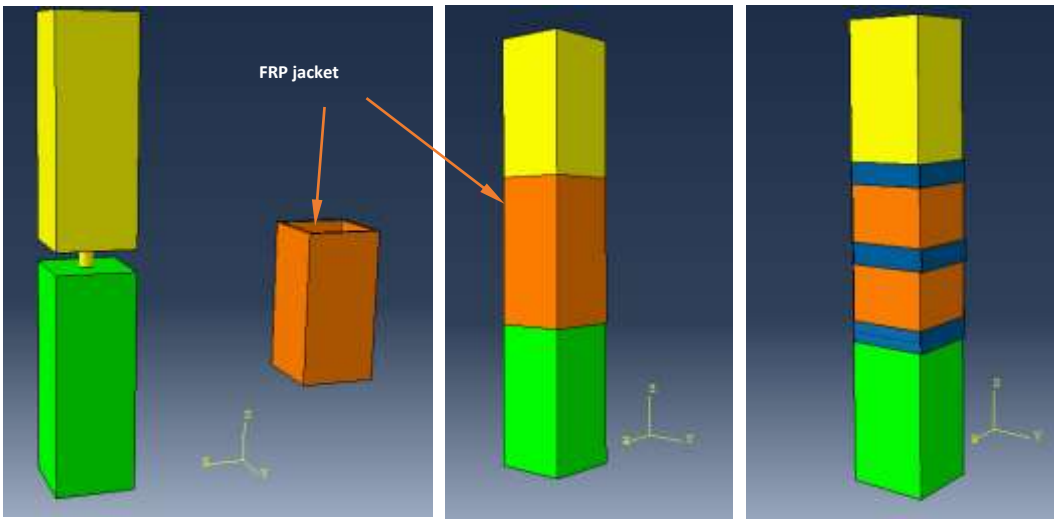

Figure 80: FRP jacket splice

Based on the size of piles in a specific construction project, the designer will determine the number of splices to be made at the site. Accordingly, the material list for the contract will include the number of sheets, the length, width, number of layers, the thickness of sheets, and the amount of resin required for installation. As discussed, for each pile splice, four sheets or one jacket is needed. The sheets can come already tapered in thickness at their ends. FRP strips will come on a spool with a pre-specified width and thickness. Alternatively, FRP single-layer sheets can be delivered to the site for layer-by-layer application.

Figure 81 shows an example for section detail for 18x18" prestressed pile spliced using FRP sheets.

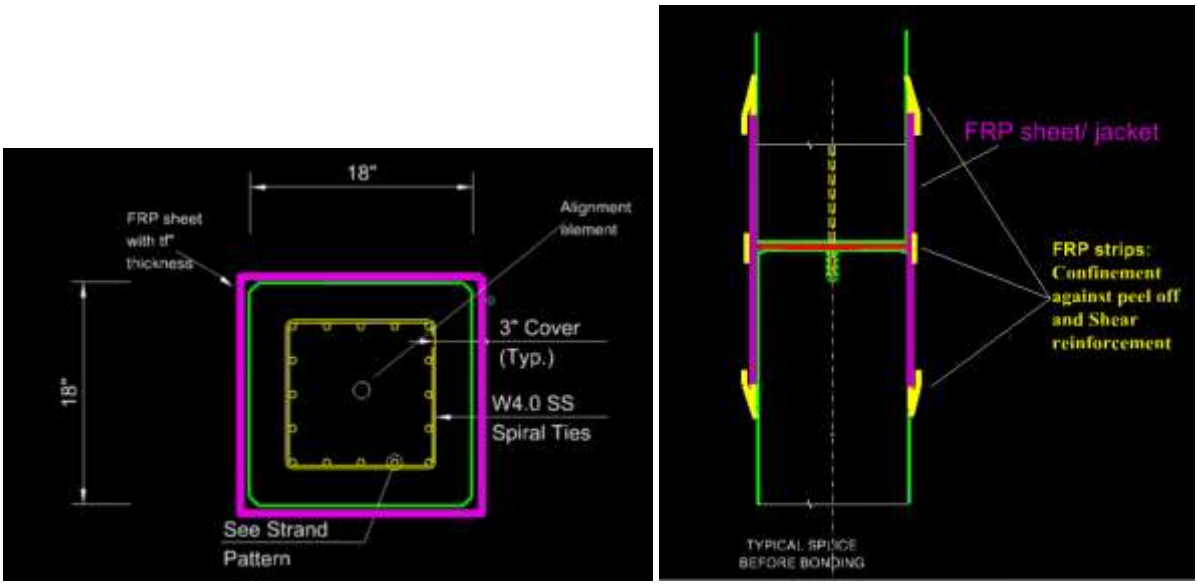

Figure 81: 18 in. square prestressed pile spliced with FRP sheet

For FRP sheet/jacket splice system subjected to pure bending, three failure scenarios are possible. The failure may initiate with the crushing of concrete that is the most preferred failure for FRP reinforced concrete elements with ductility consideration. Failure initiated with FRP rupture is the least preferred mode of failure and shall be avoided as much as possible. The third type of failure is associated with debonding or bond failure between FRP and concrete. The latter is believed to perform more favorable than rupture of FRP. For the case of pile splice, compressive forces will exist in the section in addition to possible bending. As such, the failure mode will shift closer to concrete crushing with increasing axial compressive load.

3.5.2.1. Time required for installation

Installation of FRP sheet/jacket splice system involves application of epoxy resin and grout which required time for curing and developing the required strength. An in-depth investigation was conducted on the workability, setting, and curing time for a variety of available epoxy resin and other grout materials to provide the user the best possible option for establishing splice connection (Khedmatgozar Dolati & Mehrabi, 2021). The results of this investigation demonstrated that epoxy grouts have working time in the range of 0.13 to 0.7 hrs. and setting time in the range of 0.2 to 0.27 hrs. They reach an average compressive strength of 3000 psi in 2

hrs. and about 6000 psi in one day. Similar data indicates a tensile strength for epoxy resins in the range of 7000 to 10000 psi depending on temperature with curing time between 12 to 24 hrs (https://usa.sika.com). Accordingly, establishing and curing a sheet/jacket splice connection would require less than 1 day.

3.5.2.2. Advantages of the FRP sheet/jacket splice system:

The new splice system is advantageous to existing methods because; a) it is considerably easier and safer to implement, b) requires little or no modifications to the pile segments to be spliced, c) the contractor can be trained easily to apply this technology, d) it is durable and corrosion-resistant and will perform better in the marine environment, e) it is environmentally friendly and lightweight, f) it provides for the required strength rapidly to allow driving of the pile to continue, g) it overcomes the shortcomings of unforeseen splices that are unable to provide the required splice strength, h) and more importantly, it is applicable to both preplanned and unforeseen splices. This technique will impact positively and considerably improve the construction operation for splicing driven piles. It will also provide for significant improvement for strength and durability of spliced piles, especially for unforeseen splice situations.

3.5.3. NSM FRP pile splice method:

The NSM FRP Pile Splice concept is developed as an alternative to the existing methods to connect driven pile segments both in preplanned and unforeseen situations. The new method provides excellent advantage especially for the unforeseen condition when other splice systems fail to provide the required capacity. The method consists of using FRP bars and strips, and an alignment element. When splicing is needed, the pile driving operation pauses, the upper pile segment is lowered and erected on top of the lower segment (Fig. 82d). To help the operation, an alignment bar protruded from the upper pile segment is placed into a hole at the center of the bottom pile segment to facilitate the installation as well as ensure the alignment (Fig. 82c). This hole can be cast for the case of preplanned and drilled for the case of unforeseen splices. Filler/bonding compound, normally epoxy grout is used inside the alignment hole in the lower segment and at the interfaces of the two pile segments. In the next step, for the case of unforeseen splicing, longitudinal grooves with required length and dimension are cut into the concrete cover of pile segments on both sides of the splice at joint location (Fig. 82e). For the case of preplanned splicing, the grooves can be precut or cast at the precast plant. FRP bars are then placed into the grooves and bonded therein with a suitable grout/filler (typically epoxy or cementitious material) (Fig. 82f). Figure 82 shows this method for connecting driven pile segments in an unforeseen situation (a: drilling hole in bottom pile segment, b and c: cutting grooves and placing an alignment bar in upper pile segment, d: placing upper segment on the bottom segment, e) cutting the same dimension of grooves in the bottom segments, and f) inserting the bars into the grooves and filling the groves with grout injection). It goes without saying that for the case of preplanned splicing, each segment can be prepared with all modifications before shipping to the site which makes this method even easier and faster to be implemented.

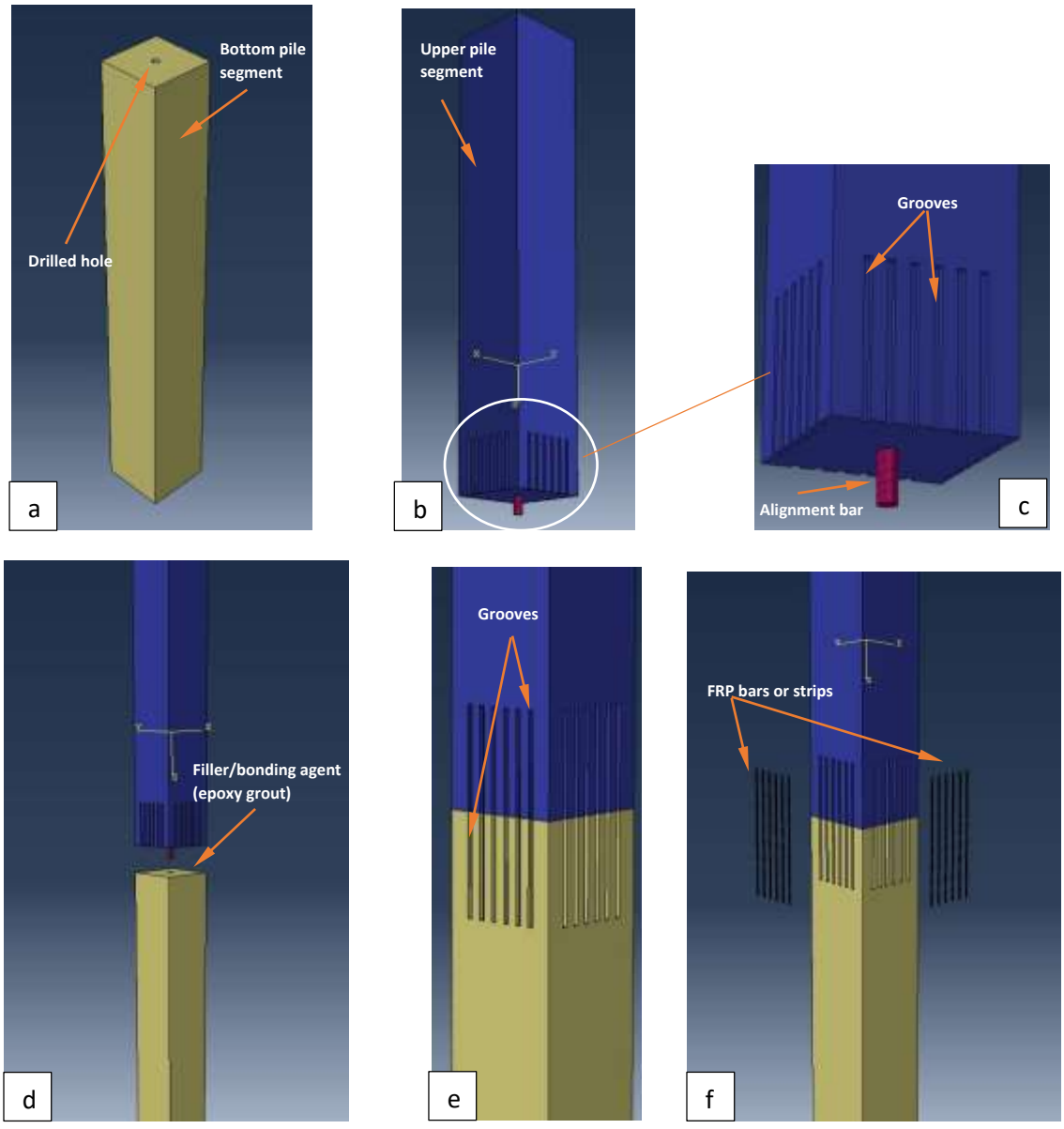

Figure 82: NSM FRP technique for splicing driven pile segments

Many factors should be considered in designing NSM FRP splice. These include the mechanical properties of FRP bars, the number as well as sizes of the FRP bars in each side, the required development length of bars (to transfer the stresses to concrete and therefore to the strands in a pile), the depth and dimension of the groove as well as their distance from each other and the edge of pile section, and the filler/bonding material properties. The grout dimension and depth should be calculated in a way that prevents debonding of FRP bars.

Near Surface Mounting (NSM) method can also be used with steel reinforcing bars including normal, high strength, and stainless steel. However, using FRP bars compared to steel in the proposed method provides many advantages such as resistance to corrosion, ease and speed of

installation (due to its lightweight), and the smaller groove size (due to the higher tensile strength).

In this splicing method, FRP strips in transverse direction are also provided to serve as shear reinforcement and special restraint to peeling and premature debonding of the bars, especially at the splice ends. These strips can also cover the entire length of surface mounted splice bar plus 6 in at both ends (with very thin thickness) serving as another layer of corrosion resistant barrier. The thickness and number of FRP strips as well as the spacing between them will be calculated for shear resistance and confinement. Figure 83 shows the NSMB splice method after applying FRP strips.

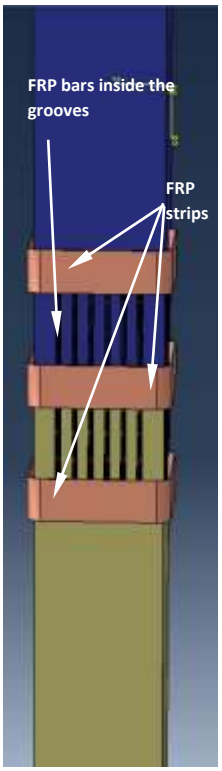

Figure 83: NSM FRP splice

Figure 84 shows an example for section detail for 18x18" prestressed pile spliced using NSM FRP splice system.

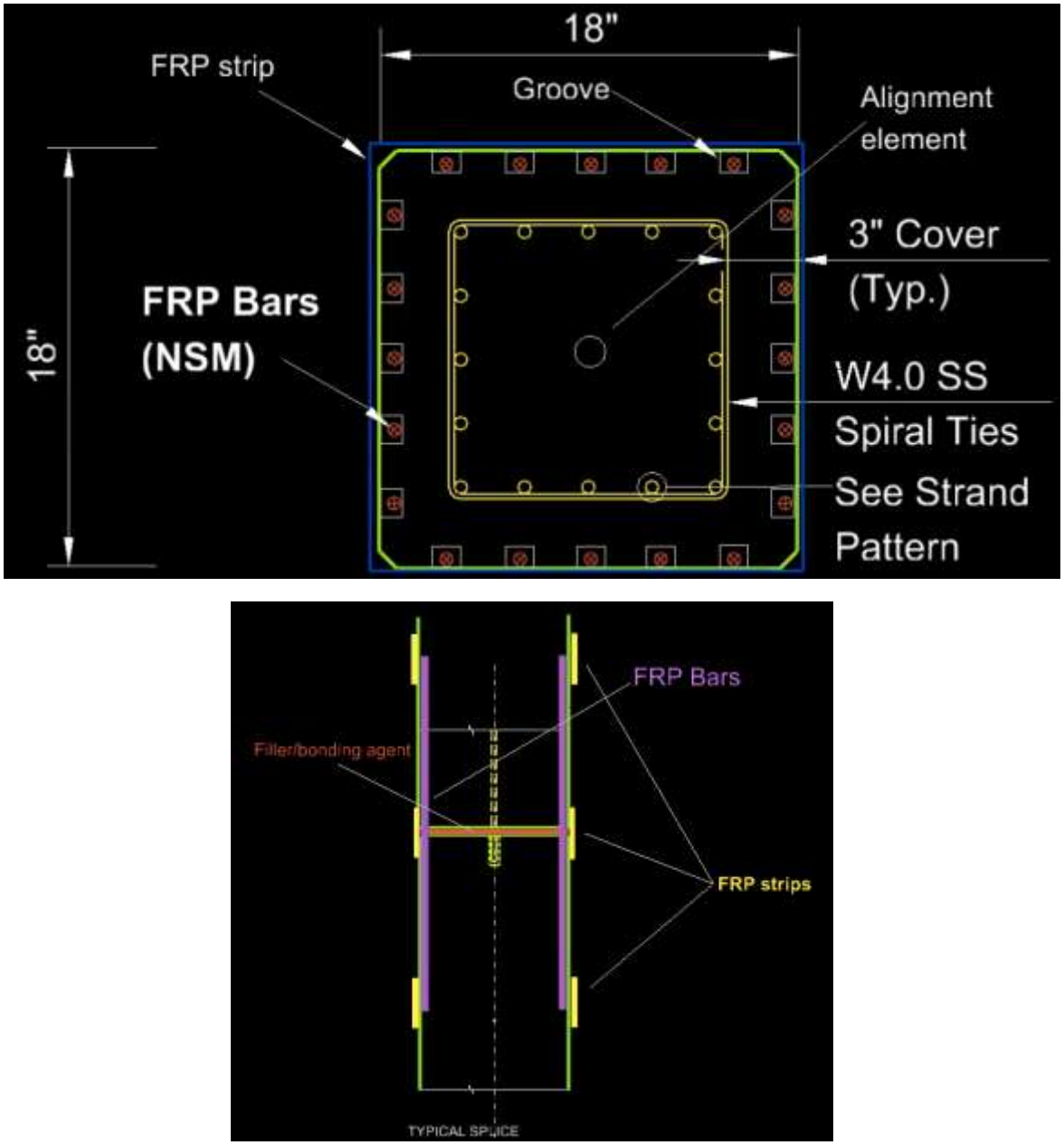

Figure 84: Section detail of the designed splice system

3.6. Comparison of currently available splicing methods with the new FRP methods

The qualitative comparison of the newly developed splicing methods with the currently available splicing methods is shown in Table 31 in terms of:

- Ease of application: This item compares the time and work required to prepare and assemble the splice system considering the precast plant and the field.
- The possibility to perform the splice system in unforeseen situation
- Cost: It involves the cost for manufacturing and installation of the splice system
- Capacity: It indicates the ability of the splice system in providing the required capacity in tension, compression, and flexure.

- Durability: It accounts for the performance of the splice system in corrosive environments

Table 31. Comparison of pile splices

Type of Splice	Possibility to perform in unforseen situation	Capacity	Ease of application	Durability (Corrosion-resistant)	Cost
Epoxy-Dowel	Yes *	Poor	Time consuming	Low**	Low
Bolted	No	Good	Moderate	Moderate	Moderate
Mechanical	No	Good	Easy***	Moderate	High
Post-tensioned	No	Good	Difficult	Moderate	Moderate
Wedge	No	Good	Difficult***	High	High
Welded	No	Good	Moderate	Low	Moderate
Bar couplers	No	Good	Easy	Low**	Low
FRP sheet/jacket	Yes	Good	Easy	High	Low
NSM FRP system	Yes	Good	Easy	High	Low
Tube	No	Moderate	Difficult	Moderate	Moderate

* The required capacity of pile segment will not be achieved
** With the application of FRP materials for dowels and reinforcement : High
*** Difficult at precast plant

This comparison is made using the information provided by the literature and other investigations reviewed in this study. From the table above, it can be concluded that the new splice systems are superior to other types as they can overcome shortcomings attributed to others. The application of FRP materials in the proposed splices provides corrosion-resistant properties, making them popular for marine environments.

Task 3 – Modeling and Analysis

The candidate details and configurations identified in the previous task will be analyzed using FE modeling and section analysis, and their structural performances will be compared to that of the existing splice details. This should result in selection of few configurations as most promising splice connections.

Section analysis was performed as reported above. This can be expanded in the upcoming progress reports.

Task 4 – Constructability Analysis

The most promising configurations will be scrutinized for their constructability according to ease of implementation, time to use, and cost.

Constructability analysis was performed during sectional analysis as reported above. The system developed for connecting PPCPs using grouted sleeve couplers of various configurations can be easily positioned at splices, their application and installation is easy, and no constructability issue is anticipated with this splice type. This discussion can be expanded in the upcoming progress reports.

Task 5 – Design Considerations

Means and methods for designing the selected splice connections will be investigated. The results will be organized in the form of a design procedure.

Design considerations were covered in the analysis reported above. This discussion can be expanded in the upcoming progress reports.

Task 6 – Draft and Final Report

A comprehensive draft final report including the activities performed in the previous tasks will be prepared and submitted first for review by the research advisory panel (RAP). The report will identify the alternative splice connection(s) for prestressed-precast concrete piles, and will attempt to provide an analysis and design procedure. After incorporating the comments received from RAP, the final report will be submitted to ABC-UTC for publication on the website.

4. Schedule

Progress of tasks in this project is shown in the table below.

Item	% Completed
Percentage of Completion of this project to Date	90%

Duration of this project is 25 months. Scope and timeline for various tasks are shown below.

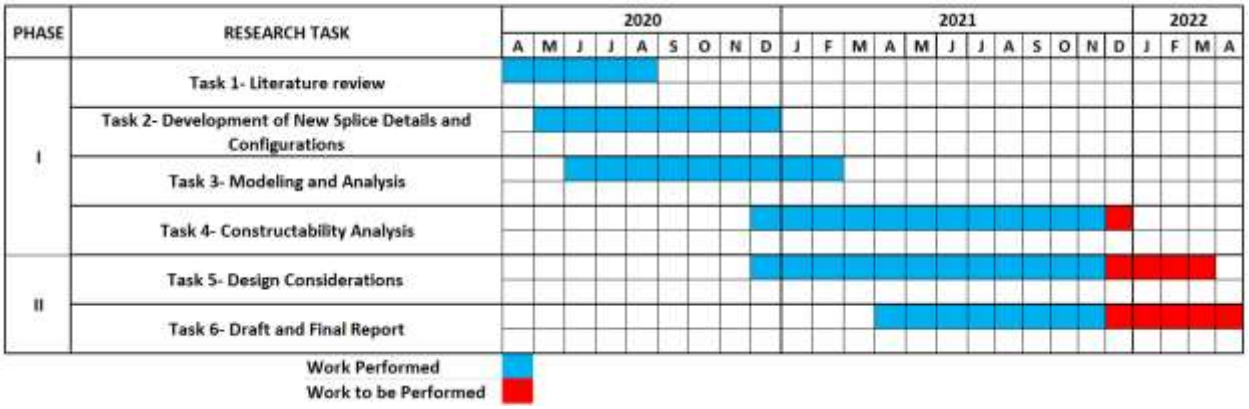

5. Reference

AASHTO (2017) AASHTO LRFD Bridge Design Specifications (8th ed.). Washington, D.C.: American Association of State Highway and Transportation Officials.

ACI-209R. (1998). Prediction of creep, shrinkage, and temperature effects in concrete structures. American Concrete Institute ACI Detroit, USA.

ACI Committee (2014) '318, Building Code Requirements for Structural Concrete (ACI 318–14) and Commentary (ACI 318R–14)', American Concrete Institute, Farmington Hills, MI, p. 519.

ASTM, A. (2014). C173/C173M-14-Standard Test Method for Air Content of Freshly Mixed Concrete by the Volumetric Method. USA: ASTM International.

ASTM, C. (1996). 496-96 "Standard Test Method for Splitting Tensile Strength of cylindrical Concrete Specimens." American Society for Testing and Materials.

ASTM, C. (1999). 882-99–Standard test method for bond strength of epoxy-resin systems used with concrete by slant shear. American Society for Testing and Materials.

ASTM, C. (2001). 1437-01. Standard test method for flow of hydraulic cement mortar. ASTM International, Pennsylvania.

ASTM, C. (2002). C 39-49. Compressive Strength of Molded Concrete Cylinders.

Alias, A. et al. (2014) 'Performance of grouted splice sleeve connector under tensile load', Journal of Mechanical Engineering and Sciences (JMES), 7, pp. 1096–1102.

Alley, E. W. (1970). Long Prestressed Piles. *Civil Engineering*, *40*(4), 50.

Annual, A. (1994). Book of Standards. A536-84, 1, 303

Belarbi, A., Dawood, M., Bowman, M., & Mirmiran, A. (2017). *Synthesis of concrete bridge piles prestressed with CFRP systems.* Texas. Dept. of Transportation. Research and Technology Implementation Office.

Belleri, A. and Riva, P. (2012) 'Seismic performance and retrofit of precast concrete grouted sleeve connections'. Prestressed Concrete Institute.

Bruce Jr, R. N., & Hebert, D. C. (1974a). Splicing of Precast Prestressed Concrete Piles: Part 1—Review and Performance of Splices. *PCI JOURNAL*, *19*(5), 70–97.

Bruce Jr, R. N., & Hebert, D. C. (1974b). Splicing of Precast Prestressed Concrete Piles: Part 2—Tests and Analysis of Cement-Dowel Splice. *PCI JOURNAL*, *19*(6), 40–66.

Canner, I. W. (2005). *Field Testing of Prestressed Concrete Piles Spliced with Steel Pipes*. University of Florida.

Cohagen, L. S. et al. (2008) A precast concrete bridge bent designed to re-center after an earthquake. TransNow Seattle, WA.

Çolak, A. (2001). Parametric study of factors affecting the pull-out strength of steel rods bonded into precast concrete panels. International Journal of Adhesion and Adhesives, 21(6), 487–493.

Cook, R. A., & McVay, M. C. (2003). *Alternatives for Precast Pile Splices*. University of Florida.

Culmo, M P. (2009). Connection Details for Prefabricated Bridge Elements and Systems (No. FHWA-IF-09-010). *Federal Highway Administration—US Department of Transportation: McLean, VA, USA.*

Culmo, Michael P, Marsh, L., Stanton, J., & Mertz, D. (2017). *Recommended AASHTO Guide Specifications for ABC Design and Construction*.

Dayton Superior Corporation. (2018). Dayton Sleeve Splices.

De la Varga, I., & Graybeal, B. A. (2015). Dimensional stability of grout-type materials used as connections between prefabricated concrete elements. Journal of Materials in Civil Engineering, 27(9), 4014246.

Einea, A., Yamane, T. and Tadros, M. K. (1995) 'Grout-filled pipe splices for precast concrete construction', Pci Journal. Citeseer, 40(1), pp. 82–93.

Florida Department of Transportation. (2021). Standard Plans - FY 2021-22. https://www.fdot.gov/design/standardplans/current/default.shtm#Bridges

FDOT. (2018). Standard specifications for road and bridge construction. FDOT Tallahassee, FL.

Fleming, K., Weltman, A., Randolph, M., & Elson, K. (2008). *Piling engineering*. CRC press.

Gamble, W. L., & Bruce Jr, R. N. (1990). Tests of 24 in. Square Prestressed Piles Spliced With ABB Splice Units. *PCI JOURNAL*, *35*(2), 56–73.

Gerwick Jr, B. C. (1968). General Report—Prestressed Concrete Piles. *Proceedings*, 1–30.

Grace, N. (2007). 5-years monitoring of first CFRP prestressed concrete 3-span highway bridge in USA. *Proceedings of the 12th International Conference on Structural Faults & Repair-2008*.

Haber, Z. B. (2013) Precast column-footing connections for accelerated bridge construction in seismic zones. University of Nevada, Reno.

Henin, E. and Morcous, G. (2015) 'Non-proprietary bar splice sleeve for precast concrete construction', Engineering Structures. Elsevier, 83, pp. 154–162.

Horeczko, G. (1995). Marine application of recycled plastics. *Restructuring: America and Beyond*, 834–837.

Iskander, M. (2003). FRP composite piling practice. *Proc. Soil Rock America 2003, XII Panamerican Conference on Soil Mechanics and Geotechnical Engineering, MIT, Cambridge, USA*, 1851–1857.

Iskander, M. G., & Hassan, M. (1998). State of the practice review in FRP composite piling. Journal of Composites for Construction, 2(3), 116–120.

Jansson, P. O. (2008). Evaluation of grout-filled mechanical splices for precast concrete construction.

Khedmatgozar Dolati, S. S., & Mehrabi, A. (2021). Review of available systems and materials for splicing prestressed-precast concrete piles. Structures, 30, 850–865. https://doi.org/https://doi.org/10.1016/j.istruc.2021.01.029

Korin, U. (2004). Mechanical splicer for precast, prestressed concrete piles. System, 79.

Li, Y., Zhou, X.-P., Qi, Z.-M., & Zhang, Y.-B. (2014). Numerical study on girth weld of marine steel tubular piles. *Applied Ocean Research*, *44*, 112–118.

Liu, T. C.-Y. (1970). Prestressed Concrete Piling-Contemporary Design Practice and Recommendations. *Journal Proceedings*, *67*(3), 201–220.

Mantawy, I., Chennareddy, R., Genedy, M., & Taha, M. R. (2019). Polymer Concrete for Bridge Deck Closure Joints in Accelerated Bridge Construction. Infrastructures, 4(2), 31.

Marsh, M. L. (2011) Application of accelerated bridge construction connections in moderate-to-high seismic regions. Transportation Research Board.

Mashal, M., White, S. and Palermo, A. (2014) 'Experimental testing of emulative connections for accelerated bridge construction in seismic areas', in Austroads Bridge Conference, 9th, 2014, Sydney, New South Wales, Australia.

Materials, A. S. for T. and. (1999). ASTM C 157: Standard test method for length change of hardened hydraulic-cement mortar and concrete. In Annual book of ASTM standards. ASTM.

Mehrabi, A.B., and Torrealba, A. (2019). *Available ABC Bridges Systems for Short Span Bridges- Course Module*. https://abc-utc.fiu.edu/wp-content/uploads/sites/52/2019/09/Progress-Report-FIU-2016-2-3-August-2019-V1-TO-POST.pdf

Mehrabi, A. B., & Farhangdoust, S. (2019). *Epoxy Dowel Pile Splice Evaluation*.

Melchers, R. E., Jeffrey, R. J., & Usher, K. M. (2014). Localized corrosion of steel sheet piling. *Corrosion Science*, *79*, 139–147.

Menotti, F., & PRANCKENAITE, E. (2008). Lake-dwelling building techniques in prehistory: driving wooden piles into lacustrine sediments. *EuroRAE*, *5*, 3–7.

Mullins, G., & Sen, R. (2015). *Investigation and development of an effective, economical and efficient concrete pile splice.* Florida. Dept. of Transportation.

Mullins, G., Sen, R., Sagüés, A., Winters, D., Morton, C., Fernandez, J., Johnson, K., DePianta, V., Vomacka, J., & Mitchell, E. (2014). *Design and construction of precast piles with stainless reinforcing steel.* Florida. Dept. of Transportation.

Navaratnarajah, V. (1981). Flexural tests on epoxy-jointed precast prestressed concrete piles. *International Journal of Adhesion and Adhesives*, *1*(5), 265–270.

NACE; (2010). ACCE International. Journal of Clinical Engineering, 35(4), 185–186. https://doi.org/10.1097/jce.0b013e3181fb9a65

OHSAKI, Y. (1982). Corrosion of steel piles driven in soil deposits. *Soils and Foundations*, *22*(3), 57–76.

Pantelides, C. P. et al. (2014) Seismic evaluation of grouted splice sleeve connections for precast RC bridge piers in ABC. Utah Department of Transportation.

Paul, A., Kahn, L. F., & Kurtis, K. (2015). *Corrosion-free precast prestressed concrete piles made with stainless steel reinforcement: construction, test and evaluation.* Georgia. Department of Transportation. Office of Research.

PCI. (2015). Calculation of Interaction Diagrams for Precast, Prestressed Concrete Piles (p. 105). PCI. www.PCI.org

Potter, W . (2007). Test Report for NMB Splice System For Sound Barrier Wall Foundation Connection. Florida Department of Transportation

Rambo-Roddenberry, M., Joshi, K., Fallaha, S., Herrera, R., Kampmann, R., Chipperfield, J., & Mtenga, P. (2016). Construction, strength, and driving performance of carbon-fiber-reinforced polymer prestressed concrete piles. *PCI Journal*.

Redd, S. C. (2016). *Strength, durability, and application of grouted couplers for integral abutments in accelerated bridge construction projects*.

Roddenberry, M., Mtenga, P., & Joshi, K. (2014). *Investigation of carbon fiber composite cables (CFCC) in prestressed concrete piles.* Florida. Dept. of Transportation.

Roddenberry, M., & Servos, J. (2012). *Prefabricated/Precast Bridge Elements and Systems (PBES) for Off-System Bridges*. Florida. Dept. of Transportation.

Rowell, S. P. and Hager, K. P. (2010) 'Investigation of the dynamic performance of large reinforcement bar mechanical couplers', in Structures Congress 2010, pp. 2059–2075.

Scholz, D. P., Wallenfelsz, J. A., Lijeron, C., & Roberts-Wollmann, C. L. (2007). Recommendations for the connection between full-depth precast bridge deck panel systems and precast I-beams. Virginia Center for Transportation Innovation and Research.

Seo, S.-Y., Nam, B.-R. and Kim, S.-K. (2016) 'Tensile strength of the grout-filled head-splice-sleeve', Construction and Building Materials. Elsevier, 124, pp. 155–166.

Shahawy, A. M. and M. (2003). Composite Pile: A Successful Drive. *Concrete International*, *25*(3).

Splice Sleeve Japan, L. (2015). ICC-ES report, NMB Japan Splice Sleeve UX.

Splice Sleeve Nort America, I. (2017). NMB Splice-Sleeve System.

Standard, A. (2013). C1437-13. Standard Test Method for Flow of Hydraulic Cement Mortar. ASTM, West Conshohocken, PA.

Tazarv, M. (2014) Next generation of bridge columns for accelerated bridge construction in high seismic zones. University of Nevada, Reno.

Tazarv, M. and Saiidi, M. S. (2015) 'DESIGN AND CONSTRUCTION OF BRIDGE COLUMNS INCORPORATING MECHANICAL BAR SPLICES IN PLASTIC HINGE ZONES'. Citeseer.

Tazarv, M., & Saiidi, M. S. (2016). Seismic design of bridge columns incorporating mechanical bar splices in plastic hinge regions. *Engineering Structures*, *124*, 507–520.

Tazarv, M., & Saiidi, M. S. (2017). Design and construction of UHPC-filled duct connections for

precast bridge columns in high seismic zones. *Structure and Infrastructure Engineering*, *13*(6), 743–753.

Vasumithran, M., Anand, K. B., & Sathyan, D. (2020). Effects of fillers on the properties of cement grouts. Construction and Building Materials, 246, 118346.

Venuti, W. J. (1980). Efficient Splicing Technique for Precast Prestressed Concrete Piles. *Journal - Prestressed Concrete Institute*, *25*(5), 102–124. https://doi.org/10.15554/pcij.09011980.102.124

Wu, Z. (2016). *Effective Post-Tensioned Splicing System for Prestressed Concrete Piles*.

Yee, A. (1973) 'New precast prestressed system saves money in Hawaii hotel', PCI Journal, 18(3), pp. 10–13.